

# Sustainable Production of Aromatics by Catalytic Aldol Condensation of Biomass-Derived Ketones

Nachhaltige Herstellung von Aromaten durch katalytische Aldolkondensation von biomassebasierten Ketonen



TECHNISCHE  
UNIVERSITÄT  
DARMSTADT

vom Fachbereich Chemie  
der Technischen Universität Darmstadt

zur Erlangung des Grades

Doktor-Ingenieur  
(Dr.-Ing.)

Dissertation  
von Phillip Reif

Erstgutachter: Prof. Dr. Marcus Rose  
Zweitgutachter: Prof. Dr. Markus Busch

Darmstadt 2023

---

---

Tag der Einreichung: 19. September 2023

Tag der mündlichen Prüfung: 13. November 2023

Reif, Phillip:

Sustainable Production of Aromatics by Catalytic Aldol Condensation of Biomass-Derived Ketones

Darmstadt, Technische Universität Darmstadt,

Jahr der Veröffentlichung der Dissertation auf TUpriints: 2023

URN: urn:nbn:de:tuda-tuprints-263309

Tag der mündlichen Prüfung: 13.11.2023

Veröffentlicht unter CC BY-NC-ND 4.0 International

<https://creativecommons.org/licenses/>

---

„Die Wissenschaft fängt eigentlich erst da an,  
interessant zu werden, wo sie aufhört.“

Justus von Liebig

---

---

## Publication list

---

Part of this thesis has been published in peer-reviewed journals. The listed scientific contributions are based on the work under the supervision of Prof. Dr. Marcus Rose at the Ernst-Berl-Institute of TU Darmstadt from January 2019 to May 2022.

### Journal publications relevant for this thesis:

P. Reif, H. Rosenthal, M. Rose, Biomass-Derived Aromatics by Solid Acid-Catalyzed Aldol Condensation of Alkyl Methyl Ketones, *Adv. Sustain. Syst.* **2020**, *4*, 1900150.

P. Reif, N. K. Gupta, M. Rose, Liquid phase aromatization of bio-based ketones over a stable solid acid catalyst under batch and continuous flow conditions, *Catal. Commun.* **2022**, *163*, 106402.

P. Reif, N. K. Gupta, M. Rose, Highly stable amorphous silica-alumina catalysts for continuous bio-derived mesitylene production under solvent-free conditions, *Green Chem.* **2023**, *25*, 1588.

### Other journal publications:

N. K. Gupta, P. Reif, P. Palenicek, M. Rose, Toward Renewable Amines: Recent Advances in the Catalytic Amination of Biomass-Derived Oxygenates, *ACS Catal.* **2022**, *12*, 10400.

### Conference presentations:

P. Reif, M. Rose, Catalytic Aromatization of Biomass-derived Ketones via Aldol Condensation, poster presented at 54<sup>th</sup> German Catalysis Meeting (*Jahrestreffen Deutscher Katalytiker*), 2021 March 16 – 19, virtual.

P. Reif, M. Rose, Biomass-derived Aromatics via Catalytic Aldol Condensation of Ketones, talk presented at the 13<sup>th</sup> European Congress of Chemical Engineering and 6<sup>th</sup> European Congress of Applied Biotechnology, 2021 Sep 20 – 23, virtual.

P. Reif, N. K. Gupta, M. Rose, Liquid-phase aromatization of biomass-derived ketones, talk presented at 5<sup>th</sup> International Symposium on Green Chemistry, 2022 May 16 – 20, La Rochelle, France.

P. Reif, N. K. Gupta, M. Rose, Liquid-phase aromatization of biomass-derived ketones, talk presented at 55<sup>th</sup> German Catalysis Meeting (*Jahrestreffen Deutscher Katalytiker*), 2022 June 27 – 29, Weimar, Germany.



---

## Acknowledgements

---

Ein besonderer Dank gebührt meinem Doktorvater *Prof. Dr. Marcus Rose* für die Überlassung des spannenden Forschungsthemas und die Möglichkeit in seinem Arbeitskreis zu promovieren. Neben dem wertvollen fachlichen Austausch habe ich insbesondere die menschliche Seite und das entgegengebrachte Vertrauen während der gesamten Promotion geschätzt.

A heartfelt thank you to *Prof. Dr. Navneet Kumar Gupta* for his constant support and the numerous late-night scientific discussions, but even more for becoming a true friend during his stay in Darmstadt. I hold many cherished memories from our conversations at the Staatstheater.

Ein herzliches Dankeschön geht auch an *Dipl.-Ing. Martin Lucas*, welcher eine große Unterstützung beim Aufbau der Anlage war und stets hilfsbereit und mit Humor bei allen technischen Fragen zur Seite stand.

Dem *Bundesministerium für Bildung und Forschung* danke ich für die Finanzierung des Projekts „BioAromatics“ (Förderkennzeichen: 031B0680), in dessen Rahmen die vorliegende Arbeit entstand.

Ich möchte ein großes Dankeschön an den gesamten Arbeitskreis Rose aussprechen für die angenehme, freundschaftliche Atmosphäre, die stete Hilfsbereitschaft und die vielen schönen Erinnerungen an gemeinsame Aktivitäten.

Herzlich bedanken möchte ich mich auch bei *Christoph Drexler, Eric Haberhauer, Dajung Jang, Konstantin Lempp, Philipp Pfeifer, Malte Schummer, Christoph Weigel* und *Timon Zankel*, die mich tatkräftig mit ihren von mir betreuten Forschungspraktika, Bachelor- und Masterarbeiten unterstützt haben.

Weiterhin danke ich allen Mitarbeitern der Mechanik- und Elektronikwerkstätten, insbesondere *Herrn Martin Schwarz*, für die technische Unterstützung. Ebenso gilt mein Dank der Sasol Germany GmbH für die unkomplizierte Bereitstellung der Katalysatoren. *Herrn Zubrod* der Shimadzu Deutschland GmbH danke ich für den freundlichen und hilfsbereiten technischen Service.

Dem großartigen Projekt *TUtor International* danke ich für die vielen wunderbaren Momente und Menschen, die ich erleben durfte, und für die Möglichkeit, mich während meiner Zeit an der Universität dort zu engagieren.

Abschließend möchte ich mich auch bei meiner ganzen Familie und meinen Freunden von Herzen für ihre stete Unterstützung und Nachsicht während des Studiums und der Promotion bedanken.

---

---

## Abstract

---

Achieving carbon neutrality and establishing a circular bioeconomy are major challenges of our time. Currently, polymers are predominantly derived from fossil resources. However, increasing demands for their sustainable production require the exploration of alternative pathways based on renewable biomass. For many monomers, aromatics are key precursors, but the large-scale production from biomass remains limited. Catalytic self-aldol condensation of biomass-derived alkyl methyl ketones over solid acid catalysts to aromatics is a promising, less explored pathway. The one-step reaction requires neither hydrogen nor precious metal catalysts. In this study, the aromatization of the model compound acetone was initially investigated under solvent-free batch and continuous flow conditions over commercially available catalysts. The goal was to identify acid catalysts with superior stability and activity and to elucidate structure-activity relationships. The most active catalyst under batch conditions proved to be unstable in the continuous flow reactor. Conversely, larger pore silica-alumina catalysts were observed to provide stable aromatization activity under flow conditions. Very high stability (> 50 h time-on-stream) combined with significant activity was found for the amorphous silica-alumina Siralox 30. The catalyst was also suitable for the aromatization of 2-butanone. Increased space-time-yield and energy-efficient product separation are feasible through solvent-free reaction conditions. Overcoming the challenges associated with catalyst deactivation represents a significant step toward the potential scale-up of the alkyl methyl ketone route and contributes to the transition to a fossil-free, renewable chemical industry.

---

## Zusammenfassung

---

Klimaneutralität und der Aufbau einer biomassebasierten Kreislaufwirtschaft gehören zu den bedeutendsten Herausforderungen unserer Zeit. Polymere werden bisher überwiegend aus fossilen Rohstoffen gewonnen, aber steigende Forderungen nach einer nachhaltigen Produktion machen die Erforschung alternativer Herstellungsrouten auf Basis nachwachsender Biomasse notwendig. Für viele Monomere stellen Aromaten wichtige Vorstufen dar, welche jedoch bisher nur in begrenztem Umfang aus Biomasse hergestellt werden können. Ein vielversprechender, bislang wenig erforschter Ansatz für die Herstellung von Aromaten ist die Selbstaldolkondensation von biomassebasierten Alkylmethylketonen über feste Säurekatalysatoren. Diese einstufige Reaktion erfordert weder zusätzlichen Wasserstoff noch Edelmetallkatalysatoren. In dieser Studie wurde zunächst die Aromatisierung der Modellsubstanz Aceton unter lösemittelfreien Bedingungen in einem Batch- und kontinuierlichen Festbettreaktor über kommerziell erhältliche Katalysatoren untersucht. Ziel war es, Säurekatalysatoren mit hervorragender Stabilität und Aktivität zu identifizieren und Struktur-Aktivitäts-Beziehungen aufzuklären. Der aktivste Katalysator unter Batchbedingungen war jedoch nicht im kontinuierlichen Rohrreaktor stabil. Dahingegen wurde unter kontinuierlichen Bedingungen eine stabile Aromatenbildung von größerporigen Alumosilikat-Katalysatoren beobachtet. Eine sehr hohe Stabilität (Standzeit >50 h) und angemessene Aktivität zeigte das amorphe Alumosilikat Siralox 30. Dieses eignete sich auch für die Aromatisierung von 2-Butanon. Erhöhte Raumzeitausbeuten sowie eine energieeffiziente Produkttrennung sind aufgrund der lösungsmittelfreien Reaktionsbedingungen möglich. Die Überwindung der mit der Katalysatordeaktivierung verbundenen Herausforderungen stellt einen wichtigen Beitrag im Hinblick auf eine mögliche Prozessskalierung sowie auf dem Weg zu einer erneuerbaren fossilfreien Chemieindustrie dar.

---

---

## Table of Contents

---

Nomenclature	viii
1.....Introduction	1
2.....State of the art	3
2.1. Routes from biomass to aromatics	3
2.1.1. Pyrolysis of lignocellulosic biomass	6
2.1.2. Diels-Alder cycloaddition of furanics	8
2.1.3. Self-condensation of alkyl methyl ketones	11
2.2. Aromatization of biomass-derived ketones	12
2.2.1. Alkyl methyl ketones from biomass	13
2.2.2. Aldol condensation of acetone to mesitylene	15
3.....Fixed-bed reactor setup	21
3.1. Overview and implementation of the reactor setup	21
3.2. Safety features for continuous operation	23
4.....Results and discussion	25
4.1. Biomass-Derived Aromatics by Solid Acid-Catalyzed Aldol Condensation of Alkyl Methyl Ketones	25
4.2. Liquid phase aromatization of bio-based ketones over a stable solid acid catalyst under batch and continuous flow conditions	43
4.3. Highly stable amorphous silica-alumina catalysts for continuous bio-derived mesitylene production under solvent-free conditions	62
5.....Conclusion and outlook	91
References	93

---

---

## Nomenclature

---

### Abbreviations

ABE	acetone-butanol-ethanol (fermentation)
APR	aqueous-phase reforming
ASA	amorphous silica-alumina
BAS	Brønsted acid site(s)
BEA	beta zeolite
BET	Brunauer-Emmett-Teller (theory)
BT(E)X	benzene, toluene, (ethylbenzene,) xylene
CAGR	compound annual growth rate
CFP	catalytic fast pyrolysis
DA	Diels-Alder (cycloaddition)
DMF	2,5-dimethylfuran
<i>E. coli</i>	<i>Escherichia coli</i>
GC	gas chromatography
HMF	5-(hydroxymethyl)furfural
HPLC	high performance liquid chromatography
IR	infrared (spectroscopy)
LAS	Lewis acid site(s)
MS	mass spectrometry
MTA	methanol-to-aromatics
PET	polyethylene terephthalate
PS	polystyrene
PTFE	polytetrafluoroethylene
TPD	temperature-programmed desorption
XRD	x-ray diffraction
XRF	x-ray fluorescence (spectroscopy)

---

## Symbols

$X$	conversion	$\text{mol mol}^{-1}$
$S$	selectivity	$\text{mol mol}^{-1}$
$Y$	yield	$\text{mol mol}^{-1}$
$W/F$	(catalyst) weight-to-flow ratio	$\text{g}_{\text{cat}} \text{ h mol}^{-1}$
WHSV	weight hourly space velocity	$\text{g g}^{-1} \text{ h}^{-1}$

## Indices

cat	catalyst
Mes	mesitylene
MesOx	mesityl oxide

---

## 1. Introduction

---

Anthropogenic climate change caused by CO<sub>2</sub> emissions from the use and depletion of fossil-based resources is one of the greatest challenges of the 21<sup>st</sup> century. To mitigate its global effects, the establishment of a circular bioeconomy based on alternative and renewable resources for energy and materials with net-zero emissions is required.<sup>[1]</sup> Biomass as a resource has great potential as it is not only renewable but its use also decreases the dependency on crude oil with fluctuating supply and prices.<sup>[2]</sup> For the chemical industry, the sustainability of polymers is a particular issue due to their ubiquity in everyday life and the increasing consumer and political demands for bio-based products.<sup>[1,3]</sup> Thus, besides the environmental impact, there is a strong financial incentive to develop more sustainable routes to polymers from biomass feedstocks. In 2020, less than 0.03% of the global biomass demand of 13.4 billion tons was used for the production of bio-based polymers, demonstrating the large unrealized potential.<sup>[4]</sup> In combination with polymer recycling, greenhouse gas emissions over the polymer lifetime can be effectively reduced with bio-based virgin plastic.<sup>[5-7]</sup> For many polymers, the precursors of their chemical building blocks are derived from aromatics as favorable properties such as rigidity and thermal stability can be promoted.<sup>[8]</sup> For polystyrene (PS), the monomer styrene is obtained via dehydrogenation of ethylbenzene. Polyethylene terephthalate (PET) is another example where one of its monomers, terephthalic acid, is formed by oxidation of *p*-xylene. PET is prevalently used for bottle packaging. Therefore, big soft drink companies such as Coca-Cola or Suntory work together with chemical companies on bio-derived alternatives for PET bottles to accommodate market demands and reduce their environmental footprint.<sup>[9,10]</sup> This requires bio-based *p*-xylene since monoethylene glycol, the second monomer, is readily available from biomass. Besides polymers, the constituent aromatics benzene, toluene, ethylbenzene, and xylene – the so-called BT(E)X mixture – are applied as solvents, fuel additives, and as adhesives.<sup>[11-13]</sup> Currently, they are obtained by catalytic reforming or steam cracking of fossil-based naphtha in crude oil refineries.<sup>[14,15]</sup> Their importance in the chemical value chain is displayed by a market size of 122 million tons (2020) with a compound annual growth rate (CAGR) of 3.76%.<sup>[16]</sup> In 2015, more than 37 million tons of *p*-xylene were used for PET and polyester fibers.<sup>[17]</sup> Due to their positioning as intermediates in the value chain, bio-based aromatics present an excellent opportunity to contribute to a shift to a carbon-neutral economy and are seen as a key enabling technology by the European Union.<sup>[2]</sup>

To produce aromatics from biomass, various strategies have been explored but two routes are prominent: the thermochemical depolymerization of lignocellulosic biomass by (catalytic) fast pyrolysis (CFP) and the Diels-Alder (DA) cycloaddition of furan derivatives with bio-dienophiles such as ethylene from sugar cane.<sup>[10,18]</sup> Pyrolysis yields a bio-oil which requires intensive purification and deoxygenation to separate the desired aromatics.<sup>[19]</sup> DA-cycloaddition is highly selective, but depending on the raw material

structure additional dehydrogenation or dehydration is required and the large-scale production of furan derivatives based on 5-(hydroxymethyl)furfural (HMF) is still demanding due to its high reactivity.<sup>[18]</sup> A less explored but very promising pathway is the self-condensation of biomass-derived alkyl methyl ketones, e.g., acetone, 2-butanone, etc. In the presence of acids, these form 1,3,5-alkylated C<sub>6</sub>-aromatics by condensation and elimination of water.<sup>[20,21]</sup> Various chemocatalytic and biotechnological pathways permit to obtain alkyl methyl ketones from existing biorefinery streams, thereby facilitating their integration.<sup>[21]</sup> The most prominent example is the ABE fermentation which yields acetone, butanol, and ethanol from biomass-derived carbohydrates.<sup>[22,23]</sup> One highly interesting approach is gas-phase fermentation to produce acetone from CO<sub>2</sub>, rendering the feedstock carbon-negative.<sup>[24]</sup> The direct formation of aromatics from alkyl methyl ketones in a one-step reaction without the need for further deoxygenation with (currently still limited) hydrogen or precious metal catalysts has the advantage of being catalyzed by robust solid acids. With well-established transalkylation processes, the self-condensation of alkyl methyl ketones is an efficient drop-in solution for BTX-aromatics.<sup>[25]</sup> While the base-catalyzed condensation of alkyl methyl ketones has been studied, mainly for the application as jet fuels<sup>[21]</sup> (C<sub>9</sub>-C<sub>16</sub>) or lubricants<sup>[26]</sup> (C<sub>24</sub>-C<sub>45</sub>) after hydrodeoxygenation, the use of solid acid catalysts for the production of 1,3,5-alkylated C<sub>6</sub>-aromatics has been limited by fast deactivation, especially under high-temperature vapor-phase conditions.<sup>[27]</sup> To overcome the challenge of insufficient catalyst stability and to enable process scale-up, the aim of this study was to better understand the structure-activity relationship of catalysts in the aromatization and to develop a selective catalytic process with high stability and aromatics selectivity under industrially-relevant continuous conditions. The presented research thus contributes to the realization of a carbon neutral circular bioeconomy as illustrated in **Figure 1**.

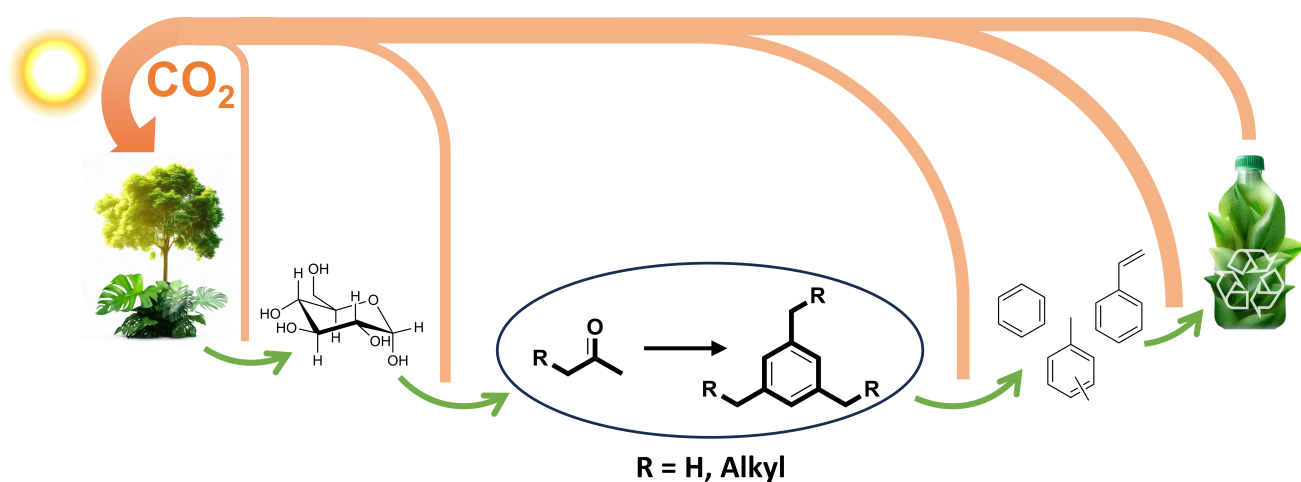


Figure 1: Bio-based aromatics are a key intermediate in the carbon neutral production of polymers.



## 2. State of the art

Several routes are being developed to produce aromatics from renewable biomass instead of limited fossil resources. An overview of the most developed and promising routes is given as a reference point for the pathway via catalytic self-condensation of biomass-derived alkyl methyl ketones discussed below. The upstream production of ketones from biomass is described and the state of the art of the aromatization of acetone, which serves as a model compound for alkyl methyl ketones, to mesitylene is presented.

### 2.1. Routes from biomass to aromatics

Biomass as a renewable feedstock is an attractive source for fuels and chemicals and can be sourced from plants.<sup>[28]</sup> While first generation biomass such as maize and edible oil seeds compete directly with food production, non-edible lignocellulosic biomass is used in the second generation, e.g., sugar cane bagasse, corn stover or rice husks, or ideally food supply chain waste.<sup>[28]</sup> The widely available lignocellulosic biomass consists of approx. 75% carbohydrates, 20% lignin, and 5% of triglycerides, proteins, and terpenes.<sup>[28]</sup> Depolymerization and the removal of oxygen are required in order to use the structural polysaccharides cellulose (40%), hemicellulose (25%), and lignin (see **Figure 2**) in downstream processing, especially for drop-in replacements.<sup>[29]</sup> The processing and valorization for the various biomass application streams are to occur in integrated biorefineries comparable to crude oil refineries. Due to the structural and chemical complexity of biomass, costs associated with processing are usually high in comparison to the feedstock costs.<sup>[29,30]</sup> Efficient processing with a limited number of reaction and separation steps is therefore important.<sup>[31]</sup>

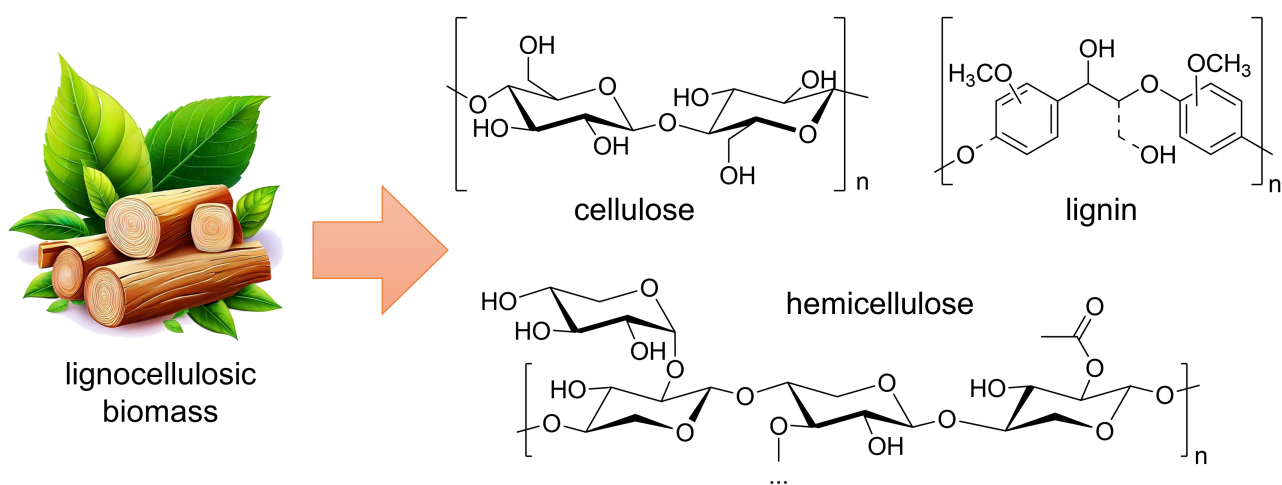


Figure 2: Polysaccharides and lignin obtained from lignocellulosic biomass. Structures adapted from references.<sup>[32,33]</sup>

The conversion and deoxygenation of biomass to platform chemicals is accomplished via fermentation, direct gasification, and chemocatalytic pathways (see **Figure 3**).<sup>[28]</sup> The monosaccharides obtained from the acid-catalyzed depolymerization of cellulose and hemicellulose are used for the fermentation to lower alcohols, e.g., ethanol, propanols, butanols, which are subsequently upgraded to ethylene, propylene, butene, isobutene, etc.<sup>[28]</sup> While lignin is already composed of aromatic monomers, it would be an ideal feedstock for biomass-derived aromatics, but its selective depolymerization is challenging and it is therefore converted by pyrolysis. Due to the importance of this process, the pyrolysis of lignocellulosic biomass is explained in more detail in the following chapter. Similarly, the DA-cycloaddition of furan derivatives is described in detail in its chapter. An overview of the other promising approaches from biomass to aromatics is given below.

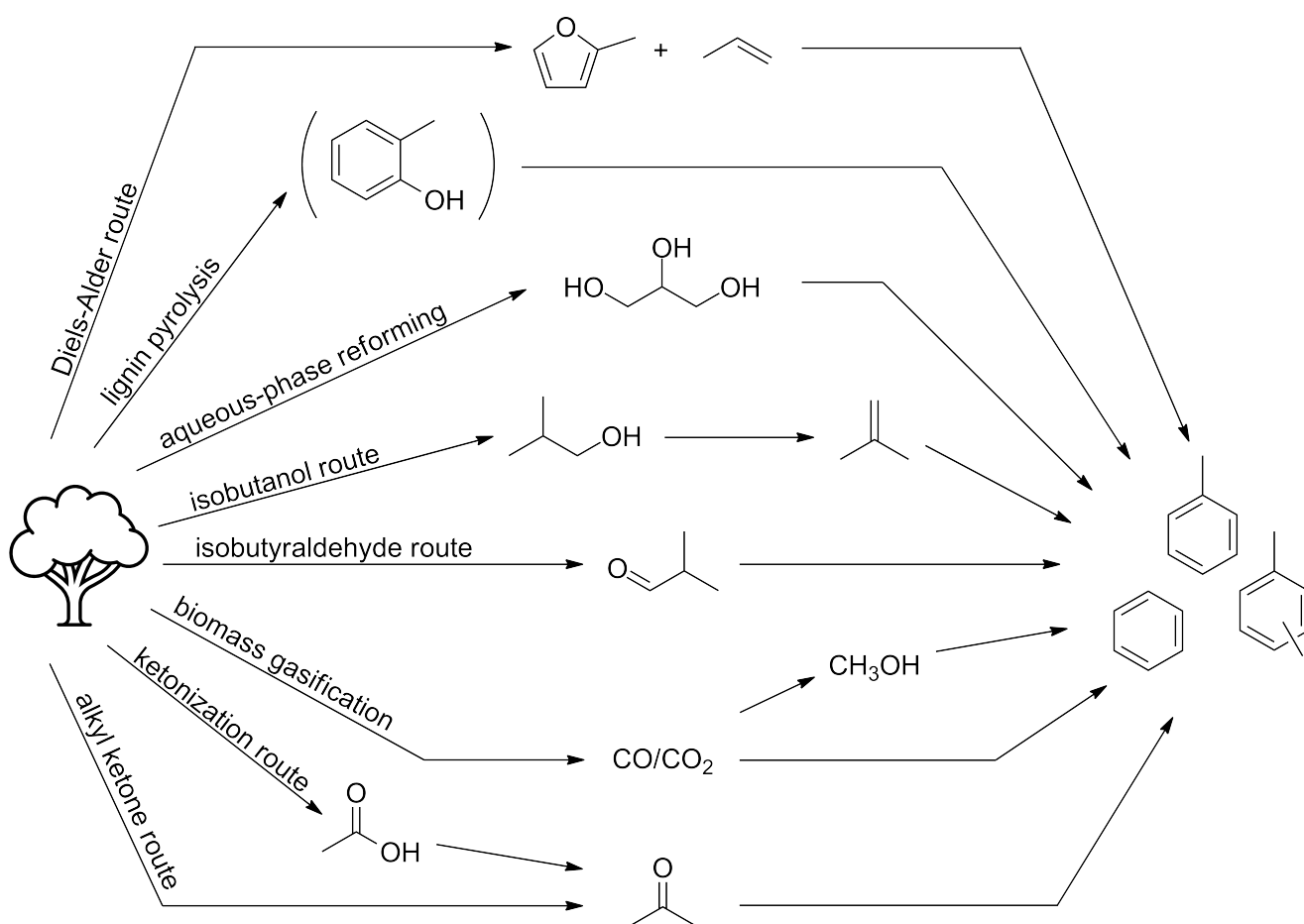


Figure 3: Schematic overview of the most prominent pathways from biomass to aromatics via their respective intermediates.

By fermenting glucose, isobutanol can be obtained from biomass and subsequently converted to aromatics via isobutene. This process has been commercialized by the company Gevo and uses multiple catalyzed reaction steps to dimerize isobutene and then cyclize it to *p*-xylene.<sup>[34]</sup> As catalysts zeolites are employed.<sup>[35]</sup> Another approach based on fermentation is the aromatization of biomass-derived

---

isobutyraldehyde over acidic H-ZSM-5 zeolites. An advantage of isobutyraldehyde is its energy-efficient separation due to its low boiling point and high vapor pressure.<sup>[36]</sup> Deischer *et al.* reported that the conversion to BTX was optimal at 400 °C and a WHSV of 3 h<sup>-1</sup> with a yield of up to 79% using a fixed-bed reactor at atmospheric pressure.<sup>[36]</sup> A productivity of 65 mmol g<sub>cat</sub><sup>-1</sup> h<sup>-1</sup> was obtained. Catalyst deactivation was observed due to coke formation and the BTX-yield dropped to 53% after 10 h time-on-stream. Calcination of the spent catalyst was shown to restore its catalytic activity.

Another important approach for biomass-derived aromatics is the aqueous-phase reforming (APR) of carbohydrate solutions, e.g., glucose, sorbitol and glycerol, are converted to hydrocarbons in the presence of solid acids and (de)hydrogenation catalysts, e.g., Pd, Pt.<sup>[10,28]</sup> This technology is used by the company Virent for the commercial production of bio-based *p*-xylene.<sup>[37]</sup> At reaction conditions of 180-300 °C and 10-90 bar H<sub>2</sub>, the aqueous sugar solution is deoxygenated into a mixture of intermediates which are then dehydrocyclized over ZSM-5 zeolites to BTX-aromatics and alkanes.<sup>[28]</sup> The aromatics are then isolated from the reaction mixture.

Carboxylic acids such as acetic acid are found in fermented waste-water streams and can be valorized to aromatics in a sequence of ketonization and aromatization over zeolite catalysts at high reaction temperatures. This approach was followed by Fufachev *et al.* who yielded 45% BTX-aromatics over a Ga/ZSM-5 zeolite after initial TiO<sub>2</sub>-catalyzed conversion of butyric acid to 4-heptanone at 450 °C and a WHSV of 1 h<sup>-1</sup>.<sup>[38]</sup> Coke formation on the catalyst was found to cause deactivation and decreases the BTX-yield with time-on-stream. Fermentative waste-water streams contain large amounts of water which has an inhibiting effect on the Ga/ZSM-5 activity. A route from acetic acid to *p*-xylene via isobutene was patented in which a combination of Zn<sub>x</sub>Zr<sub>y</sub>O<sub>z</sub> and ZSM-5 catalysts is used.<sup>[18,39]</sup> A detailed review on the ketonization of carboxylic acids for biomass valorization including to aromatic compounds was recently provided by Boekaerts and Sels.<sup>[40]</sup>

The methanol-to-aromatics (MTA) route is based on the gasification of biomass to syngas from which biomass-derived methanol is produced.<sup>[12]</sup> Methanol is seen as a highly relevant platform chemical from which a wide product portfolio is available. The aromatization of methanol is a multi-step process utilizing acidic zeolites at reaction temperatures of 370-400 °C and atmospheric pressure.<sup>[18]</sup> The reaction is usually performed in fixed-bed reactors and catalyst deactivation by coking is common.<sup>[41]</sup> It follows a carbenium ion mechanism in the formation of higher aliphatic and aromatic hydrocarbons, e.g., toluene, xylenes, and other aromatics, from C<sub>1</sub>-C<sub>4</sub> feeds.<sup>[42]</sup> Using a SiO<sub>2</sub>/Zn/P/ZSM-5 catalyst a 61.7% *p*-xylene yield was achieved from methanol.<sup>[43]</sup> The MTA process is highly promising as the production of methanol from biomass or by CO/CO<sub>2</sub> hydrogenation is intensively researched.<sup>[44]</sup>

In addition to the methanol route, CO and CO<sub>2</sub> can be used directly as feedstocks for aromatics. The selective hydrogenation of CO<sub>2</sub> to aromatics is a highly interesting approach as it is carbon-negative and thus a “dream reaction”. Ni *et al.* showed a promising aromatics selectivity with a composite catalyst of

---

ZnAlO<sub>x</sub> and H-ZSM-5 with an aromatics selectivity of 73.9% (excluding CO selectivity) at 320 °C and 30 bar in a fixed-bed reactor.<sup>[45]</sup> Catalyst productivity was still low with 15 mg g<sup>-1</sup> h<sup>-1</sup> due to 9.1% CO<sub>2</sub> conversion. The reaction to aromatics was reported to proceed via formation of methanol, dimethyl ether, and olefins as intermediates. Addition of Cr<sub>2</sub>O<sub>3</sub> was shown to improve the *p*-xylene selectivity.<sup>[46]</sup>

### 2.1.1. Pyrolysis of lignocellulosic biomass

The direct conversion of lignocellulosic biomass to aromatics by pyrolysis is a highly promising thermochemical route as it turns low-cost solid biomass into a renewable aromatic-rich liquid.<sup>[47]</sup> It is one of the main pathways for biomass valorization besides gasification and hydrolysis.<sup>[48]</sup> Especially lignin is an interesting feedstock for pyrolysis and a good source for aromatic molecules as it is composed of various aromatic units. The most common ones are coumaryl alcohol, coniferyl alcohol, and sinapyl alcohol.<sup>[49]</sup> Due to its structural complexity, it has a low susceptibility to processing by methods other than pyrolysis. Large quantities of lignin are produced as a by-product in the pulp and paper industry and are used energetically for power generation.<sup>[50]</sup> While the global production of lignin would be sufficient to meet the global demand for aromatic molecules, the selective depolymerization of lignocellulosic biomass remains a challenge due to the aforementioned high structural complexity.<sup>[28]</sup>

In pyrolysis, the biomass composite is treated by rapid heating (>500 °C s<sup>-1</sup>) to high temperatures of 550-750 °C under oxygen-free conditions and yields a liquid bio-oil, vapors, water, and char.<sup>[19,51]</sup> The pyrolysis vapors are either directly and rapidly condensed to a bio-oil or passed over a catalyst for further conversion to target compounds such as aromatics.<sup>[18]</sup> The bio-oil formed by depolymerization is a complex mixture of oxygenated compounds and contains 15-35 wt% of water and a low amount of solid particles.<sup>[48]</sup> Due to the high oxygen content and low selectivity, further deoxygenation and purification are required in order to substitute fossil-sourced chemicals.<sup>[19]</sup> By upgrading the pyrolysis vapors with acidic catalysts, broad fractions of monoaromatic compounds can be obtained.<sup>[52,53]</sup> This consecutive process in combination with very short residence times is the above mentioned CFP and produces a bio-oil of higher quality and yield and suppresses char formation in comparison to conventional pyrolysis without catalyst and lower heating rates.<sup>[47,51]</sup> The short residence time minimizes secondary reactions.<sup>[51]</sup>

The inexpensive, solvent-free production of a renewable bio-oil in a simple, single-step reaction with short residence times is one of the biggest advantages of CFP.<sup>[18,19,54,55]</sup> The process conditions allow the direct use of non-food competing lignocellulosic biomass and the high versatility is suited for integration into a biorefinery where the produced aromatics and olefins fit in the existing infrastructure for the production of bio-fuels and bio-chemicals from all types of biomass.<sup>[18,48,52]</sup> Besides the bio-oil, CO and CO<sub>2</sub> are formed as off-gases, which can be further valorized downstream. Upgrading of the bio-oil is

---

essential as its formation is not selective and a heterogeneous mixture of over 300 different compounds is obtained.<sup>[56]</sup> The most common are carboxylic acids, aldehydes, ketones, alcohols, glycols, phenols and phenol derivatives, and carbohydrates.<sup>[57]</sup> Combined with the high oxygen content, this results in a thermally unstable product with a low heating value that degrades over time.<sup>[10,19]</sup> The carboxylic acids present make the bio-oil corrosive.<sup>[51,57]</sup> Due to the lack of quality, it cannot be used directly, e.g., for fuel applications as envisaged, and must be upgraded before use.<sup>[19]</sup>

For the catalytic treatment, acidic zeolites such as H-ZSM-5 or H-Y are most commonly used as they efficiently remove oxygen as CO, CO<sub>2</sub>, and H<sub>2</sub>O vapors, produce the desired products, and increase the C/O ratio.<sup>[47,51]</sup> The zeolites promote aromatization due to their shape-selectivity and thus allow the formation of monoaromatic compounds from uncondensed pyrolysis vapors.<sup>[55]</sup> Yield and selectivity are controlled by tuning of the acidity and pore size of the catalyst.<sup>[47]</sup> Carlson *et al.* found that H-ZSM-5 produced the highest aromatic yield and least amount of coke.<sup>[19]</sup> Puértolas *et al.* introduced mesopores to obtain hierarchical H-ZSM-5 zeolites and found an improved aromatization activity and catalyst stability as the number of accessible Brønsted acid sites (BAS) and the decarbonylation rate increased.<sup>[48]</sup> Fast heating rates and high catalyst-to-feed ratios further maximize aromatics yield and lower coking. But too high catalyst loadings can lead to trapping of the pyrolysis vapors and deactivation by coking.<sup>[51]</sup> To improve the aromatics selectivity in CFP, doping of the zeolite catalysts with Ga was found beneficial.<sup>[52]</sup> The Ga-doped zeolites increase the rate of decarbonylation and olefin aromatization. In general, a high density of BAS is beneficial for aromatics production in the upgrading of pyrolysis vapors. The catalytic upgrading step can be performed *in situ* in a single reactor where biomass and catalyst are in contact or *ex situ* where the pyrolysis vapors are transferred to a sequential reactor setup.<sup>[51]</sup> *In situ* CFP leads to higher bio-oil yields but also faster catalyst deactivation. *Ex situ* CFP allows better temperature control of the catalyst bed, resulting in improved product composition and longer catalyst life due to reduced catalyst coking. But it is also associated with higher investment costs as a second reactor is required. The suppression of coke formation, the heterogeneous structure of lignocellulosic biomass, and low H/C ratio of the bio-oil are some of the multi-scale challenges that CFP faces in the substitution of petroleum-sourced chemicals.<sup>[19,58]</sup> Alternatively, oxygen functionalities can be removed by hydrodeoxygenation which requires additional hydrogen and metal hydrogenation catalysts.<sup>[56]</sup>

The conversion of biomass to aromatics in CFP proceeds by a series of reaction steps. First, anhydrous sugars are formed from the lignocellulosic biopolymers. Then, a series of oligomerization, decarbonylation, and dehydration steps occur in the zeolite pores, leading to aromatics.<sup>[18,49,51]</sup> The reaction pathway to aromatics follows a hydrocarbon pool mechanism in which light olefins, e.g., ethene and propene, are formed by dealkylation and then oligomerized to aromatics. Lignin is converted to hydrocarbon pool precursors by demethylation and demethoxylation. An overview of the complex

---

reaction network for the catalytic upgrading of bio-oil to aromatics over acidic catalysts is given by Puértolas *et al.*<sup>[48]</sup>

While silica-alumina catalysts such as zeolites are rather inexpensive, the pyrolysis process is energy-intensive and leads to carbon losses in the form of solid coke, CO<sub>x</sub>, and unwanted side products. Catalyst deactivation by undesired coking is a major obstacle and is caused by pore blocking and active site poisoning.<sup>[47]</sup> Kim *et al.* found that the phenolic hydroxyl groups in lignin monomers promote coke formation and repolymerization, which can lead to a reduced aromatics yield.<sup>[55]</sup> The catalytic activity can be restored by calcination of the zeolite catalysts. The resulting product composition is highly dependent on the biomass source and the upgraded bio-oil requires further separation in order to obtain highly pure compounds, e.g., aromatics.<sup>[18]</sup>

Nevertheless, several companies have worked on commercialization of the technology for the production of bio-based fuels and aromatics. Anellotech Inc. was co-founded by G. W. Huber and D. Sudolsky and uses low-cost primary feedstock as well as zeolite catalysts to turn solid biomass into liquid fuels and aromatics.<sup>[18,59]</sup> In their process, a bio-oil is formed at a reaction temperature of 400-600 °C, high heating rate (>500 °C min<sup>-1</sup>), and a short residence time (<2 min).<sup>[10,59]</sup> In Europe, the first pilot plant for lignin-based aromatics was recently opened by VITO in Mol, Belgium, in October 2022.<sup>[60]</sup> The pilot plant is designed for the production of up to 100 kg of renewable aromatics per day by catalytic depolymerization of lignin with hydrogen. The proprietary technology is developed under the Biorizon consortium and is funded by the European Regional Development Fund.

CFP of lignocellulosic biomass is a potentially effective and robust way to utilize all components of biomass as chemical feedstocks. However, current challenges in the selective depolymerization indicate that large-scale commercial production of bio-oil derived aromatics requires further research efforts and is only expected in the long term.<sup>[58]</sup>

### 2.1.2. Diels-Alder cycloaddition of furanics

The selective formation of biomass-derived aromatics can be achieved through [4+2]-DA cycloaddition of furan derivatives with suitable dienophiles such as alkenes and consecutive aromatization by dehydration or dehydrogenation over acidic catalysts.<sup>[18,61]</sup> This reaction of a conjugated diene with a dienophile allows the production of monoaromatic monomers with very high feedstock atom efficiency in comparison to the complex product mixtures obtained by pyrolysis.<sup>[11,62]</sup> Furans are important renewable platform molecules that are obtained from lignocellulosic C<sub>6</sub>-sugars such as glucose and fructose which are dehydrated to HMF by acid catalysis.<sup>[63,64]</sup> HMF is selectively converted by hydrogenation to the widely used diene 2,5-dimethylfuran (DMF) with yields of 76-79%.<sup>[17,65]</sup> DA-cycloaddition of DMF with ethylene and subsequent aromatization of the formed cycloadduct yields the

very important aromatic *p*-xylene which is the precursor for terephthalic acid. Besides DMF, HMF can be converted to other furanic dienes in high yields, e.g., 2-methylfuran by hydrogenation (>90% yield) or furan by decarbonylation (>99% yield).<sup>[11]</sup>

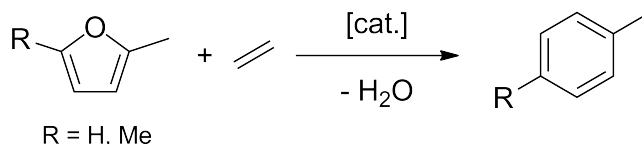


Figure 4: Aromatics formed by [4+2]-Diels-Alder cycloaddition of furan derivatives with ethylene.

The second starting material ethylene is obtained in high yield and purity from biomass via dehydration of ethanol which is produced in large quantities by fermentation of sugars.<sup>[11]</sup> The production of bio-ethylene from sugarcane has been commercialized by Braskem.<sup>[66,67]</sup> Other dienophiles, e.g., acrolein, maleic anhydride, 2,2,2-trifluoroethylacetate or propylene, are also accessible from biomass and can be used for the formation of *p*-xylene with suitable dienes.<sup>[11,18,68]</sup> A comprehensive overview of the formation of aromatics by DA-cycloaddition of bio-based compounds was provided by Settle *et al.*<sup>[11]</sup> The reaction proceeds by coupling of the diene and dienophile and formation of a six-membered ring, the cycloadduct.<sup>[11]</sup> Depending on the starting materials, elimination of water or hydrogen then yields the desired aromatic compound in high selectivity. Significant amounts of energy are required to initialize the cycloaddition, so that the reaction is usually performed at 200-300 °C and 20-60 bar of ethylene.<sup>[18,62]</sup> Under these reaction conditions *p*-xylene yields of up to 97% from DMF and ethylene were reported.<sup>[11,69]</sup>

Since DA-cycloaddition is thermodynamically controlled and forms an unstable cycloadduct, it benefits from a low reaction temperature. The subsequent aromatization is therefore carried out at high reaction temperatures to shift the reaction equilibrium towards the stable aromatic products.<sup>[70]</sup> However, the high temperature can also lead to an increase in the retro-Diels-Alder reaction which reduces the overall reaction yield of the aromatic product.<sup>[71]</sup> An alternative approach is to completely saturate the intermediate first by hydrogenation, followed by dehydration to form the aromatic compound. The direct reaction of furan derivatives, e.g., DMF and 2-methylfuran, with dienophiles is feasible due to their electron-rich alkyl substituents which stabilize charged intermediates.<sup>[70]</sup> The electron-withdrawing substituents on furfural and HMF therefore limit the direct DA-cycloaddition.<sup>[62]</sup> In the formation of *p*-xylene from DMF and ethylene, the initial DA-cycloaddition step is rate-determining since the subsequent dehydration to aromatics is effectively catalyzed by BAS.<sup>[72]</sup> The DA-cycloaddition proceeds thermally without a catalyst but is strongly catalyzed by Lewis acids.<sup>[73]</sup> The reaction benefits from confinement in the micropores of zeolites. Therefore, zeolites are often used as they combine BAS and Lewis acid sites (LAS). The subsequent aromatization benefits from BAS. In order to increase the aromatics yield tandem



---

catalysts are important that combine properties to catalyze both consecutive reactions and thus allow to perform the reaction in one system. Moderately acidic zeolites are therefore used for dehydration.<sup>[64]</sup> Since the formation of aromatics from furan derivatives and suitable dienophiles is a consecutive reaction, suitable tandem catalysts are required to catalyze both reaction steps over a single catalyst, ideally in one-pot type reactions. Lewis acid catalysts are very effective for the DA-cycloaddition because they drastically reduce the required activation energy. The subsequent aromatization of the cycloadduct by dissociation of water is effectively catalyzed by Lewis and more commonly Brønsted acid catalysts such as zeolites in proton form, polyoxometalates or heteropoly acids which are highly tunable multifunctional catalysts.<sup>[11,68]</sup> The tandem catalysis can therefore proceed via two modes: using Lewis acidic catalysts for the DA-cycloaddition and Brønsted acids for the aromatization or using tandem Brønsted-Lewis acid catalysts for both DA-cycloaddition and aromatization.<sup>[11]</sup> If dehydrogenation of the cycloadduct is required, platinum group metals are also effective.<sup>[11]</sup> In some cases, this is also achieved over BAS on zeolites through a carbocation-based mechanism.<sup>[11]</sup> In a one-pot reaction, a very high yield of 90% *p*-xylene was achieved by Chang *et al.* using a Lewis acidic Zr-BEA (Si/Zr=168) zeolite to tandem catalyze the DA-cycloaddition and aromatization of DMF with ethylene in comparison to 30-34% yield reported for the stepwise conversion.<sup>[11,68,74]</sup> They found that the reaction rate was proportional to the number of LAS and that deactivation decreased as the reaction was not selective for the hydrolysis by-product 2,5-hexanedione.

Using heterogeneous catalysts, continuous flow synthesis of *p*-xylene is feasible and up to 83% yield was reported by Mendoza Mesa *et al.* from DA-cycloaddition of DMF and acrylic acid over an H-beta zeolite (Si/Al=150) at 100% DMF conversion.<sup>[11,17,75]</sup> The use of acrylic acid allows a fully liquid route without the need for external gas pressure and the use of a lower reaction temperature of 473 K. The formed DA-cycloadduct is intermediately dehydrated to 2,5-dimethylbenzoic acid and finally decarboxylated to *p*-xylene. The residence time in the flow reactor was 10.1 min and an excess of acrylic acid was used. Under these reaction conditions, the catalyst was stable for 10 h time-on-stream and could be restored by calcination in air. The high selectivity of the reaction was based on the combination of high acid site density and surface area of the catalyst used. Teixeira *et al.* found that the direct use of liquid ethanol as a dienophile, instead of relying on pressurized gaseous ethylene, lowered the reaction barrier for the [4+2]-DA-cycloaddition over zeolite H-USY-12, significantly increasing the initial formation rate to *p*-xylene at 300 °C.<sup>[64]</sup>

The DA-cycloaddition gives selectively access to various aromatics. Toluene is formed by the reaction of 2-methylfuran and ethylene. For the consecutive reaction steps, catalyzed by the strong Lewis acid AlCl<sub>3</sub> at 250 °C and 30 bar, a yield of 70% toluene was reported after 24 h.<sup>[73]</sup> Toluene can also be formed from furan and propylene, albeit in lower yields.<sup>[11,61]</sup> Ethylbenzene, the precursor for styrene, is obtained with over 80% selectivity from 1,3-butadiene by dehydrocyclodimerization at 400 °C in



---

continuous flow.<sup>[76]</sup> A highly selective formation of the terephthalic acid replacement diethyl terephthalate is viable by DA-cycloaddition of biomass-derived *trans,trans*-diethylmuconate and ethylene with over 80%.<sup>[77]</sup> Through DA-cycloaddition and the wide variety of available addends from biomass, it is also possible to form functional alternative aromatic monomers which are not directly accessible from petroleum sources.<sup>[11]</sup>

Advantages of the DA-cycloaddition are its very high selectivity and atom efficiency which makes it an effective process for transforming biomass-derived compounds into aromatic chemicals. A downside is the high price of furanic raw materials as the production of HMF, which has enormous potential as a raw material, is challenging due to its high reactivity and instability.<sup>[18,28]</sup> As feedstock costs directly impact final product costs, the high costs associated with low yields are currently the biggest drawback of the route and hamper commercialization of producing aromatics via DA-cycloaddition of furanics.<sup>[11]</sup> Further improvements and increased selectivity for the conversion of sugars to biomass-derived furans is therefore required.<sup>[78]</sup> In comparison with petroleum-based *p*-xylene production, the harsher reaction conditions required for the pathway via DA-cycloaddition lead to higher costs.<sup>[62]</sup> Under process conditions, the microporous zeolite catalysts deactivate by coke formation over time. One cause for this is the hydrolysis of DMF to 2,5-hexanedione in a competing side reaction as 2,5-hexanedione which can further polymerize and then lead to coking.<sup>[64]</sup> This side reaction is inhibited by doping catalysts with Zr and Al.<sup>[62]</sup>

### 2.1.3. Self-condensation of alkyl methyl ketones

The selective self-aldol condensation of alkyl methyl ketones to biomass-derived aromatics is an alternative pathway that is currently being explored.<sup>[79–82]</sup> Alkyl methyl ketones are obtained from biomass through various chemocatalytic and biotechnological routes.<sup>[21,29]</sup> The most well-known is the ABE fermentation of bio-based carbohydrates to acetone, butanol, and ethanol with the bacterium *Clostridium acetobutylicum*. A century ago, ABE fermentation was used for the industrial acetone production before large amounts of acetone were obtained as a by-product in the cumene oxidation to phenol.<sup>[83]</sup> The self-aldol condensation of biomass-derived ketones is catalyzed by acids and bases and yields water as the sole condensation product.<sup>[84]</sup> It is therefore an efficient deoxygenation strategy for biomass conversion without requiring additional hydrogen or precious metal catalysts. Aromatics are formed by sequential cyclotrimerization of three alkyl methyl ketones in the presence of acid catalysts (see **Figure 5**).<sup>[84]</sup> In the case of acetone, the simplest alkyl methyl ketone, only the C<sub>9</sub>-aromatic mesitylene is formed as an aromatization product.

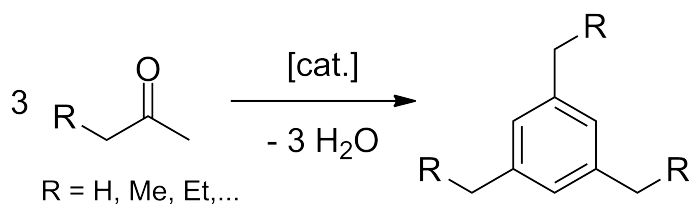


Figure 5: Self-condensation of alkyl methyl ketones to 1,3,5-alkylated C<sub>6</sub>-aromatics by sequential cyclotrimerization.

While the general pathway and reaction have been known and studied for a long time, the focus was usually on using the C-C coupling reaction during aldol condensation to increase the carbon chain length and transform biomass-derived ketones to compounds suitable for fuel applications.<sup>[21,26]</sup> The self-condensation of alkyl methyl ketones for the purpose of aromatics production was less explored. For acetone, it was mostly studied using mineral acid catalysts or under gas-phase conditions where rapid catalyst deactivation by coking occurred.

The aldol condensation of longer alkyl methyl ketones to bio-fuels or lubricants is usually catalyzed by base catalysts and entails subsequent hydrodeoxygenation of the oligomers.<sup>[21,26,85]</sup> During these studies the formation of trimer aromatics was also observed during the initial screening of acid catalysts. In the literature, the self-condensation to aromatics is reported for 2-butanone<sup>[81,86,87]</sup>, 2-pentanone<sup>[85]</sup>, 2-hexanone<sup>[21,82,88]</sup>, 2-heptanone<sup>[85,89]</sup>, 2-nonanone<sup>[26]</sup>, and C<sub>10</sub>-ketones<sup>[26]</sup>. The aromatization of these longer ketones yields alkyl aromatics which can be subsequently upgraded to the desired compounds by established transalkylation reactions.<sup>[90]</sup> Utilizing high-temperature gas-phase conditions, Fuhse and Bandermann explored the conversion of various ketones to aromatics over H-ZSM-5 at 673 K.<sup>[91]</sup>

The promising aromatization strategy by selective aldol condensation of alkyl methyl ketones in a one-step reaction using existing biorefinery streams, such as acetone production by ABE fermentation, therefore warrants a more detailed investigation, aiming at a robust and technically feasible aromatization process under milder reaction conditions. The complete pathway from biomass to alkyl methyl ketones and the subsequent aldol condensation reactions are therefore described in detail in the following section. Here, the state of the art of the conversion of acetone to mesitylene is presented, as it is a model compound for all alkyl methyl ketones and has been studied the most.

## 2.2. Aromatization of biomass-derived ketones

Biomass-derived aromatics by self-condensation of alkyl methyl ketones is based on the accessibility from biomass and suitable reaction conditions. In this section, the pathways from biomass to alkyl methyl ketones are first summarized to establish the basis of this route. The aromatization of alkyl methyl ketones is described in detail for acetone, which serves as a model compound for the highlighted route. Understanding the reaction to the aromatic acetone trimer mesitylene provides guidance on how to

---

optimize the formation of higher alkyl aromatics from ketones. The reaction network of the self-aldol condensation of acetone, the intricacies of the catalytic condensation with solid acids, and the challenges posed by catalyst deactivation are also presented.

### 2.2.1. Alkyl methyl ketones from biomass

Ketones are important solvents and are produced industrially on a large scale.<sup>[92]</sup> Of the most important alkyl methyl ketone, acetone, more than 6 million tons are produced annually as a coproduct of the phenol production by cumene oxidation.<sup>[83,93]</sup> The high demand for phenol has directly increased the production scale of acetone. 2-butanone, also known as methyl ethyl ketone, is the second most important alkyl methyl ketone and is produced industrially by dehydrogenation of 2-butanol in high yields of >90% on Cu or Zn-catalysts at 400-550 °C.<sup>[94]</sup> In 2005, more than 1 million tons of 2-butanone were produced globally. Since there is also a market for ketones with longer alkyl chains, 2-heptanone and 2-octanone are produced industrially by reductive condensation of acetone with butyraldehyde and pentanal, respectively.<sup>[92]</sup> Like most of the chemical industry, the industrial production of ketones is based on fossil resources. The starting materials for the acetone production by cumene oxidation are benzene and propene.<sup>[83]</sup> For 2-butanone, *n*-butene derived from petrochemical C<sub>4</sub>-raffinates is first hydrogenated to 2-butanol.<sup>[94]</sup> However, ketones are also available from biomass and ABE fermentation, yielding acetone, butanol, and ethanol which used to be the main route to acetone more than a century ago. Today, alternative pathways based on renewable biomass are being explored and optimized for high alkyl methyl ketone yields.

The most important pathway is the mentioned ABE fermentation with the bacterium *Clostridium acetobutylicum* which produces acetone, *n*-butanol, and ethanol in a mass ratio of 3:6:1 from various sugars and carboxylic acids.<sup>[95]</sup> The fermentation process was used industrially for the production of acetone and butanol in large-scale until the end of the 1950s when it became no longer economically viable due to the rise of the petrochemical industry.<sup>[22]</sup>

The ABE fermentation mixture was used by the Toste group to obtain larger methyl ketones such as heptan-4-one, nonan-4-one, and undecane-6-one by Pd-catalyzed alkylation of acetone with the other alcohols obtained by fermentation in the presence of a base.<sup>[95]</sup> Renewable production of acetone is very important for obtaining higher bio-methyl ketones as various pathways rely on the alkylation with acetone such as the dehydration of biomass-derived alcohols to terminal olefins and consecutive alkylation with a ketone.<sup>[96][21]</sup> For this, both lignocellulosic and traditional biofuels crops such as corn and sugarcane can be used to produce useful sugars for this process which can then be fermented.<sup>[21]</sup> In the works of Balakrishnan and Sacia<sup>[21,26]</sup>, the pathways to biomass-derived ketones are laid out such as microbial fermentation for the direct biological synthesis of C<sub>9</sub>-, C<sub>11</sub>-, and C<sub>13</sub>-methyl ketones.<sup>[97]</sup> The

---

renewable production of 2-butanone is possible by acid-catalyzed dehydration of 2,3-butanediol which is obtained by fermentation of lignocellulosic and traditional biofuel crops.<sup>[21]</sup> Direct biological production of 2-butanone from glucose is also feasible in genetically engineered *Escherichia coli* (*E. coli*) bacteria. An *E. coli* strain was engineered to synthesize 2-butanone from glucose by extending the 2,3-butanediol synthesis reaction sequence.<sup>[98]</sup> Another pathway to 2-butanone with a yield of 67.5% is oxidative decarboxylation of levulinic acid over cupric oxides at 300 °C.<sup>[99]</sup> Levulinic acid is obtained upstream by acid-catalyzed hydrolysis of HMF which is an important platform molecule. By genetically engineering *E. coli*, Srirangan *et al.* were able to coproduce acetone and 2-butanone with 42% total yield from bio-derived glycerol.<sup>[100]</sup> The bio-oil that is formed during CFP also contains acetone which after separation can be used for further upgrading.<sup>[57,81]</sup> The Dumesic group showed that hydrodeoxygenation of biomass-derived aqueous sugar solutions leads to an organic phase with an 80% decreased oxygen content and a high concentration of ketones, e.g., 2-butanone, 2-pentanone, 2-hexanone, among other mono-functional hydrocarbons.<sup>[29]</sup>

Larger alkyl methyl ketones such as 2-pentanone and 2-hexanone can be synthesized by ring-opening hydrogenolysis of furan derivatives.<sup>[85]</sup> 2-Pentanone is obtained from 2-methylfuran which is the product of the hydrodeoxygenation of xylose-derived furfural.<sup>[21,101]</sup> Similarly, 2-hexanone is obtained in high selectivity (98%) from DMF. By the above mentioned alkylation of the ABE fermentation products acetone, butanol, and ethanol, also 2-heptanone is obtained with 38% yield.<sup>[95]</sup> Hydrogenated long-chain C<sub>8</sub>-C<sub>16</sub> fatty acids extracted from vegetable oils are a source for long-chain alkyl methyl ketones by alkylation with acetone.<sup>[102]</sup>

Gas phase fermentation which uses waste gas feedstocks is a way to produce carbon-negative acetone with great potential.<sup>[24]</sup> Building a value chain on top of this would allow the sustainable production of many derived products. Due to the high importance of acetone as a renewable platform chemical, there is also research to optimize the ABE fermentation, for example by co-culturing with acetate addition and thus increase the acetone concentration in the fermentative supernatant.<sup>[23]</sup> Ketonization of carboxylic acids presents an upgrading reaction which allows to transform compounds commonly available from biomass and waste sources to ketones, e.g., acetic acid to acetone.<sup>[40]</sup> It is performed at high reaction temperatures of 350-500 °C in the presence of metal catalysts. Fufachev *et al.* used a tandem approach based on this to first ketonize butyric acid over TiO<sub>2</sub> and subsequent aromatization by sequential aldol condensation reactions over Ga/ZSM-5 to yield C<sub>10+</sub>-aromatics.<sup>[38]</sup>

Although there is still much potential for optimization in the conversion of biomass to methyl ketones, the routes are promising for the renewable production of methyl ketones. The ketones can then be used as feedstocks for larger molecules and even oligomerized for fuel applications. While this is possible by hydrodeoxygenation at high temperatures over acidic zeolite catalysts, the self-aldol condensation of

---

methyl ketones presents a more energy-efficient and selective route to linear and branched oligomers as well as alkylated aromatics which is described in the following section for acetone.

### 2.2.2. Aldol condensation of acetone to mesitylene

The self-condensation of acetone is a pathway to aromatics that is catalyzed by acid and base catalysts and produces water as the condensation product. This C-C coupling reaction allows the simultaneous formation of longer alkyl chains and deoxygenation which is highly relevant for biomass-derived compounds to reduce their O/C-ratio and decrease functionalization for the chemical value chain. Alkyl aromatics can be formed by acid-catalyzed cyclotrimerization of alkyl methyl ketones. For instance, acetone yields 1,3,5-trimethylbenzene, known as mesitylene, but the same reaction principle also applies to homologues of acetone. Using base catalysts, the non-aromatic cyclization product isophorone is obtained. While the conversion of acetone to mesitylene was already applied using H<sub>2</sub>SO<sub>4</sub> as catalyst more than 100 years ago, catalytic conversion of biomass-derived alkyl methyl ketones to alkylated aromatics was proposed by the Dumesic group in the context of biomass utilization for chemical production in more recent times.<sup>[103-106]</sup> Research on the self-condensation of biomass-derived alkyl methyl ketones usually focuses on the formation of hydrocarbons suitable for fuel or lubricant production, but aromatization of these alkyl methyl ketones has been less explored.<sup>[21]</sup> Since acetone represents the simplest alkyl methyl ketone, it is a suitable model compound, albeit with higher reactivity due to lower steric hindrance. The following is a detailed review of the acid-catalyzed self-condensation of acetone to mesitylene.

#### Reaction network

The reaction network formed by the self-condensation of acetone is complex due to the sustained reactivity of the formed carbonyl products. This promotes consecutive aldol condensations based on the acidity of the  $\alpha$ -H atom and ensuing keto-enol tautomerism.<sup>[107]</sup> Acids or bases activate the ketones, and through nucleophilic attack of the carbonyl group of another acetone molecule, the adduct diacetone alcohol is formed.<sup>[108]</sup> Diacetone alcohol rapidly dehydrates to the dimer mesityl oxide and thus can often not be isolated under reaction conditions. Two isomers of the  $\alpha,\beta$ -unsaturated ketone can be formed: mesityl oxide and isomesityl oxide.<sup>[109]</sup> Under typical reaction conditions mesityl oxide is the main product. It can react with another acetone molecule which leads to the trimeric phorones of which several isomers are possible.<sup>[110]</sup> Further oligomerization by consecutive aldol condensations of phorones with acetone to tetra-, penta- and oligomers can occur. Besides oligomerization, the C<sub>9</sub>-phorones can cyclize intramolecularly by 1,6-aldol condensation or 1,6-Michael addition to mesitylene and isophorone, respectively.<sup>[108]</sup> In the presence of acids, the condensation of phorones to the desired

aromatic trimer mesitylene by dehydration is favored.<sup>[84]</sup> Contrary, base catalysts, such as KOH, favor the formation of the non-aromatic oxygenated cyclotrimer isophorone. Faba *et al.* found that  $\alpha$ -isophorone can dehydrate to mesitylene in the presence of acids while this does not apply for the typically formed  $\beta$ -isophorone.<sup>[79]</sup>

The reaction network of the acetone self-condensation is displayed in **Figure 6**. Due to the large number of reactive products, a complex reaction network is formed as oligomerization and intra- and cross-molecular aldol condensations occur in parallel, rendering the selective formation of mesitylene or aromatics from alkyl methyl ketones a challenging task. Aldol condensations are equilibrium reactions and therefore the reaction steps prior to the cyclization are reversible. In the presence of strong acid sites,  $\beta$ -scission reactions are possible which cleave C-C bonds and lead to condensate cracking and formation of olefinic and carboxylic acid products.<sup>[20]</sup> This represents a decomposition pathway that is usually tried to be avoided. The  $\beta$ -scission of mesityl oxide yields acetic acid and isobutene.<sup>[111]</sup> It is typically seen on stronger acid sites as a sign of catalyst deactivation due to coke formation and blocking of the acid sites. In the case of homologous alkyl methyl ketones, the reaction network becomes even more complex as the formation of many positional isomers is possible.

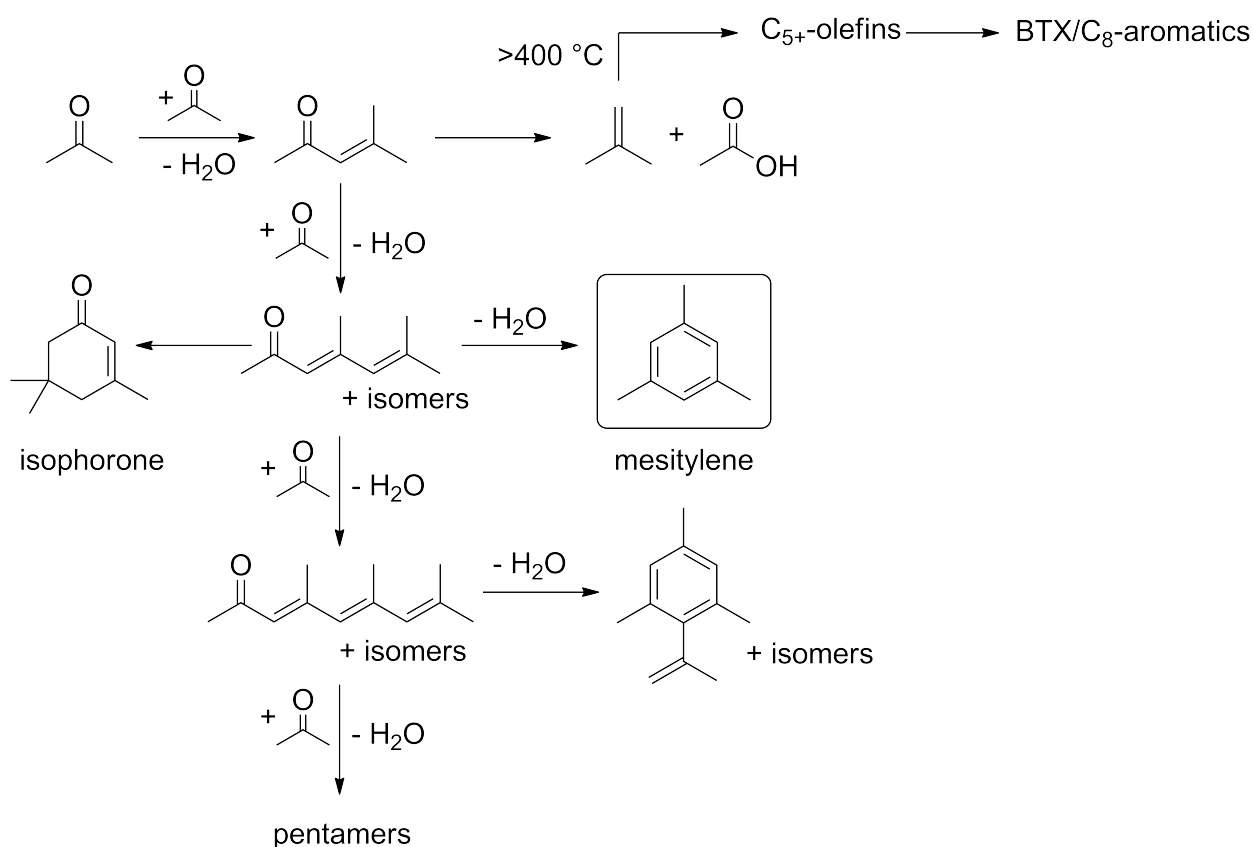


Figure 6: Reaction network of the acetone self-condensation.

---

At high reaction temperatures  $>400\text{ }^{\circ}\text{C}$ , dehydration by aldol condensation is no longer the preferred catalytic pathway but decarbonylation to CO and decarboxylation to  $\text{CO}_2$  with high acetone conversion become predominant.<sup>[81]</sup> Under these conditions, the main products are isobutene and other olefins that are intermediates to aromatics via olefin-to-aromatics pathways. While  $\text{C}_9$ -aromatics such as mesitylene are initially formed, BTX-aromatics and  $\text{C}_8$ -aromatic xylenes are preferentially formed at high temperatures and gas phase conditions. Despite high aromatics selectivity under these conditions, rapid catalyst deactivation prevents long-term catalyst stability.

### Reaction conditions and catalysts for mesitylene formation

Acids are the preferred catalysts for the aromatization of acetone by self-aldol condensation. A wide variety of different catalysts and reaction conditions have been studied since Robert Kane first described the conversion of acetone to mesitylene with concentrated sulfuric acid in 1838.<sup>[104]</sup> By acetone condensation with liquid mineral acids such as sulfuric acid and HCl significant yields of mesitylene (10-36%) were achieved in combination with distillation over extended reaction times of 24 h.<sup>[105,106,112]</sup> The use of strong acid catalysts significantly promotes dehydration and aromatization, thus conventional Brønsted acid catalysts were most commonly used for mesitylene formation during the early developments.<sup>[84]</sup> But homogeneous acid catalysts have considerable downsides in terms of corrosiveness, catalyst separation, and gypsum-formation during downstream neutralization.<sup>[113]</sup> Mitchell and Reid therefore studied the acetone conversion over solid silica gel at  $500\text{ }^{\circ}\text{C}$  in a gas-phase reaction and obtained 17% mesitylene yield.<sup>[114]</sup> These high temperature ( $300\text{-}500\text{ }^{\circ}\text{C}$ ) gas-phase conditions represent the best studied reaction conditions for acetone condensation for which various solid acids have been tested such as zeolites (H-ZSM-5<sup>[115]</sup>, H-Y<sup>[27]</sup>, H-BEA<sup>[20]</sup>), Fe-MCM-41<sup>[116]</sup>,  $\text{MgAl}_2\text{O}_4$ <sup>[108]</sup>, Cs-doped  $\text{TiO}_2$ <sup>[117]</sup>, Mg-Zr<sup>[110]</sup> or  $\text{CaC}_2$ <sup>[118]</sup>. Among these, the highest mesitylene yield of 28% was found for Cs-doped  $\text{TiO}_2$  at  $300\text{ }^{\circ}\text{C}$ .<sup>[117]</sup> While aromatics selectivity is increased under these conditions, catalyst deactivation by rapid coking is also promoted, restricting the development of a continuous catalytic process.<sup>[119-121]</sup>

Other solid acid catalysts and reaction conditions were studied as well: Paulis *et al.* prepared highly acidic  $\text{Nb}_2\text{O}_5$  and obtained a mesitylene selectivity of 49% under differential conversion conditions at  $250\text{ }^{\circ}\text{C}$  and 6 bar.<sup>[122]</sup> According to Salvapati *et al.* high pressure in combination with high temperature and an excess of acid benefit the aromatization.<sup>[84]</sup> Under these conditions, Benson *et al.* reported 27.8% mesitylene yield for the catalytic deoxygenation of acetone at 71 bar and  $500\text{ }^{\circ}\text{C}$  using 100% anatase  $\text{TiO}_2$  to test the influence of Lewis acidity.<sup>[123]</sup> Interestingly, Ivakhnov *et al.* observed a very high mesitylene yield of 60.1% under extreme supercritical conditions of  $500\text{ }^{\circ}\text{C}$  and 600 bar in absence of any catalyst.<sup>[124]</sup> A high mesitylene yield of 25.7% was also reported for a dual catalyst bed consisting of a first layer of  $\text{TiO}_2$  and a consecutive layer of Al-MCM at  $250\text{ }^{\circ}\text{C}$  and 2.5 bar at a WHSV of  $4\text{ h}^{-1}$ .<sup>[79]</sup> The



---

rationale behind the stacking of catalysts was that TiO<sub>2</sub> selectively catalyzes the dimerization of acetone, while Al-MCM effectively promotes the aromatization. This strategy was chosen to prevent rapid catalyst deactivation through polycondensation on acid sites. The to date highest mesitylene yield of 79.9% was reported by Wu *et al.* over a tantalum phosphate catalyst at 200 °C and atmospheric pressure (WHSV=1.45 h<sup>-1</sup>).<sup>[80]</sup> Through intermittent oxygen treatment, the spent catalyst could be recycled 10 times.

An inherent problem of studying the acetone self-condensation is the rapid deactivation of acid catalysts due to oligomerization and coking by strongly-adsorbed species.<sup>[125]</sup> While the activity of silica-alumina catalysts can usually be regenerated by simple calcination, the development of technical processes requiring long-term catalyst stability is hampered. Larger pore catalysts such as zeolite H-Y or mesoporous MCM-41 have been found beneficial for extending catalyst stability.<sup>[126]</sup> Alternatively, addition of hydrogen and metal-doping of catalysts, often employed in dual bed configuration with acid catalysts, allows high aromatics yields and longer catalyst life.<sup>[127,128]</sup> Accordingly, Herrmann and Iglesia used Pt functions and excess hydrogen to prevent catalyst deactivation and assess the elementary steps in acetone dimerization on aluminosilicates.<sup>[109]</sup>

The selective formation of mesitylene is shown to benefit from strong acid sites but also high mass transport via large catalyst pores. While reaction temperatures above 300 °C increase mesitylene selectivity, catalyst stability is a concern due to rapid deactivation. The use of special catalysts such as tantalum phosphate is one option, another is to look more closely at the deactivation and use lower reaction temperatures while maintaining high acetone selectivity.

### **Reaction mechanism and active sites for condensation and aromatization**

Studying the reaction steps of the aldol condensation of acetone is challenging as they proceed rapidly, simultaneously, and are mostly reversible equilibrium steps before the cyclization leading to isophorone or mesitylene.<sup>[108]</sup> So is the formation of diacetone alcohol equilibrium-controlled.<sup>[84]</sup> The prevalent coke formation under reaction conditions makes accurate kinetic measurements under steady-state conditions difficult as the catalyst quickly deactivates.<sup>[27,129]</sup> To date, there is no final verdict in literature whether the aromatization of acetone is catalyzed by BAS or LAS.

To tackle the catalyst deactivation under reaction conditions and study the condensation over zeolite catalysts, Herrmann and Iglesia incorporated Pt-functions and elucidated the acetone dimerization under hydrogen-controlled reaction conditions which prevented coking.<sup>[109]</sup> The BAS present on the zeolite catalysts otherwise led to rapid deactivation. In their study, the condensation reaction was found to occur exclusively on BAS without contribution of LAS. The C-C bond formation proceeds over an H-bonded acetone with another acetone molecule and thus is the kinetically-relevant step. It is mediated by a bimolecular transition state consisting of a C<sub>3</sub>-alkenol and a protonated acetone molecule. The



---

condensation rate is proportional to the acetone pressure and number of accessible protons.<sup>[20]</sup> Based on their findings, an elementary step mechanism for the acetone condensation was proposed which describes the pathway to C<sub>6</sub>-products on zeolitic BAS.<sup>[109]</sup> The consecutive reaction steps for the formation of mesitylene were not included in the mechanism. It was stated that mesitylene binds strongly on BAS and leads to rapid deactivation of the active sites under reaction conditions.<sup>[109]</sup>

Using different metal-substituted MCM-materials, e.g., Fe-MCM-41, Kosslick *et al.* found that aromatization benefits from lower Brønsted acidity whereas higher Brønsted acidity leads to increased isobutene formation.<sup>[116]</sup> The decomposition product isobutene is formed by cleavage of C-C bonds on BAS. Two different pathways lead to its formation on zeolites depending on the involvement of water.<sup>[20]</sup> At high reaction temperatures >300 °C, mesityl oxide can coordinate to Lewis acid-base pairs and subsequently undergo conversion to surface acetate species and gas-phase isobutene by nucleophilic attack of surrounding OH-groups.<sup>[130]</sup>

The mechanism of the aldol condensation of acetone depends on the catalyst nature and the density of active sites. The elementary steps follow the same pattern on acid and base catalysts: 1) adsorption of reactants, 2) enolization of the carbonyl compound, 3) C-C coupling reaction and bond formation, 4) dehydration of the adduct, 5) desorption of  $\alpha,\beta$ -unsaturated oxygenates.<sup>[131]</sup> But on base catalysts, e.g., MgO, enolization is the rate-limiting step and the reaction kinetics can be modeled by a unimolecular Langmuir-Hinshelwood mechanism. In contrast, on acid catalysts the C-C coupling step is rate-limiting, resulting in a bimolecular reaction mechanism. By varying the acid site density on MCM-41-SO<sub>3</sub>H catalysts, it was possible to further differentiate and elucidate the reaction mechanism for acid catalysts. For high density acid catalysts, site cooperation is possible which leads to a Langmuir-Hinshelwood-type mechanism. For low acid site densities, no adsorbed electrophile is in the vicinity of the activated enol to be attacked which fits to an Eley-Rideal mechanism. In this case, the reaction rate per site is much lower and increases with ketone concentration for low density acid catalysts.

The acetone condensation is also catalyzed by TiO<sub>2</sub> which possess Lewis acid-base site pairs. These alter the surface environment and thus require an adapted reaction mechanism. This was studied by Lin *et al.* through vapor-phase condensation of acetone over single-facet TiO<sub>2</sub>.<sup>[129]</sup> On TiO<sub>2</sub>, acetone binds on the Lewis acidic Ti-sites of the catalyst and forms an enolate intermediate. On metal oxides, e.g., TiO<sub>2</sub> or MgO, both Lewis acid and Brønsted base sites are required as the reaction proceeds via two adjacent reaction intermediates. The acetone condensation then precedes via intermolecular C-C coupling between the formed enolate and acetone hydrogen-bonded to the vicinal surface OH-group. In their work, they found that the C-C coupling reaction step was likely to be kinetically relevant. Since the participation of two acetone molecules adsorbed on vicinal active sites is required, the reaction likely proceeds via a Langmuir-Hinshelwood reaction mechanism on TiO<sub>2</sub>. The proposed elementary step reaction mechanism for the aldol condensation on TiO<sub>2</sub> is started with the equilibrium adsorption of two

---

acetone molecules on Ti- and vicinal O-sites. The enolate is formed through abstraction of the  $\alpha$ -H-atom by the basic O-site. The nucleophilic attack of the enolate C=C-bond on the carbonyl carbon of the adjacent acetone leads to the C-C-bond formation and finally the aldol product.

In their study of microkinetic reaction models, Dellon *et al.* identified that the activated cation dimer condensation product is the key branching point in the catalytic self-condensation mechanism of acetone.<sup>[111]</sup> Under reaction conditions where  $\beta$ -scission occurs, isobutene and acylium ions are formed which lead to xylene formation. In the case where deprotonation prevails, the physisorbed dimer intermediate mesityl and isomesityl oxide are formed and present required intermediates for the consecutive mesitylene formation pathway via trimeric phorones.<sup>[110]</sup> As a result, the various competing and subsequent pathways in the catalytic self-condensation of acetone lead to a complex product mixture.

The acid-catalyzed aromatization of acetone to mesitylene is a highly interesting route as it allows the production of fully bio-based aromatics. The established ABE fermentation yields acetone but also provides access to higher alkyl methyl ketones and is subject to continued optimization through research activities. Meanwhile, an easily accessible and low-cost acetone stream already exists with the large-scale production of acetone as a by-product of phenol production. Understanding and optimizing the mesitylene formation from acetone in a continuous catalyzed process is the key intermediate step in substituting the various fossil-based (alkyl) aromatics at the foundation of the chemical industry since trans- and dealkylation processes were established and operated commercially.

---

### 3. Fixed-bed reactor setup

---

The experimental details are described in the specific sections of the published articles. An overview of the fixed-bed reactor setup specifically designed and constructed to study the aromatization of methyl ketones is provided below for future reference.

#### 3.1. Overview and implementation of the reactor setup

Based on preliminary results, a flow reactor setup was designed for reaction conditions of up to 400 °C and 160 bar under liquid phase or supercritical conditions. Reactions are catalyzed over a heated fixed-bed of catalyst particles inside the reactor. The resulting product stream is continuously monitored by a downstream online-GC with automatic liquid product sampling.

The reaction setup consists of several sections and components which are illustrated by following the path from the ketone starting material to the aromatic product: The liquid alkyl methyl ketone is fed with the HPLC pump P100 (Knauer 40P with pump head cooling) via a heated line from the storage tank TK100 into the bottom end of the reactor (**Figure 7**). The reactor itself is constructed of a 3/4"-stainless steel tube (1.4404, inner diameter: 1.58 cm) with VCR fittings for simple mounting and dismounting. A 4 mm stainless-steel thermocouple jacket equipped with 6 type-J Fe-CuNi-thermocouples (TIR1-6) is fitted along the axis of the reactor. The position of the catalyst bed is fixed in the middle zone of the reactor between TIR3 and TIR4 with glass wool, stainless steel balls (1.0 mm diameter) and stainless-steel inserts above and below.

The inserts reduce the dead volume of the reactor and keep the catalyst bed in place as the weight of the upper insert prevents fluidization of particles in the catalyst bed. The reactor is heated over a length of 21 cm with a two-zone vertical electric furnace (HORST, 160 W each). The temperatures of the zones are controlled based on the readings at TIR 3 and TIR 4. In a standard experiment, both are set to the same temperature to ensure an isothermal catalyst bed during the reaction.

The product solution exiting from the top of the reactor is first filtered (0.5 micron) and then cooled to 15 °C in the double pipe heat exchanger E100, connected to a thermostat (Huber Ministat 240). To improve the accuracy of GC measurements, a GC standard can be added from TK200 via a second HPLC pump P200 (Knauer 40P with pump head cooling). The two streams are united in a tee fitting in the pressurized section of the reaction setup. The reactor pressure is controlled by a dome-loaded back pressure regulator (Equilibar U3L) in combination with a digital process pressure controller (Bronkhorst El-Press P-822CV), connected to a 300 bar Argon line. The product mixture with the internal standard is analyzed by online-gas chromatography (Shimadzu GC-2030, FID, MEGA-5, H<sub>2</sub>) by sampling from the product stream with an automated injector for liquids. The accumulated product solution is stored in the tank TK300. By continuously monitoring the weight of TK100 and TK300, the mass balance under

the studied reaction conditions is evaluated. A photo of the final reactor setup is depicted in **Figure 8**. The complete setup is controlled via a proprietary software developed by Martin Lucas. The GC is controlled with Shimadzu's LabSolution software package which is also used for analysis of the measured data.

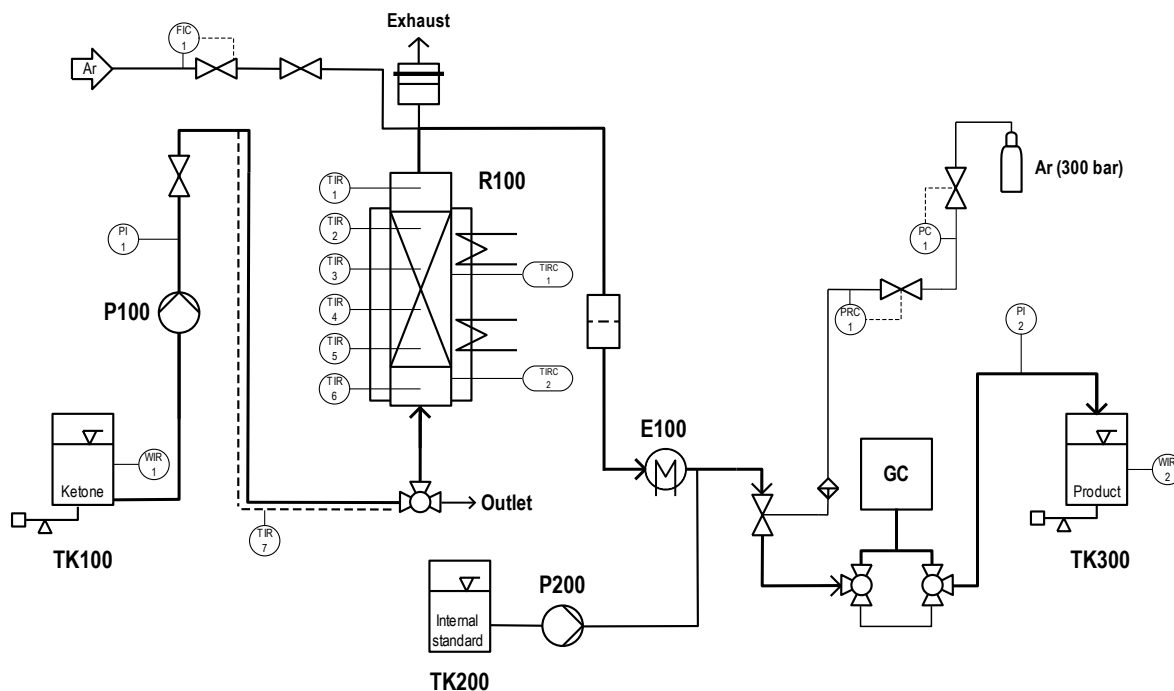


Figure 7: Process flow diagram of the fixed-bed reactor.



Figure 8: Front view of the laboratory fixed-bed reactor setup.

---

### 3.2. Safety features for continuous operation

The reactor setup was built for studying the alkyl ketone aromatization over extended periods of time. Therefore, built-in safety features are mandatory to ensure safe operation of the reaction setup and to prevent potentially hazardous conditions. Furthermore, through rigorous prior assessment of the experimental risk level and implementation of the precautions, it is possible to operate the reactor without constant supervision. Safety considerations were therefore an integral part of the design phase. The first point to consider is the environment of the reaction setup: a high level of safety is achieved by placing the entire setup in a closed fume hood with constant ventilation and exchange of atmosphere. This ensures that any potential leaks are kept in a closed environment. Leaking gases or vapors are immediately removed by ventilation and cannot accumulate in the fume hood. Ventilation is controlled and monitored by university site management. In the event of a ventilation problem, a loud warning sound is played over a siren which signals all operator activity in the fume hood to be stopped. For a safe shutdown of the reactor setup, the temperature controllers are located outside the fume hood and are accessible without endangering the operator. By turning off the controllers, power supply to the electric furnace is cut and heating of the reactor is stopped. This precaution applies to all electrical equipment. Stainless-steel 1.4404 and PTFE tubing is used where appropriate to provide maximum chemical compatibility with the reaction solution and high corrosion resistance to support continuous operation of the setup.

In addition to these more general precautions, reactor and reaction specific features were implemented: A safety relief is required to perform reactions under pressure to prevent a possible bursting of the equipment under critical conditions where the pressure exceeds the mechanical limits of the reaction vessel. In this reaction setup, a rupture disc (Sitec, 160 bar) is implemented at the top of the reactor directly below the fume hood exhaust. In the event of a rapid pressure build-up above 160 bar, the disc ruptures, and the pressure is released by venting the reactor contents into the exhaust. To prevent this scenario, the reactor pressure up- and downstream of the catalyst bed is constantly monitored to detect any pressure build-up, e.g., by blocking of the reactor. If the pressure difference exceeds 10 bar, the electronically controlled back-pressure valve automatically opens to relieve the pressure build-up. This also causes the reactor heating to shut down and the pumps to stop. Increasing the tubing size downstream of the reactor from 1/8" to 1/4" ensures that in the event of high gas formation, all material can be transported through the larger cross-section and no blockage will occur. In this downstream section, a 0.5 micron in-line filter removes any mobilized catalyst particles from the product stream that could otherwise damage the backpressure valve or injector. The pipe-in-pipe heat exchanger is angled downward to prevent blocking by agglomerations that may form in the cooling section.

During the experiments, liquid handling is required. Therefore, it is important to avoid overflow of the product storage tank and a sufficiently filled ketone storage tank during the course of the experiment.

---

To minimize the release of organic substances from the storage tanks into the fume hood, the storage tanks are placed inside stainless-steel trays. As a further precaution, both pumps are shut down when a fill level of 85% is reached. This is calculated from the monitored weight of the product storage tank. Continuous monitoring, refilling, and emptying of the storage tanks is required during the experiments. The GC injector is sealed from the online injector by two special gaskets made of PTFE/maroon that wear with repeated injections. They must be replaced regularly to prevent damage to the GC from leaking product solution. Additionally, the drift of the GC baseline was monitored at 150 °C for 10 min after every 5<sup>th</sup> run to check for leakage from the online injector. Increases in the baseline drift are a sign of increased leakage and warrant a timely gasket replacement.

With the safety features and precautions described, it was possible to successfully perform aromatization experiments that lasted 10 days. During this period, the ketone and product storage tanks were refilled and emptied daily, and temperature, pressure and volumetric flow rates were checked frequently.

---

## 4. Results and discussion

---

The following section provides summaries of the published articles and how they are connected. The journal articles and their supporting information are attached to the individual chapters.

### 4.1. Biomass-Derived Aromatics by Solid Acid-Catalyzed Aldol Condensation of Alkyl Methyl Ketones

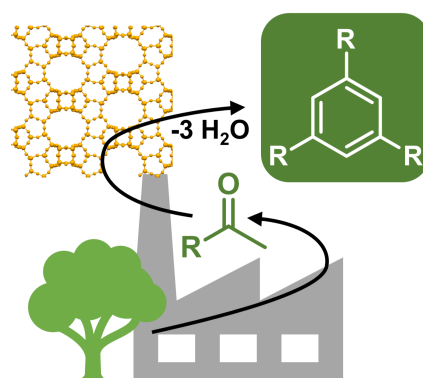
Authors: P. Reif, H. Rosenthal, M. Rose

Journal: *Advanced Sustainable Systems*

Date: 24 June 2020

DOI: <https://doi.org/10.1002/adsu.201900150>

© 2020 The Authors. Published by WILEY-VCH Verlag GmbH & Co. KGaA, Weinheim. This is an open access article under the CC BY-NC-ND 4.0 license.



The research presented here for biomass-derived aromatics is driven by developing a more sustainable alternative pathway utilizing ketones as platform chemicals from biorefinery streams and targeting industrial relevance. The first research paper published in *Advanced Sustainable Systems* focused on identifying suitable, commercially available catalysts for the aromatization of the model compound acetone to the aromatic trimer mesitylene under milder, liquid phase batch conditions.<sup>[132]</sup> A wide range of different solid acid catalysts was screened as they promote the self-condensation to mesitylene, can be easily separated in a continuous technical process, and do not lead to salt formation. In total, more than 16 different catalysts were tested including various types of zeolites, cation exchange resins, amorphous silica-alumina, and others. The sulfonic ion exchange resin Purolite CT275DR was identified as the most active and promising candidate based on its 9% mesitylene yield at 130 °C due to its highest number of acid sites. The beta-zeolite H-BEA 35 and the amorphous silica-alumina Siralox 70/170 HPV were also found suitable. H-ZSM-5 did not show any activity. The number of acid sites and pore size geometry of zeolites were identified as crucial factors regarding activity. For the three selected catalysts, the influence of reaction temperature (130-190 °C), time (3-15 h) and pressure (40-145 bar) was evaluated comparatively. In general, the aromatization activity increased with reaction temperature which was especially significant for the ASA Siralox 70/170 HPV at 190 °C. The reaction progress was studied with the most active catalyst Purolite CT275DR by sampling from the reaction mixture. Under batch conditions, a strong initial increase in conversion was found followed by a phase of declined

---

activity. Water formed as a by-product in the self-aldol condensation of acetone has been shown to be a potential inhibitor under reaction conditions, as it can interact with the surface ions of the resin. This could cause the observed decline in activity. In summary, the feasibility of the route towards aromatic products by deoxygenation of biomass-derived ketones with technical solid acid catalyst under liquid phase reaction conditions was successfully demonstrated.





# Biomass-Derived Aromatics by Solid Acid-Catalyzed Aldol Condensation of Alkyl Methyl Ketones

Phillip Reif, Hannah Rosenthal, and Marcus Rose\*

Cyclotrimerization of biomass-based alkyl methyl ketones exhibits great potential as a route to biomass-derived aromatics by a sustainable valorization of biorefinery streams. In this study, acetone is used as a model reagent to screen solid acid catalysts for the aldol condensation reaction to the aromatic trimer mesitylene. From a broad catalyst screening promising activity is shown by the cation exchange resin PuroLite CT275DR, the beta-zeolite H-BEA 35, and aluminosilicate Siralox 70/170 HPV which are used to further investigate reaction parameters. Acetone conversion and mesitylene yield increase with temperature and time, while yield of the intermediate mesityl oxide decreases. This effect is also found for higher quantities of catalyst acid sites and is accompanied with an increased side product formation which negatively affects total product selectivity. Analyzing the reaction progress shows a significant drop in catalyst productivity after an initial start-up phase. This observation is linked to a deactivation of the catalyst which involves water that is formed during the condensation reaction of acetone. Obtained results confirm the general viability of the aromatization of alkyl methyl ketones and can be considered the first step to an alternative sustainable route to biomass-derived aromatics compared to other currently discussed routes.

## 1. Introduction

With a global annual production of 103 Mio. t (2012) for benzene, xylene, and toluene (BTX), aromatics are an important intermediate in chemical industry used for a wide array of products.<sup>[1]</sup> Obtained via catalytic reforming of naphtha, they are precursors for monomers used in the polymer industry, e.g., *p*-xylene for polyethylene terephthalate and styrene for polystyrene, and other commodity products such as solvents, plasticizers, and adhesives.<sup>[2]</sup> In the context of climate change and limitation of fossil resources, their wide application in consumer products drives a growing demand for their sustainable

P. Reif, H. Rosenthal, Prof. M. Rose  
Ernst-Berl-Institute of Technical and Macromolecular Chemistry  
Department of Chemistry  
Technical University of Darmstadt  
Alarich-Weiss-Straße 8, Darmstadt 64287, Germany  
E-mail: rose@tc2.tu-darmstadt.de

The ORCID identification number(s) for the author(s) of this article can be found under <https://doi.org/10.1002/adsu.201900150>.

© 2020 The Authors. Published by WILEY-VCH Verlag GmbH & Co. KGaA, Weinheim. This is an open access article under the terms of the Creative Commons Attribution-NonCommercial-NoDerivs License, which permits use and distribution in any medium, provided the original work is properly cited, the use is non-commercial and no modifications or adaptations are made.

DOI: 10.1002/adsu.201900150

production. To meet this demand, strong research efforts have been made to obtain aromatics from renewable biomass over the past years. Among these catalytic fast pyrolysis, the utilization of the abundant but structurally complex lignin-fraction of wood by depolymerization and the selective Diels–Alder cycloaddition of biomass-derived furan derivatives with alkenes to specific aromatic compounds present the most fundamental routes.<sup>[3]</sup> Thermochemical or chemocatalytic processing of lignin via (catalytic) fast pyrolysis gives a bio-oil containing a heterogeneous mixture of over 300 compounds.<sup>[4]</sup> In addition to separating the aromatic compounds from the bio-oil, it is necessary to deoxygenate them via hydrotreating, associated with enormous challenges, to insert them in downstream processes developed for aromatics.<sup>[5]</sup> Due to the heterogeneous structure of lignin which strongly depends on its biomass source, a selective depolymerization to specific aromatics which

substitute petroleum-sourced ones can only be expected in the long run.<sup>[6]</sup> High separation costs and overall low yields decrease the route's economic viability to date.<sup>[3]</sup> By catalytic treatment of pyrolysis vapors with acidic zeolites such as ZSM-5 at temperatures above 400 °C broad fractions of monoaromatic compounds can be obtained.<sup>[7]</sup> Selective formation of specific aromatics is achieved via Diels–Alder cycloadditions with subsequent aromatization through dehydrogenation or dehydration.<sup>[2]</sup> As biomass-based dienes, furan derivatives produced from 5-hydroxymethylfurfural (HMF), e.g., 2,5-dimethylfuran (DMF), are suitable. They are reacted with biomass-based dienophiles, e.g., acrolein, ethylene, or propylene, to Diels–Alder adducts. For the formation of *p*-xylene from DMF and ethylene, yields of over 90% have been reported.<sup>[8]</sup> However, the mass production of the precursor HMF, often envisioned as a biomass-derived platform chemical,<sup>[9]</sup> has not been established yet due to its challenging high reactivity. An economically viable route to aromatics via Diels–Alder cycloaddition therefore also depends on mass-scale availability of HMF and other furanic derivatives.

In order to overcome the limitations posed on existing routes to biomass-derived aromatics, facile accessibility to suitable feedstock and integration into an infrastructure for value added chains are advantageous. Such a platform for biomass-derived intermediates was devised by the Dumesic group who converted aqueous solutions of sugars to monofunctional hydrocarbons such as ketones and alcohols and thus reduced the primary oxygen content by 80%.<sup>[10]</sup> As a valorization step for ketones

produced by this process, acid-catalyzed aldol condensation with subsequent hydrogenation to alkanes was proposed. It was also mentioned that in the absence of hydrogen, selectivity is shifted to the more stable aromatics which are formed by self-condensation of three ketone molecules under water formation. Based on this principle, the Bell group showed the formation of cyclic, acyclic and aromatic trimers from *n*-alkyl methyl ketones via base-catalyzed aldol condensation in the context of bio-based aviation fuels.<sup>[11]</sup> Moreover, accessibility of C<sub>3</sub>–C<sub>7</sub> methyl ketones from biomass via hybrid biological/chemical and purely chemical pathways was outlined, e.g., acetone from the 100-year old acetone-butanol-ethanol fermentation process in which butanol and ethanol are produced as byproducts.

In contrast to these approaches on the hydrodeoxygenation of nonaromatic trimers to branched, cyclic alkanes, it is also feasible to increase the aromatics yield and thus, create a route to biomass-based aromatics that has not attracted any attention in the recent past. Besides greater utilization of biorefinery streams, the route benefits from its simplicity of a single reaction step and does neither require hydrogen for deoxygenation nor expensive precious metal catalysts, which immensely contributes to lower costs. Conceived as a sustainable drop-in solution for petroleum-sourced aromatics, the cyclotrimerization of alkyl methyl ketones via acid- or base-catalyzed aldol condensation of alkyl methyl ketones to 1,3,5-substituted C<sub>6</sub>-aromatics is highly promising. The reaction proceeds via Michael addition and 1,6-aldol condensation reactions over dimers to trimer condensates which but the aromatic can further oligomerize, thus spanning a rather complex reaction network (Figure 1).<sup>[11]</sup> Alkylation chemistry to obtain direct replacement of BTX-aromatics is established and well known and can help shifting the product spectrum into the desired direction.

As model reagent for studying the cyclotrimerization reaction to produce aromatics, acetone was chosen as its production in biorefinery processes is already realized and it is the simplest of all available alkyl methyl ketones. Therefore, only one aromatic trimer condensate as main product can be formed: mesitylene (Mes). Hence, our objective was the selective formation of mesitylene despite the many possible side reactions. While acid- and base-catalyzed self-condensation of acetone have been proposed and studied in the past nearly one century ago, little focus was given to optimizing the aromatic yield or applying technically suitable solid catalysts.<sup>[12]</sup> Common understanding

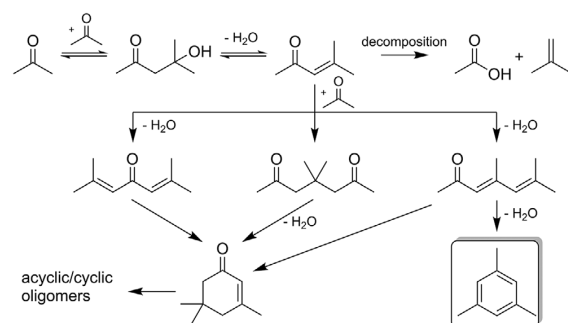


**Figure 1.** Simplified reaction scheme of the consecutive aldol condensation reactions of acetone to the trimeric products mesitylene and isophorone.

is that base catalysts favor mesityl oxide (MesOx) formation and the consecutive reaction toward isophorone while acids promote mesitylene formation.<sup>[13]</sup> Consequently, solid acid catalysts were studied to increase the aromatic yield of the self-condensation of acetone in liquid phase. In this work, suitable solid catalysts for acetone to mesitylene conversion, influence of reaction parameters, and reaction kinetics are presented.

## 2. Results and Discussion

### 2.1. Screening of Solid Acid Catalysts

More than 16 solid acid catalysts were initially screened for the selective aromatization of the model reagent acetone to mesitylene. The screening focused on heterogeneous catalysts due to their intrinsic advantages of simple product removal and susceptibility to wide reaction conditions. Moreover, in prior tests with homogeneous acids, e.g., *p*-toluenesulfonic acid, strongly acidic, phase-separated product mixtures of an organic and an aqueous phase occurred. These limited characterization by gas chromatography (GC) as acids can damage the GC column and reported yields can be altered by processing of the product mixture. Based on literature, three classes of solid acids were chosen for screening: different types of zeolites, amorphous aluminosilicates, and acid cation resins.<sup>[14]</sup> Additionally, Nb<sub>2</sub>O<sub>5</sub> was tested.<sup>[15]</sup> Employed catalysts are commercially available in order to facilitate possible scale-up in a later process development.

To assess the catalyst activity for liquid-phase acetone aromatization, initial reaction conditions were mild at 130 °C and 3 h. For these, acetone conversion  $X_{Ac}$  was in almost all cases

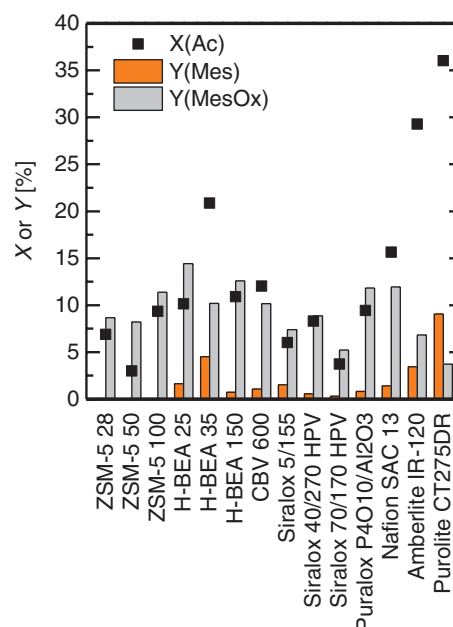


**Figure 2.** Results of  $X_{Ac}$ ,  $Y_{Mes}$ , and  $Y_{MesOx}$  for selected solid acid catalysts screened in the condensation reaction of acetone at 130 °C and 3 h.

<16% (Figure 2) and only significantly higher for the catalysts H-BEA 35 (21%), Amberlite IR-120 (29%), and Purolite CT275DR (36%). Of interest for the selective aromatization is the product distribution, and here specifically the yields for mesitylene  $Y_{Mes}$  and mesityl oxide  $Y_{MesOx}$ . For the ZSM-5 zeolites,  $Y_{Mes}$  below 0.1% were found irrespective of their silica-to-alumina ratio. The consecutive reaction from formed mesityl oxide ( $Y_{MesOx} < 10\%$ ) to mesitylene is thus not catalyzed by ZSM-5 zeolites under reaction conditions. Slightly higher activities were observed for the different aluminosilicates which yielded up to 1.5% mesitylene for Siralox 5/155. The overall best performance based on conversion and mesitylene yield was shown by the sulfonated ion exchange resins. For Purolite CT275DR,  $Y_{Mes}$  not only exceeded  $Y_{MesOx}$  by more than 5% but also the highest  $Y_{Mes}$  of 9% was found. Promising results were also obtained for the second-best performing catalyst H-BEA 35, a beta zeolite in proton form, with an  $Y_{Mes}$  of 4.5%. Interestingly, other beta zeolites with higher or lower silica-to-alumina ratios were significantly less active for the consecutive reaction.

In this assessment of the activity, potentially formed side products, such as isophorone, were not considered. While for the Purolite-catalyzed reaction significant amounts of isophorone (4%) were detected, this is not the case for the aluminosilicate catalysts (0–0.8%) under reaction conditions (see Figure S2, Supporting Information). As catalysts were screened for the aromatization reaction of acetone, the yield of mesitylene was the main criterion.

Differences in conversion and yield of three different catalysts were assessed for their statistical significance in later experiments (see Figure S2, Supporting Information). Repeating identical experiments multiple times gives standard deviations of  $\approx 2\%$  and  $0.2\%$  for conversion and yields, respectively. A comparable statistical error is therefore assumed for the screening experiments.

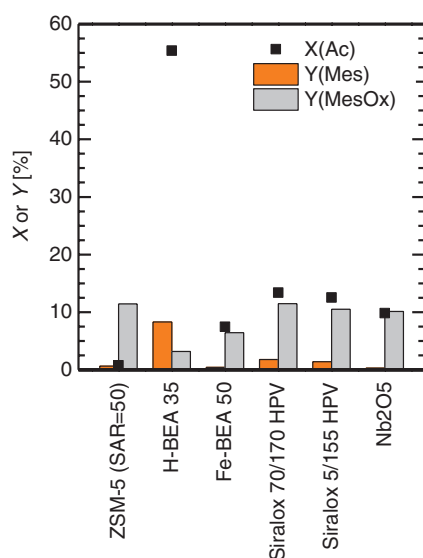


**Figure 3.** Results of  $X_{Ac}$ ,  $Y_{Mes}$ , and  $Y_{MesOx}$  for solid acid catalysts of lesser activity screened in the condensation reaction of acetone at 160 °C and 6 h.

Catalytic activity is strongly influenced by the reaction conditions. Therefore, five catalysts that showed lesser activity at aforementioned reaction conditions were tested at an elevated temperature of 160 °C and prolonged reaction time of 6 h. Results are depicted in Figure 3 and also include  $Nb_2O_5$  and Fe-BEA 50 which both showed a negligible activity under previous conditions so that they were not listed earlier.

Despite the harsher conditions, catalytic activity for the acetone aromatization did not increase for most catalysts and mesitylene yields were generally lower than 0.6%. One notable exception is the significant increase in  $Y_{Mes}$  from 0.3 to 1.8% for the aluminosilicate Siralox 70/170 HPV which was also highly selective as over 99% of acetone was converted to either mesitylene or mesityl oxide. The substantial influence of reaction conditions is marked by the significant increase in activity of H-BEA 35 for which  $Y_{Mes}$  exceeded  $Y_{MesOx}$  and over 55% acetone was converted. Latter is a sign of decreased selectivity and increased side product formation as the desired product yields did not increase similarly. It must be mentioned in the discussion of the screening experiments that in some cases  $X_{Ac}$  was lower than the actual products yield. This is likely caused by errors in measurement of the highly volatile compounds acetone and cyclohexane, the internal standard, due to losses by either adsorption on the catalyst surface or vaporization. Assessment of the reactor blank activity shows that even at an elevated temperature of 220 °C less than 1% of acetone is converted and no significant amounts of products are detected (see Figure S3, Supporting Information). However, it is also demonstrated that the measurement of very low conversions is error-prone and subject to a significant statistical error.

Noticeable are the differences in the activity of the various zeolites for the condensation reaction to mesitylene. This could be a result of their different pore sizes as first data on the acid site densities from temperature-programmed  $NH_3$ -desorption ( $NH_3$ -TPD) measurements shows only little difference (see Figure S4, Supporting Information).

More analysis and characterization are required for optimizing the catalytic activity due to the complex cyclotrimerization reaction of three acetone molecules inside a zeolite pore and the various effects present in zeolite catalysis, such as acid strength and density and pore and channel size.

Overall, the catalysts H-BEA 35, Siralox 70/170 HPV, Amberlite IR-120, and Purolite CT275DR were the most promising candidates for the acid-catalyzed aldol condensation to mesitylene based on the screening results. Due to the chemical similarity of the two strongly acidic, sulfonated cation exchange resins, the subsequent screening of the reaction conditions time and temperature focused on the more active Purolite catalyst as well as the two aluminosilicates. An explanation for the higher activity of Purolite could be its higher weight capacity of  $5.2 \text{ eq kg}^{-1}$ <sup>[16]</sup> compared to  $2.2 \text{ eq kg}^{-1}$  calculated for Amberlite<sup>[17]</sup> which results in a higher concentration of catalytically active sites on the Purolite surface.

## 2.2. Influence of Reaction Parameters

The three selected catalysts were subject to a variation in reaction temperature (130, 160, and 190 °C) and reaction time

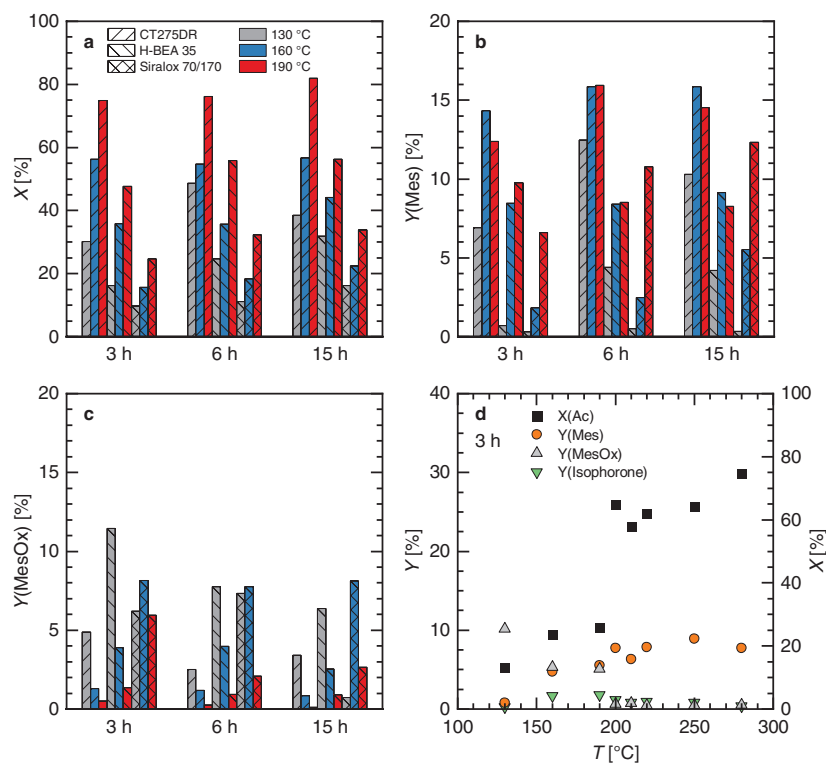


**Figure 4.** Results for the three selected catalysts Pulolite CT275DR, H-BEA 35, and Siralox 70/170 HPV in the reaction parameter screening for a) acetone conversion, b) mesitylene yield, and c) mesityl oxide yield at different reaction times, respectively. d) Results of the temperature variation for H-BEA 35 at 3 h.

(3, 6, and 15 h). For all catalysts conversion of acetone increased continuously with reaction temperature while  $Y_{\text{MesOx}}$  declined as it reacts to consecutive products (Figure 4a). Differences in activities of the catalysts become apparent by taking into account the maximum acetone conversion as more than 82% of acetone are converted with Pulolite CT275DR at 190 °C after 15 h, considerably more than for H-BEA 35 (56%) and Siralox 70/170 HPV (34%). This could be attributed to the higher quantity of acid sites per catalyst mass for Pulolite CT275DR. Since equal amounts of catalysts were employed, a higher site density increases the total number of acid sites present in the reaction system. For a just comparison of activities, catalysts are required to be dried preceding and added according to their amount of acid sites. However, the type and strength of acidity need to be addressed as well in further characterization.

A continuous increase in  $Y_{\text{Mes}}$  with temperature is only observed for Siralox 70/170 HPV, particularly from 160 to 190 °C which implies that it requires a high temperature due to a higher activation barrier to become active for catalyzing the aromatization reaction. In case of H-BEA 35 and Pulolite CT275DR,  $Y_{\text{Mes}}$  does not further increase but remains constant from 160 to 190 °C. Maximum yields for mesitylene (H-BEA 35: 10%, Siralox 70/170 HPV: 12.5%, Pulolite: 16%) and mesityl oxide (H-BEA 35: 12.3%, Siralox 70/170 HPV: 8%, Pulolite: 5%) are in a comparable range (Figure 4b,c). The

decrease of  $Y_{\text{MesOx}}$  with reaction temperature can be explained with mesityl oxide being a reaction intermediate of which less is yielded when consecutive trimerization reactions are promoted. On the other hand, the observed rise in  $X_{\text{Ac}}$  for higher reaction temperatures is caused by an increasing formation of side products which compete with the formation of mesitylene. As side products water, isobutylene from the decomposition of intermediate products,<sup>[15]</sup> trimer condensates phorone and isophorone as well as higher oligomers such as acyclic and aromatic tetramer condensation products were identified through GC-mass spectrometry (MS) analysis (see Figure S5, Supporting Information). Depending on the catalyst, 90–95% of the total product amount detected in GC-analysis can be assigned to the main products for the studied reaction temperatures of 160–190 °C. As such 88–99% of the product yield consists of mesitylene, mesityl oxide and isophorone for 160 °C (see Figure S2, Supporting Information). Nevertheless, errors in conversion and yield occur due to the high volatility of acetone and the reaction intermediates and the likely formation of carbonaceous deposits. Concluding, catalyst selectivity decreases with increasing temperature and increasing quantity of acid sites as mesityl oxide is increasingly converted to undesired by-products instead of mesitylene.

Assessing the influence of reaction time on the self-condensation of acetone shows that the main reaction progress occurs

in the first 3 h and approaches maximum values for conversion and yields afterward. A general increase of  $X_{Ac}$  and  $Y_{Mes}$  and decrease of  $Y_{MesOx}$  over time is only apparent for H-BEA 35 and Siralox 70/170 HPV at 130 and 160 °C and is less pronounced for higher temperatures. Reaching the equilibrium of the reaction or catalyst deactivation over time could explain the observed behavior. Deactivation could be either caused by pores blocked by formed by-products or buffering of the acidic protons of the catalyst by the water formed as by-product of the condensation reaction. As catalyst conversion increases with time and temperature total product yields for mesitylene and mesityl oxide do not increase similarly. This is likely due to promoted catalyst deactivation for higher temperatures and longer reaction times. Fast recycling combined with reactivation of the catalyst could potentially yield significant product amounts.

The polymeric nature of cation exchange resins limits their use to temperatures of  $\approx 180$  °C in case of Purolite CT275DR due to the insufficient thermal stability. In order to gain insight into the influence of higher reaction temperatures the beta-zeolite H-BEA 35 was tested in a temperature range from 200 to 280 °C. For H-BEA 35 a significant increase in conversion from 26% to 65% is observed for a 10 °C increase in temperature from 190 to 200 °C (Figure 4d). The greater acetone conversion is accompanied by only a minor increase in  $Y_{Mes}$  whereas the yield of the intermediate product mesityl oxide decreases to below 0.5%. For the higher temperature reactions tested, phase separation of the product mixture occurred. The two separating phases had to be resolubilized by adding 30 wt% of 1,4-dioxane as phase solubilizer for GC analysis. Regarding a future process development based on the cyclotrimerization of alkyl methyl ketones, the phase separation that occurs during the reaction could be used to separate water from the desired products, the aromatics, thus shifting the reaction equilibrium. The influence of water on the catalytic activity of the reaction system and the effects on catalyst stability and activity has to be assessed in advance though.

As mentioned above, formation of undesired by-products increases drastically with temperature while selectivity to mesitylene declines. Above 200 °C decomposition of intermediate products is becoming increasingly pronounced as shown by the presence of acetic acid in the reaction mixture. This emphasizes once more the complexity of the reaction in terms of possible side reactions and desired product selectivity. Albeit a generally increased formation of side products, isophorone yield similarly to mesityl oxide yield decreases with higher temperatures and can only be detected in traces above 200 °C. Due to the microporous nature of zeolites, reaction pressure can potentially influence the acetone condensation reaction. But a variation of the autoclave pressure from 40 to 145 bar showed only a negligible pressure dependence for the H-BEA 35 catalyst at 160 °C (Figure S6, Supporting Information). A slight increase in  $Y_{Mes}$  and decrease in  $X_{Ac}$  and  $Y_{MesOx}$  is observed for pressures of 95 bar and higher.

### 2.3. Reaction Kinetics

For a better understanding of the reaction and the influence of reaction time on intermediates and product formation, the

progress of reaction was followed by taking samples of the reaction mixture in a batch reactor over the course of a total reaction time of 300 min. A 300 mL stirring autoclave that features a sampling line was used to study the time-resolved reaction progress at 130, 150, and 170 °C. Reaction temperatures were limited to 170 °C to accommodate for the maximum operating temperature of the catalyst. Furthermore, maximum  $Y_{Mes}$  were obtained at 160 °C. The reaction had to be scaled-up by a factor of 30 based on the acetone volume due to the larger reactor. The catalyst amount was reduced to 2.5 wt%. As catalyst the cation exchange resin Purolite CT275DR was investigated since it showed the highest activity in the screening of reaction parameters and required lower temperatures for activation than Siralox 70/170 HPV. Since the reactor was loaded with catalyst and starting material acetone prior to heating up, a first sample was taken when the final reaction temperature was reached. This marked the start of the reaction and was set as 0 min. The data obtained from following the reaction progress support the results found in the parameter screening: acetone conversion increases with time and temperature (Figure 5). More interesting is the fact that the reaction progress can be subdivided into two consecutive phases: in the first 20 min the reaction is very fast and  $X_{Ac}$  and  $Y_{MesOx}$  increase linearly. 20–30 min into the reaction,  $Y_{MesOx}$  goes through a maximum. This is especially pronounced for higher reaction temperatures. Two explanations are feasible: 1) The formation of water or by-products limits the further course of the reaction or 2) the reaction kinetics of the initial acetone condensation step and the consecutive reaction, i.e., growth/aromatization of mesityl oxide, are different. For the latter reason it is conceivable that the initial step is of second order as a bimolecular reaction occurs while in the second case the reaction is of first order regarding the concentration of mesityl oxide and acetone. At 130 °C a slower formation with a later maximum of mesityl oxide is observed. Formation of the consecutive reaction product mesitylene starts delayed as its intermediate must be formed first and  $Y_{Mes}$  is only significant after 10 min. Characteristic for this 20 min long start-up phase where almost two thirds of acetone are converted is the steep slope for  $X_{Ac}$ . In the subsequent second phase acetone conversion slows down immediately which is marked by a significant decrease of the slopes for  $X_{Ac}$  and  $Y_{MesOx}$  since the reaction to its consecutive products increases. However,  $X_{Ac}$  and  $Y_{Mes}$  steadily increase over the full reaction time of 300 min. It can be concluded that no equilibrium state is reached during the reaction time. Over the course of the reaction not only the yields are shifted from mesityl oxide to mesitylene but also the overall selectivity decreases as formation of side products increases which is the main contributor to the rising acetone conversion. During the start-up phase at 130 °C acetone, diacetone alcohol, mesityl oxide, phorone, isophorone, and mesitylene are detected via GC-MS with their sum representing 99.9% of the total GC area. Higher reaction temperatures lead to longer heat-up phases. Thus, formation of side products and mesitylene are already observed at  $t = 0$  min.

Concerning the reaction temperature, reaction progresses run almost parallel when monitored by  $X_{Ac}$  and  $Y_{Mes}$  for 130–170 °C, especially during the start-up phase. In the reaction parameter screening a maximum for  $Y_{Mes}$  was obtained

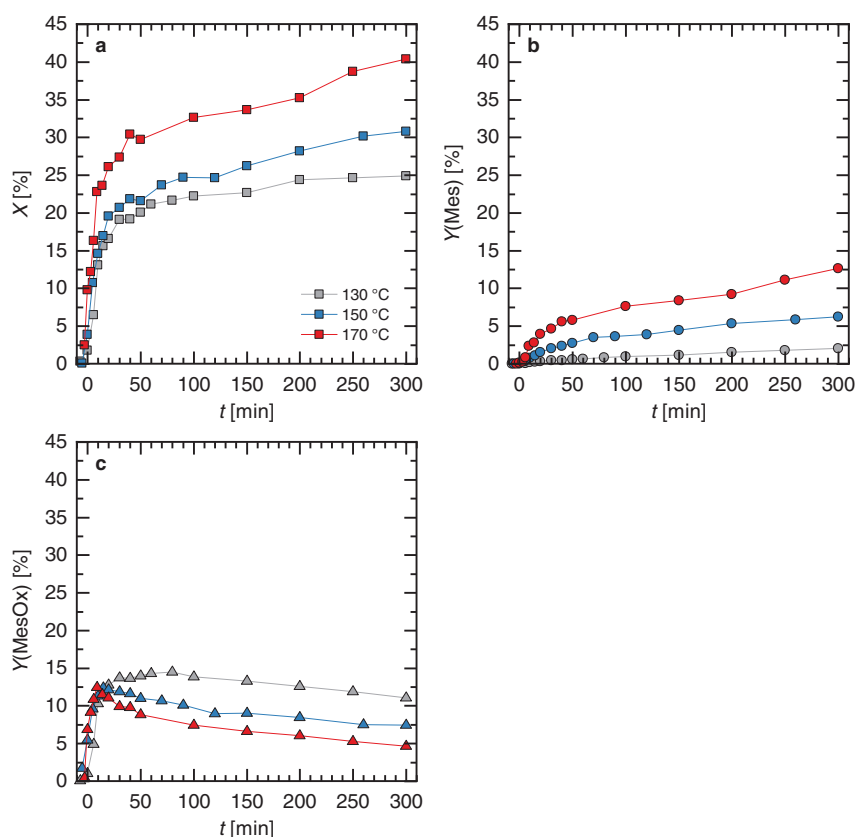


**Figure 5.** Time-resolved a) acetone conversion, b) mesitylene yield, and c) mesityl oxide yield for the acetone condensation reaction with Purolite CT275DR at 130, 150, and 170 °C (straight lines connect the measured points just for clarity and to indicate trends).

at 160 °C. Although this is not replicated in the time-resolved experiments, the general trend of a constant increase of  $X_{\text{Ac}}$  with reaction temperature is confirmed.

### 2.3.1. Catalyst Conversion Activity and Productivity

The preceding observations are clarified by investigating the catalyst conversion activity which is defined as the amount of converted acetone  $n_{\text{Ac}}$  per catalyst mass  $m_{\text{cat}}$  and time  $t$  and determined via linear regression of the data in the two reaction phases (see Figure 6a). These two phases can be clearly distinguished by the abrupt change in catalyst conversion activity around 20 min. While for 130 and 150 °C the converted amount of acetone per catalyst mass in the start-up phase is 6–7 and 9.8 mmol g<sup>-1</sup> min<sup>-1</sup> at 170 °C, a drastic decline is noted for the second phase when the conversion activity drops below 0.3 mmol g<sup>-1</sup> min<sup>-1</sup>. The sudden decrease in catalyst activity is also observable in the formation of products, particularly for mesityl oxide (see Figure 6b). Productivity for both mesityl oxide and mesitylene after the start-up phase flattens and is significantly reduced for the remainder of the reaction. On the one hand this shows that temperature has a major influence on

catalyst conversion activity. On the other hand, this represents a decrease in activity of more than 95% which can be an indicator for a drastic inhibition of the reaction caused by catalyst deactivation or change in reaction order due to the mechanism and concentration dependence as described above. However, the catalyst is not completely deactivated since mesitylene productivity monotonically increases with time. Plausible explanations for catalyst deactivation could be blocking of the catalyst pores by formed reaction and side products, such as oligomers but also water of which three molecules are formed for every molecule of mesitylene. A water film on the catalyst surface can lead to inhibition of the acidic surface centers by creating a buffer solution with H<sub>3</sub>O<sup>+</sup>-ions which would decrease the acidic strength considerably. Additional mass transfer limitations posed by an aqueous acidic phase would further contribute to a decrease in catalyst activity. Besides water, oligomerization products formed by the high quantity of acid sites in the pores can mechanically block pores and thus hinder access to a substantial number of catalytically active centers. In fact, Podrebarac et al. assumed heavier side products to be the cause for the observed deactivation of an Amberlite IR-900 anion exchange resins in hydroxide form when investigating the conversion of acetone to diacetone alcohol and mesityl oxide.<sup>[18]</sup> For the studied Purolite CT275DR



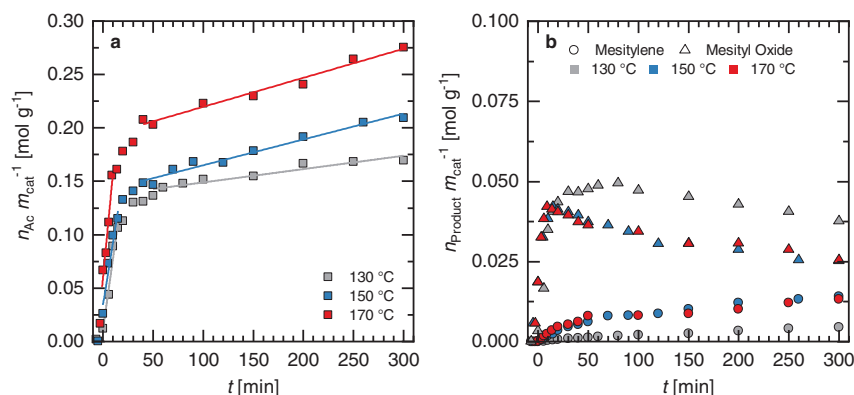


**Figure 6.** a) Converted amount of acetone  $n_{Ac}$  and b) formed products mesitylene and mesityl oxide per catalyst mass  $m_{cat}$  to determine the catalyst activity of Purolite CT275DR.

catalyst, an increase in catalyst mass of 9.3% is observed after reaction at 160 °C for 3 h (see Table S1, Supporting Information). At low reaction temperatures under 200 °C carbonaceous deposits on acid catalysts are nonpolyaromatic and stem mainly from condensation and rearrangement steps.<sup>[19]</sup> Besides coke formation on the catalyst surface, nondesorbed reaction products such as mesitylene can add to the catalyst mass. Their strong adsorption to the catalyst's acid sites can contribute to the catalyst deactivation. Further investigations of the species adsorbed on the catalyst surface must be conducted to understand in more detail what causes the decrease in activity and to what extent catalyst deactivation occurs.

#### 2.4. Influence of Water on the Reaction

Formation of an acidic aqueous phase on the catalyst surface could cause catalyst deactivation and would imply a change from heterogeneous to homogeneous catalysis. To further address the influence of water on the reaction progress of the acetone self-condensation, the catalyst and reagent acetone were dried before the reaction to remove residual water and compared to untreated conditions. Additionally, an experiment with a molecular sieve (3 Å) was performed to remove the water formed during the reaction. The results for the reaction progress of the two variants in comparison to the one under standard conditions without dried reactant or additives are displayed in Figure 7.

Notably, under dry conditions higher acetone conversions were obtained which is supported by an activity increase of 1.6 times in the start-up phase illustrated by a much steeper slope. Albeit, this increase does not transfer to the second phase where the curves of dry and standard conditions run parallel. Removal of residual water from Purolite CT275DR and acetone increases the initial acidic strength of the catalyst, thus preventing the immediate formation of a buffer solution which can lead to catalyst deactivation. Since the shifted equilibrium further accelerates the reaction in the start-up phase, formation of water increases rapidly as does the decrease in catalyst activity. Based on the assumption that water is the limiting factor in the reaction, in situ removal of water should result in a higher

catalyst activity. Using a 3 Å molecular sieve, progress of the start-up phase is highly similar to the one under dry reaction conditions. But the reaction does not proceed past 100 min as displayed by the constant conversion and yield curves. Inside the pores of the molecular sieve ion exchange of Na<sup>+</sup>- or K<sup>+</sup>-ions with H<sub>3</sub>O<sup>+</sup>-ions can occur and is facilitated by water formation during the reaction which increases ion mobility in the reaction system. Consequently, catalytically active H<sub>3</sub>O<sup>+</sup>-ions are removed from the reaction mixture and catalyst activity is diminished. Using a molecular sieve is therefore not suitable for the investigation of a water-free system for the aldol condensation reaction of acetone.

As an alternative means to study the catalyst deactivation which occurs during the start-up phase, fresh catalyst was added after 50 min. This resulted in acetone conversion and mesitylene yield increasing further (Figure S7, Supporting Information). Instead of an increase in  $Y_{MesOx}$  which would be expected based on the reaction progress without addition of

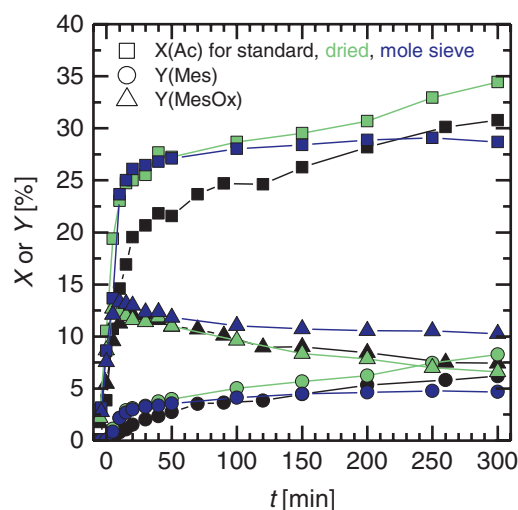


**Figure 7.** Comparison of the reaction progress for the catalyst Purolite CT275DR under dry (acetone and catalyst dried prior to reaction) and standard conditions and the addition of a mole sieve to the reaction.

fresh catalyst, a decrease occurred, implying that mesityl oxide is converted to the consecutive product mesitylene. No change in the two step behavior of the reaction is apparent when adding the fresh catalyst, thus, disproving the theory of the influence of water on the two reaction steps and on the other hand proving the dependence on the higher reaction order of the initial condensation reaction and the subsequent further reaction of mesityl oxide and acetone of lower reaction order. The increase observed for  $X_{Ac}$  and  $Y_{Mes}$  of  $\approx 10\%$  is less prominent compared to the initially added catalyst. This indicates that the deactivation of the catalyst is caused by species in the reaction mixture, e.g., water or oligomers that are formed during reaction.

### 3. Conclusion

As suitable solid acid catalysts for catalyzing the aldol condensation reaction of acetone to mesitylene we identified the beta-zeolite H-BEA 35, the cation exchange resin Purolite CT275DR, and the aluminosilicate Siralox 70/170 HPV. Regarding the influence of reaction time it was noted that in the first 3 h of reaction the majority of acetone was converted. Mesitylene yield increased with higher reaction temperatures and longer reaction times which also increased formation of side products. Latter was also emphasized by higher surface acid group densities of the catalysts, negatively affecting the total product selectivity. Progress of the reaction was found to take place in two phases with an initial 20 min long start-up phase characterized by high catalyst acetone conversion activity and a subsequent phase which was marked by an immediate apparent decrease in activity probably due to the subsequent reaction of lower reaction order. Water plays a role in the deactivation of the catalyst and thus presents a challenge for future optimization of the reaction to aromatics.

The investigated self-condensation of acetone to mesitylene demonstrates the potential of an innovative route to aromatics via cyclotrimerization of alkyl methyl ketones. A comparison with other more established routes is not yet permissible due to the early stage of the research that requires further optimizations of the catalyst selectivity and studying the cyclotrimerization reaction of longer alkyl methyl ketones, such as 2-butanone. The results present a first step toward a better understanding of the required reaction conditions and will be followed by investigation of the kinetics in a continuous reactor setup.

### 4. Experimental Section

All materials were used as received without further purification. Acetone ( $\geq 99.5\%$ ) and 1,4-dioxane ( $\geq 99.5\%$ ) were purchased from Carl Roth, cyclohexane ( $\geq 99.9\%$ ) from Sigma-Aldrich. Catalysts were either supplied by their manufacturer or commercially available and were used as received.  $Nb_2O_5$  (98.5%) was purchased from Alfa Aesar.

**Screening of Catalysts and Reaction Parameters:** A 45 mL batch autoclave (Parr MRS 5000 series) equipped with a polytetrafluoroethylene-inlet and magnetic stirring bar (500 rpm) was loaded with acetone (3.950 g, 68 mmol) and solid acid catalyst (0.198 g, 5 wt%). Cyclohexane (1.431 g, 17 mmol) was added as internal standard in the catalyst screening experiments. Reactors were purged twice with argon during which the

stirring speed was set to 100 rpm. They were then pressurized with argon (25 bar) and heated to the specified reaction temperature and time at a speed of 500 rpm. The reactors were cooled down in an ice-water bath before the product solution was filtered and analyzed by GC and GC/MS. In reaction parameter screening experiments, 1,4-dioxane (30 wt%) was added as internal standard and phase solubilizer.

**Kinetic Experiments:** Acetone (150 mL, 2.0 mol) and catalyst Purolite CT275DR (2.96 g, 2.5 wt%) were added to a stirred tank reactor from Parr featuring a sampling line. The purged reactor was pressurized with argon (20–40 bar) and heated to the specified reaction temperature. For the duration of reaction (300 min), the reaction mixture was stirred at 1000 rpm and samples (1–2 mL) were taken in regular intervals.

**Acetone Condensation under Dry Conditions:** Analogous to the reaction procedure for the temporal reaction progress of the acetone condensation, the reaction proceeded either in the presence of a molecular sieve (3 Å, 6.14 g) or with predried acetone and catalyst. Reactant acetone was dried over a molecular sieve (3 Å) and catalyst Purolite CT275DR was dried at 80 °C under vacuum.

**Product Characterization via GC:** Samples for GC analysis were usually prepared by adding 70 wt% of the filtered product solution to 30 wt% of the internal standard 1,4-dioxane. In reactions in which cyclohexane was added initially, filtered product solutions were used directly. Quantitative analysis was performed with a Shimadzu GC-2010 Plus with flame ionization detector and qualitative analysis with a GCMS-QP2010SE, both equipped with a Macherey-Nagel Optima WaxPlus column.

**$NH_3$ -TPD:** Zeolitic acid sites were quantified by temperature-programmed desorption of adsorbed  $NH_3$ . Catalyst samples (100 mg) were initially calcined for 1 h at 600 °C under  $N_2$ -atmosphere to remove residual water. Subsequently, at 140 °C the sample was loaded with  $NH_3$  (2 vol%  $NH_3$  in  $N_2$ , 20 mL  $min^{-1}$ ) for 20 min, followed by desorption of the physisorbed  $NH_3$  in  $N_2$ -flow (100 mL  $min^{-1}$ ). Afterward, the sample was heated to 600 °C (10 K  $min^{-1}$ , 100 mL  $min^{-1}$   $N_2$ ) and desorbed  $NH_3$  was detected by Fourier-transform-IR.

### Supporting Information

Supporting Information is available from the Wiley Online Library or from the author.

### Acknowledgements

The authors gratefully acknowledge financial support from the German Federal Ministry of Education and Research (Grant No. 031B0680).

### Conflict of Interest

The authors declare no conflict of interest.

### Keywords

aldol condensation, aromatics, biomass, biorefinery, catalysis, ketones

Received: December 20, 2019

Revised: June 5, 2020

Published online:

[1] Nexant Chem Systems, Global Chemicals Demand Estimate, White Plains, New York, 2012.



- [2] A. E. Settle, L. Berstis, N. A. Rorrer, Y. Roman-Leshkóv, G. T. Beckham, R. M. Richards, D. R. Vardon, *Green Chem.* **2017**, *19*, 3468.
- [3] A. Maneffa, P. Prielcel, J. A. Lopez-Sanchez, *ChemSusChem* **2016**, *9*, 2736.
- [4] Q. Bu, H. Lei, A. H. Zacher, L. Wang, S. Ren, J. Liang, Y. Wei, Y. Liu, J. Tang, Q. Zhang, R. Ruan, *Bioresour. Technol.* **2012**, *124*, 470.
- [5] X. Y. Wang, R. Rinaldi, *Angew. Chem., Int. Ed.* **2013**, *52*, 11499.
- [6] D. Dodds, B. Humphreys, in *Catalytic Process Development for Renewable Materials* (Eds: P. Imhof, J. C. v. d. Waal), Wiley-VCH, Weinheim, Germany **2013**.
- [7] Y.-T. Cheng, J. Jae, J. Shi, W. Fan, G. W. Huber, *Angew. Chem.* **2012**, *124*, 1416.
- [8] C.-C. Chang, H. Je Cho, J. Yu, R. J. Gorte, J. Gulbinski, P. Dauenhauer, W. Fan, *Green Chem.* **2016**, *18*, 1368.
- [9] A. A. Rosatella, S. P. Simeonov, R. F. M. Frade, A. M. Afonso, *Green Chem.* **2011**, *13*, 754.
- [10] R. M. West, E. L. Kunkes, D. A. Simonetti, J. A. Dumesic, *Catal. Today* **2009**, *147*, 115.
- [11] E. R. Sacia, M. Balakrishnan, M. H. Deaner, K. A. Goulas, F. D. Toste, A. T. Bell, **2015**, *8*, 1726.
- [12] a) J. A. Mitchell, E. E. Reid, *J. Am. Chem. Soc.* **1931**, *53*, 330; b) R. Adams, R. W. Hufferd, *Org. Synth.* **1922**, *2*, 63.
- [13] G. S. Salvapati, K. V. Ramanamurty, M. Janardanarao, *J. Mol. Catal.* **1989**, *54*, 9.
- [14] a) A. G. Gayubo, A. T. Aguayo, A. Atutxa, R. Aguado, M. Olazar, J. Bilbao, *Ind. Eng. Chem. Res.* **2004**, *43*, 2619; b) A. G. Panov, J. J. Fripiat, *J. Catal.* **1998**, *178*, 188.
- [15] M. Paulis, M. Martín, D. B. Soria, A. Díaz, J. A. Odriozola, M. Montes, *Appl. Catal., A* **1999**, *180*, 411.
- [16] Purolite CT275DR Product Data Sheet, <https://www.purolite.com/product-pdf/CT275DR.pdf> (accessed: November 2019).
- [17] Rohm and Haas, Amberlite IR120 H Product Data Sheet, [https://nshosting.dow.com/doc-archive/business/ier/ier\\_for\\_industrial\\_water\\_treatment/amberlite\\_ir120\\_h/tds/amberlite\\_ir120\\_h.pdf](https://nshosting.dow.com/doc-archive/business/ier/ier_for_industrial_water_treatment/amberlite_ir120_h/tds/amberlite_ir120_h.pdf) (accessed: November 2019).
- [18] G. G. Podrebarac, F. T. T. Ng, G. L. Rempel, *Chem. Eng. Sci.* **1997**, *52*, 2991.
- [19] M. Guisnet, P. Magnoux, *Appl. Catal., A* **2001**, *212*, 83.

---

Copyright WILEY-VCH Verlag GmbH & Co. KGaA, 69469 Weinheim, Germany, 2020.

**ADVANCED  
SUSTAINABLE  
SYSTEMS**

## Supporting Information

for *Adv. Sustainable Syst.*, DOI: 10.1002/adsu.201900150

**Biomass-Derived Aromatics by Solid Acid-Catalyzed Aldol  
Condensation of Alkyl Methyl Ketones**

*Phillip Reif, Hannah Rosenthal, and Marcus Rose\**

## Supporting Information

**Biomass-derived Aromatics by Solid Acid-catalyzed Aldol Condensation of Alkyl Methyl Ketones**

Phillip Reif, Hannah Rosenthal, Marcus Rose\*

**Calculation of acetone conversion  $X_{Ac}$  and product yields  $Y$ :**

Acetone conversion and product yields are calculated based on the following formulas.  $n_{Ac,0}$  is the amount of acetone in the sample if the sample only consisted of acetone and the internal standard (IS), i.e., before reaction.

$$X_{Ac} = \frac{n_{Ac,0} - n_{Ac}}{n_{Ac,0}}$$

$$Y_{Mes} = \frac{3 n_{Mes}}{n_{Ac,0}} \quad Y_{MesOx} = \frac{2 n_{MesOx}}{n_{Ac,0}}$$

$$Y_{Isophorone} = \frac{3 n_{Isophorone}}{n_{Ac,0}}$$

The amount of substances in the samples is obtained with response factors RF via GC calibration curves, according to following formulas:

$$\frac{A_i}{A_{IS}} = \frac{w_i}{w_{IS}} RF$$

$$n_{Ac,0} = \frac{(1 - w_{IS})m_{sample}}{M_{Ac}}$$

$$n_i = \frac{w_i m_{sample}}{M_i}$$

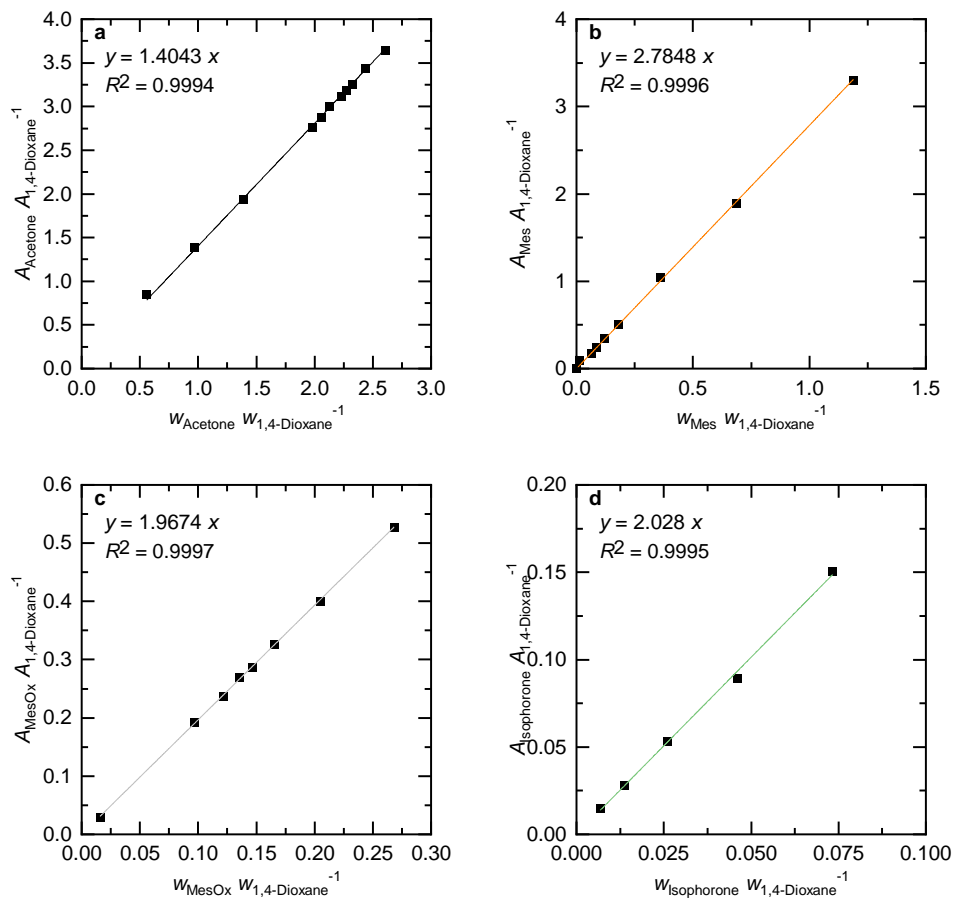


**Figure S1.** GC-calibration curves including calibration factors based on the internal standard 1,4-Dioxane for (a) acetone (b) mesitylene (c) mesityl oxide and (d) isophorone.

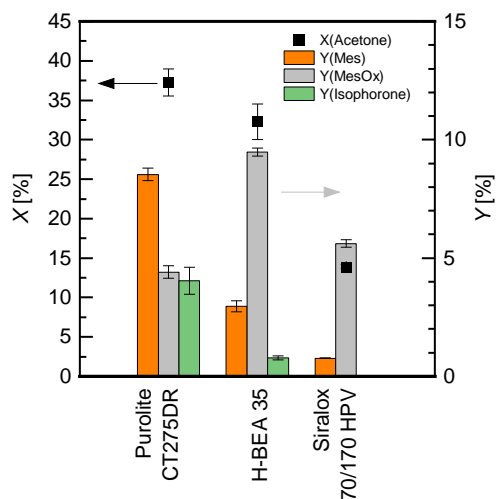


**Figure S2.** Main product distribution and statistical error of 3-5 identical experiments for each of the three selected catalysts at 160 °C and 3 h reaction time.

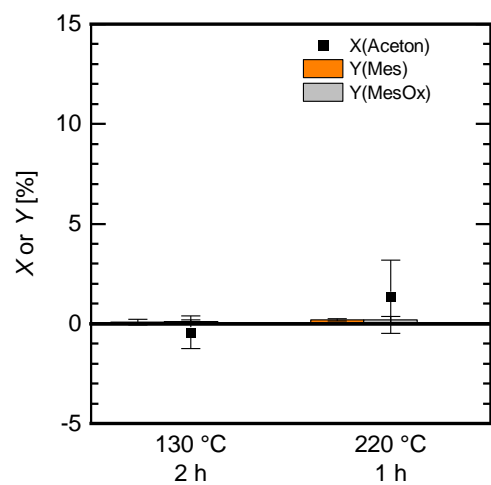


**Figure S3.** Blank activity of the 45 mL reactor vessel with PTFE inlet for the conversion of acetone.

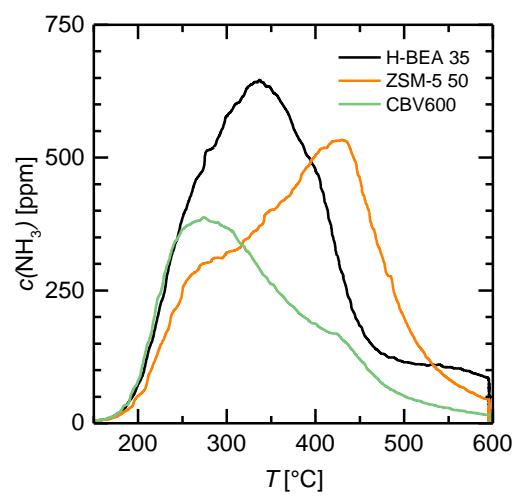


**Figure S4.** Temperature-dependent  $\text{NH}_3$ -desorption of zeolites in H-form.

**Comparison of zeolite catalyst activity, pore size and acid site density:**

In section 2 different zeolites are screened for the aromatization reaction. Comparison of their different activities with their pore sizes hints at an effect of the zeolite pore size. The pore size is largest for the Y-zeolite CBV600 with 0.74 nm compared to those of the beta and MFI-type zeolite ZSM-5 with 0.59 and 0.46 nm, respectively.<sup>[1]</sup> Since the kinetic diameter of mesitylene is relatively large with 0.76 nm<sup>[2]</sup> it is probably too bulky for the 10-ring pore system of ZSM-5 and thus its formation is limited while the larger pores of 12-ring pore systems of the beta and Y-zeolite are better accommodating for the cyclotrimerization reaction.<sup>[3]</sup> Limited formation of acetone trimer condensates with ZSM-5 zeolites was also observed in experiments by Komatsu et al.<sup>[4]</sup> Acid site density of the zeolites is less probable to cause the lacking activity for ZSM-5 zeolites in the acetone aromatization based on NH<sub>3</sub>-TPD measurements which give a comparable density of 0.523 mmol g<sup>-1</sup> and 0.587 mmol g<sup>-1</sup> for ZSM-5 (SAR = 50) and H-BEA 35, respectively (**Figure S4**). On the other hand, the slightly lower activity of CBV600 can be related to its lower acid site density of 0.327 mmol g<sup>-1</sup>.

**References:**

- [1] C. Beaulocher, L. B. McCusker, Database of Zeolite Structures, <http://www.iza-structure.org/databases/>, accessed: 2019.
- [2] S. T. Wilson, in *Introduction to Zeolite Science and Practice* (Eds: J. Cejka, H. van Bekkum, A. Corma, F. Schueth), Elsevier, Amsterdam, The Netherlands **2007**, Ch. 4.
- [3] A. Martínez, M. A. Arribas, S. Moussa, in *Zeolites in Catalysis: Properties and Applications* (Eds: J. Čejka, R. E. Morris, P. Nachtigall), Royal Society of Chemistry **2017**, Ch. 10.
- [4] T. Komatsu, M. Mitsuhashi, T. Yashima, in *Stud. Surf. Sci. Catal.*, Vol. 142 (Eds: R. Aiello, G. Giordano, F. Testa), Elsevier **2002**, p. 667.

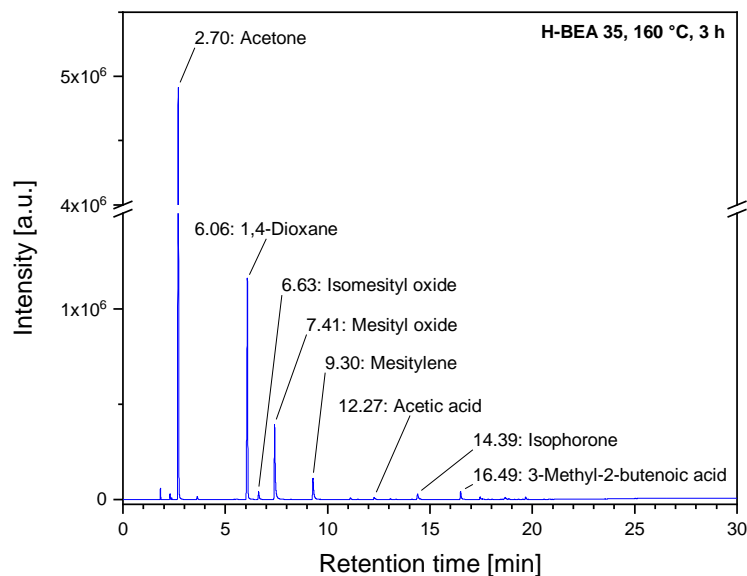


**Figure S5.** Representative GC-chromatogramme of the product mixture of the reaction catalyzed by H-BEA 35 at 160 °C after 3 h with marked retention times for main and side products.

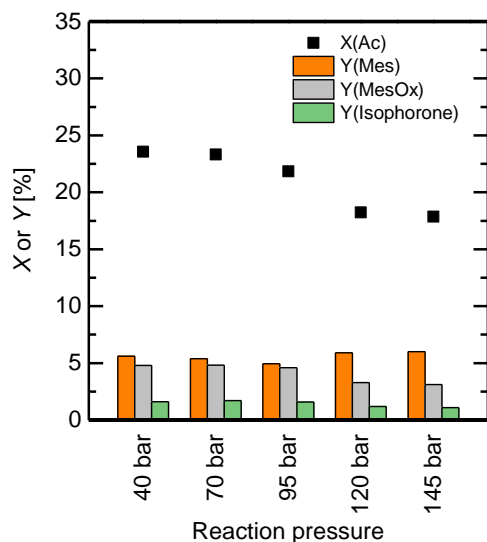


**Figure S6.** Results for different reaction pressures for acetone conversion and product yields of the acetone self-condensation reaction with H-BEA 35 at 160 °C.

**Table S1.** Comparison of Purolite CT275DR catalyst mass before ( $m_{\text{cat},0}$ ) and after reaction ( $m_{\text{cat,reactor}}$ ) at specified conditions. Noted are the sums of the catalyst mass for three identical reactions. The catalyst was dried at 60 °C under vacuum before the reaction and was washed with water before drying after the reaction.

Reaction conditions	$m_{\text{cat},0}$ [g]	$m_{\text{cat,reactor}}$ [g]	Relative increase
160 °C, 3 h	1.5049	1.6446 <sup>b</sup>	9.3 %
190 °C, 6 h	1.5032	1.5354	2.1 %

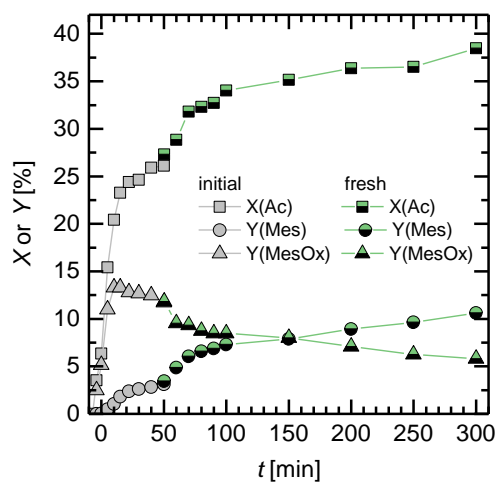


**Figure S7.** Reaction progress at 150 °C of  $X_{\text{Ac}}$ ,  $Y_{\text{Mes}}$  and  $Y_{\text{MesOx}}$  with Purolite CT275DR and addition of fresh catalyst after 50 min.



## 4.2. Liquid phase aromatization of bio-based ketones over a stable solid acid catalyst under batch and continuous flow conditions

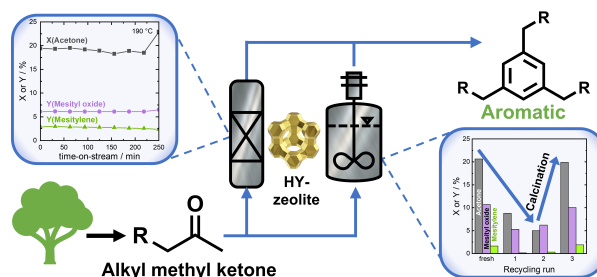
Authors: P. Reif, N. K. Gupta, M. Rose

Journal: Catalysis Communications

Date: 10 January 2022

DOI: <https://doi.org/10.1016/j.catcom.2022.106402>

© 2022 The Authors. Published by Elsevier B.V. This is an open access article under the CC BY-NC-ND 4.0 license.

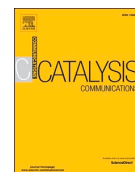


Besides catalyst activity, stability is a crucial factor and concern when upscaling a chemical process targeting later-stage industrial relevance. The results of its assessment under liquid phase batch and flow conditions were published in *Catalysis Communications*.<sup>[133]</sup> It was found that the highly active cation exchange resin Purolite CT275DR used as a benchmark is not stable under reaction conditions as the leaching of active sulfonic sites was observed in catalyst recycling experiments. The catalyst is therefore not suitable for scale-up and was not considered in the further process development. In comparison, the activities of the recycled zeolites H-BEA 35 and H-Y were strongly decreased but could be restored completely by simple calcination in air. The different catalysts were also studied under liquid phase flow conditions. For this, a fixed-bed reactor was set up with online-GC-analytics which allowed continuous monitoring of catalyst activity. The results obtained in the flow reactor at a WHSV of 8 h<sup>-1</sup> underpinned that Purolite CT275DR is not a suitable catalyst for a technical process as its mesitylene formation activity was marginal. Furthermore, due to its polymeric nature, it is not thermally stable at increased reaction temperatures. Very low yields were also observed for zeolite H-BEA as its pore size is too narrow for the bulky mesitylene molecule, and thus only surface acid sites were active. Among the assessed catalysts, only the larger pore zeolite H-Y was found suitable for the reaction conditions as it showed steady-state acetone conversion and mesitylene formation at 190 °C for 250 min time-on-stream. It can be concluded that porosity not only plays a role in catalyst activity but is also critical for stability in the aromatization of ketones. The continuous removal of products from the catalyst surface under liquid phase flow conditions benefits stability compared to the gas-phase conversion of acetone. Given its performance in the acetone condensation, zeolite H-Y was also applied successfully in the self-condensation of the higher alkyl methyl ketones 2-butanone and 2-pentanone to aromatics. Their utilization would allow further value addition of biorefinery streams and gives access to styrene-type monomers from biomass for example.



Contents lists available at ScienceDirect

Catalysis Communications

journal homepage: [www.elsevier.com/locate/catcom](http://www.elsevier.com/locate/catcom)

## Liquid phase aromatization of bio-based ketones over a stable solid acid catalyst under batch and continuous flow conditions

Phillip Reif, Navneet Kumar Gupta<sup>\*</sup>, Marcus Rose<sup>\*</sup>

<sup>a</sup> Technical University of Darmstadt, Department of Chemistry, Alarich-Weiss-Straße 8, 64287 Darmstadt, Germany

### ARTICLE INFO

#### Keywords:

Aromatics  
Liquid phase catalysis  
Zeolite  
Acid catalyst  
Biomass-derived ketones

### ABSTRACT

Herein, we describe a one-step process for renewable aromatics from biomass-derived ketones over solid acid catalysts under liquid phase batch and flow conditions. The ion exchange resin was highly active for aromatics due to high acidic strength but leaching of acidic sites caused low stability. In contrary, zeolite HY showed a lower activity but higher stability in batch by regenerability and was stable in flow for 250 min-on-stream. HY is further applicable for the conversion of higher ketones (butanone and pentanone). This work contributes towards an industrially important aromatic production from biogenic ketones and thus an economical and sustainable process.

### 1. Introduction

Aromatics are highly demanded commodity chemicals from petroleum resources. For instance, *p*-xylene, mesitylene, etc. are used for the production of high-volume polyethylene terephthalate, solvents, fuel components, and other chemical intermediates [1,2]. The high octane number of aromatics provides additional advantages in the use as octane enhancer [3]. While having unique features for a wide range of industrial applications, the expanded use of aromatics is challenging due to diminishing fossil resources and global concerns of CO<sub>2</sub> emissions. Therefore, utilization of renewable resources for the sustainable production of aromatics is a key challenge to satisfy growing industrial demands. To overcome this, aromatic production from biomass-derived furanics has been studied over solid acid catalysts [4]. In this process, aromatic skeletons are produced in high yields by tandem Diels-Alder cycloaddition followed by dehydration. However, low yields of furanics from sugars are the main obstacle for large-scale aromatic production [5].

The development of a single-step process for aromatics from biomass-derived platform chemicals will bring significant advances. Therefore, aromatics production from biogenic alkyl methyl ketones is considered an industrially relevant pathway. A variety of chemo-catalytic and biotechnological routes have been proposed from biomass to alkyl methyl ketones such as decarboxylation of levulinic acid to 2-butanone or ABE-fermentation to acetone and consecutive alkylation to 2-pentanone [6]. The aromatic mesitylene can be synthesized via self-

condensation from acetone using conventional Brønsted acid catalysts, e.g., H<sub>2</sub>SO<sub>4</sub> or HCl [7]. However, one serious drawback of the process is the energy-inefficient separation or removal of inorganic byproducts, e.g., gypsum (produced by neutralization treatment) from the reaction solution [8]. Heterogeneous catalysts, e.g., ion exchange resins, zeolites, metal oxides, have been reported as an alternative for aromatics at 300–450 °C [9–11]. In general, the high reaction temperature and in situ generated water restrict the continuous process due to the formation of heavy coke and subsequent catalyst deactivation [12–14]. Recently, we showed that the liquid phase conversion of acetone to mesitylene can also take place at lower reaction temperatures of around 150 °C over solid acid catalysts [15]. However, a deeper understanding of the catalyst stability under various reaction conditions is essential for further scale-up. Thus, designing suitable high-performance recyclable heterogeneous catalysts becomes crucial for the efficient catalytic conversion of renewable ketones into aromatics. Additionally, this pathway can also be used for byproduct valorization of the conventional phenol synthesis via the cumene process where large volumes of acetone are produced, thus increasing its potential for value addition [16].

Herein, we have investigated the efficient conversion of various biomass-derived alkyl methyl ketones to aromatics over a stable and reusable solid acid catalyst in liquid phase batch and flow conditions. Heterogeneous acid catalysts can efficiently catalyze the aromatization of alkyl methyl ketones in multiple steps (Scheme 1). Since the conversion of alkyl methyl ketones to aromatics is a complex phenomenon involving several intermediates [6], such as dimers, trimers, tetramers,

<sup>\*</sup> Corresponding authors.

E-mail addresses: [navneet.gupta@gast.tu-darmstadt.de](mailto:navneet.gupta@gast.tu-darmstadt.de) (N.K. Gupta), [marcus.rose@tu-darmstadt.de](mailto:marcus.rose@tu-darmstadt.de) (M. Rose).

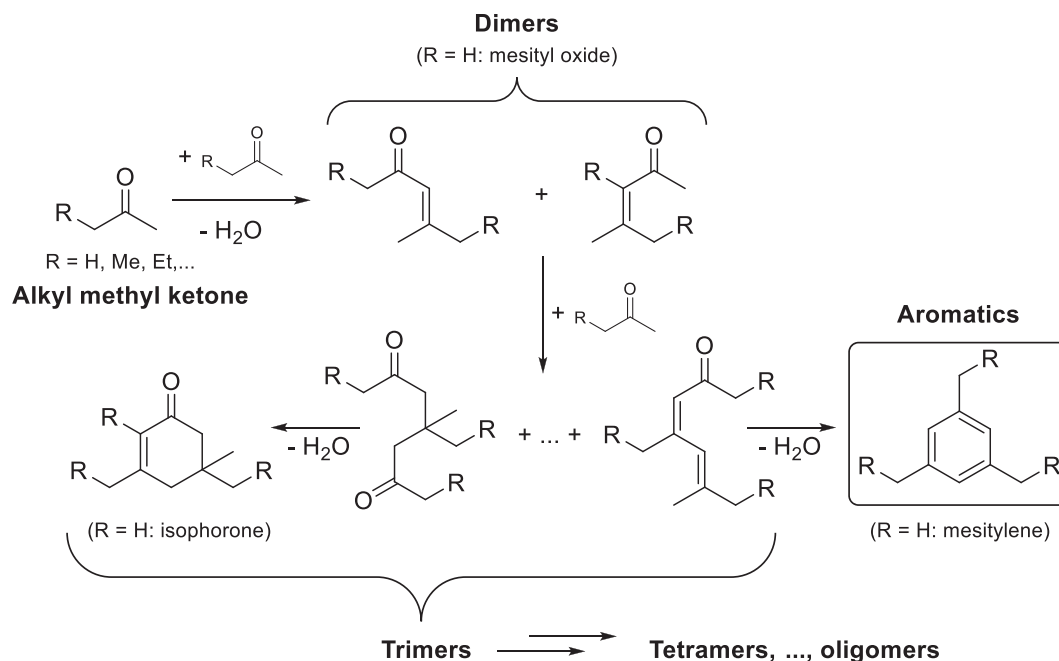
<https://doi.org/10.1016/j.catcom.2022.106402>

Received 1 November 2021; Received in revised form 22 December 2021; Accepted 7 January 2022

Available online 10 January 2022

1566-7367/© 2022 The Authors. Published by Elsevier B.V. This is an open access article under the CC BY-NC-ND license

(<http://creativecommons.org/licenses/by-nc-nd/4.0/>).



**Scheme 1.** Simplified reaction scheme for the acid-catalyzed self-condensation of alkyl methyl ketones to aromatics without depicting possible positional isomers.

and oligomers, the formation of linear/branched chains was also studied together with aromatics. The interplay between structural features and acid sites for the solvent-free transformation of various alkyl methyl ketones to their corresponding aromatics is evaluated.

## 2. Experimental

### 2.1. Catalysts and Reagents

As starting materials acetone (99.9%), 2-butanone (99.5%), and 2-pentanone (99.5%) were purchased from Sigma-Aldrich and used as received. For GC-quantification, 1,4-dioxane (99.5%, Carl Roth), mesityl oxide (97%, Sigma-Aldrich), mesitylene (99%, Acros Organics), isophorone (97%, Sigma Aldrich), and triethylbenzene (97%, Sigma-Aldrich) were used.

Cation exchange resin Purolite CT275DR (also denoted as Purolite) was supplied by Purolite® and beta-zeolite H-BEA 35 by Clariant. Zeolite HY-60 was obtained from Alfa-Aesar. All catalysts were used as received.

### 2.2. Catalytic reaction studies

#### 2.2.1. Catalytic testing in batch reactor

Catalytic reactions in batch experiments were typically performed by adding 150 mL ketone and 2.5 wt% catalyst to the autoclave (300 mL, Parr) which is then pressurized with 30 bar Ar and heated to the reaction temperature while stirring at 1000 rpm [15]. After completion of the reaction, filtered samples of the reaction mixture were analyzed using gas chromatography (Shimadzu GC-2010 Plus) with a capillary column (Restek RTX-5 Amine) and 1,4-dioxane as an internal standard. Furthermore, the identification of products was confirmed by GC coupled with mass spectrometry (Shimadzu GCMS-QP2010SE). For the higher ketones 2-butanone and 2-pentanone, products were quantified based on the concept of the effective carbon number (see SI).

For kinetic experiments, the amounts of aromatics and oligomers were monitored from the initial stage of the reaction by sampling of the

reaction solutions in specific intervals maintaining a constant Ar pressure for the remaining experiment.

#### 2.2.2. Catalyst stability in batch and flow conditions

Recycling of catalysts was carried out in the presence of 10 g acetone and 5 wt% catalyst in 45 mL batch reactors equipped with PTFE-inlets. After purging three times, reactors were pressurized with 40 bar Ar and heated to reaction temperature which was maintained for 3 h while stirring at 500 rpm. Afterwards, reactors were cooled down, filtered product samples were taken, and spent catalysts were separated from the reaction mixture. Before reuse in the next run, catalysts were washed with acetone and dried at 100 °C overnight. Calcination of spent zeolites was performed at 550 °C (6 h, 2 K min<sup>-1</sup>) under 100 NmL min<sup>-1</sup> air flow.

Catalytic reactions in flow conditions were performed in a stainless-steel fixed-bed reactor (length of 300 mm, ID of 15.75 mm). A schematic diagram of the fixed-bed reactor used in this work is shown in Fig. S1. The reactor was loaded with 3 g of catalyst fixed in the center of the reactor by stainless-steel beads and quartz wool and two thermocouples were placed in the catalyst bed to monitor the accurate temperature. Bed volume was kept constant. The feed consisting of pure acetone was introduced into the heated reactor (100–190 °C) via an HPLC pump at a rate of 0.5 mL min<sup>-1</sup>. The reactor pressure was maintained at 40 bar with a backpressure regulator. The product solution stream was analyzed via online GC (Shimadzu GC-2030) equipped with a MEGA-5 column and FID detector ( $T = 40$  °C, 3 min, 10 K min<sup>-1</sup> to 250 °C, and isothermal for 1 min). Conversion and yield were determined based on relative response factors for the internal standard 1,4-dioxane.

### 2.3. Catalyst characterization

The density of acid sites on the fresh zeolite catalysts was determined by temperature-programmed desorption of NH<sub>3</sub> [15]. Samples (approx. 100 mg) were dried in N<sub>2</sub> flow at 600 °C (3 h), then NH<sub>3</sub> was adsorbed at 140 °C (2 vol% NH<sub>3</sub> in N<sub>2</sub>, 20 mL min<sup>-1</sup>) for 20 min. After desorption of the physisorbed NH<sub>3</sub>, the sample was heated to 600 °C with 10 K min<sup>-1</sup> and NH<sub>3</sub> was detected by FT-IR. The strength of acid sites was classified

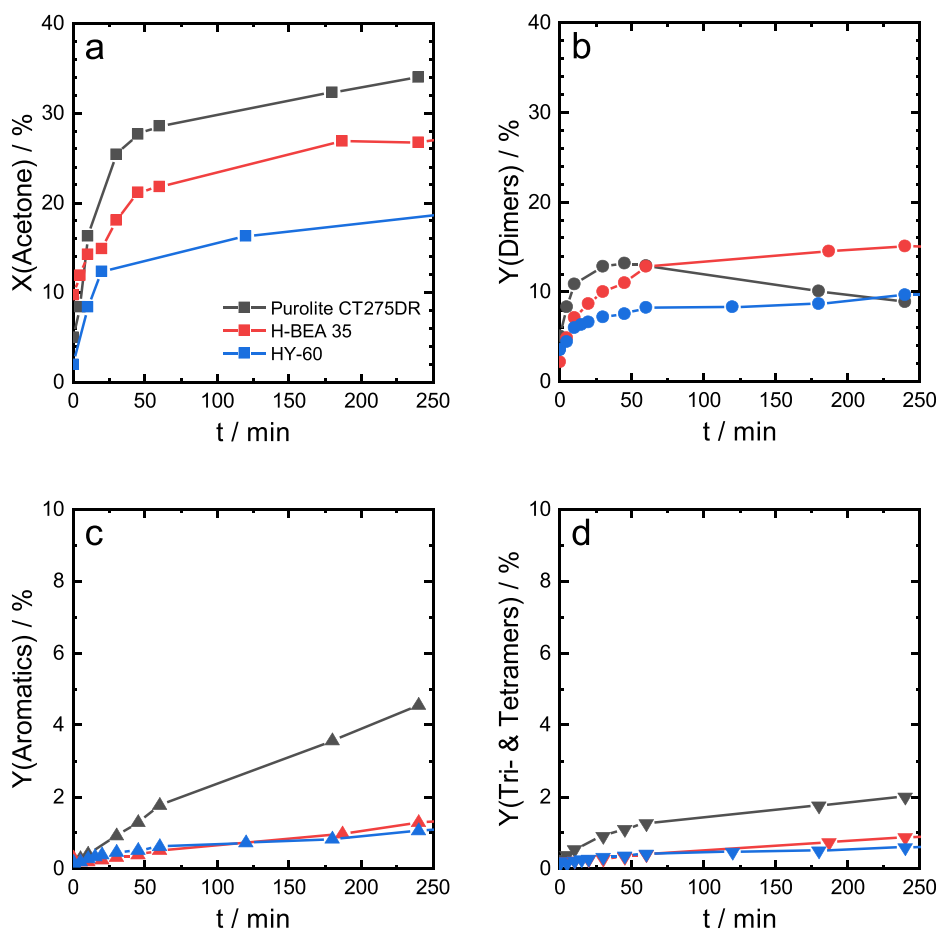


Fig. 1. Comparison of the batch reaction progress for Purolite CT275DR, H-BEA 35, HY-60 at 150 °C: acetone conversion (a) and molar product yields of dimers (b), aromatics (c), tri- and tetramers (d).

as follows: < 250 °C weak, 250–450 °C medium, and > 450 °C strong [17].

To evaluate the carbon deposition during ketone aromatization, thermogravimetric analysis (TGA, Netzsch STA 449 FE Jupiter) was performed. In the procedure, 20 mg of spent catalyst was placed in a TGA crucible and subjected to a TGA scan from 40 to 1000 °C (temperature ramp of 5 K min<sup>-1</sup>) in synthetic air flow (100 NmL min<sup>-1</sup>).

The sulfur content of the sulfonic ion exchange resin catalyst was determined by X-ray fluorescence (XRF) on an Epsilon 4 by Malvern Panalytical with Ag-cathode.

Powder X-ray diffraction (XRD) data of zeolites were obtained on a Bruker D2-Phaser using Cu-K- $\alpha$ -radiation ( $\lambda = 1.5406 \text{ \AA}$ ). The voltage of the radiation tube was 30 kV and the current 40 mA. Diffraction patterns were measured in the  $2\theta$ -range of 5–45° at 0.03° intervals and a step time of 2 s.

### 3. Results and discussion

#### 3.1. Reaction progress of different solid acid catalysts for acetone conversion

In a prior catalyst screening, solid acid catalysts such as zeolites, ion exchange resins, and amorphous silica-alumina were examined for the direct conversion of acetone to mesitylene in the liquid phase at

130–160 °C [15]. It clearly indicated that the acidic catalysts Purolite CT275DR as well as H-BEA 35- and HY-zeolite had higher conversion and good selectivity towards mesitylene starting from acetone. To compare the previously observed activity behavior of Purolite CT275DR with other active catalysts, the reaction progress of the catalysts H-BEA 35 and HY-60 were assessed under identical conditions of 150 °C and 2.5 wt% of catalyst in a batch reactor (see Figure 1). While both types of catalysts converted acetone to the desired aromatics, Purolite CT275DR was superior in both acetone conversion and mesitylene yield which suggests that the Brønsted acid sites are apparently effective for the aromatization. Consistent with the reaction progress found for Purolite CT275DR, all three catalysts show a distinct behavior of two consecutive phases with a high initial activity in the first 20–30 min and a subsequent activity drop. This could be attributed to saturation of active sites by reactants and/or products, thus leading to a decrease in activity over time.

A constant increase in acetone conversion and product yields of aromatics and oligomers is observed for all three acid catalysts. The considerably higher activity of Purolite CT275DR leads to a maximum in the yield of the dimer mesityl oxide of 13% after 50 min and a constant decrease afterward as the dimer reacts in consecutive reaction steps. H-BEA 35 shows the 2nd highest activity with a maximum acetone conversion of 26% (compared to 34% for Purolite CT275DR and 18% for HY) which can mainly be contributed to the dimerization step as it

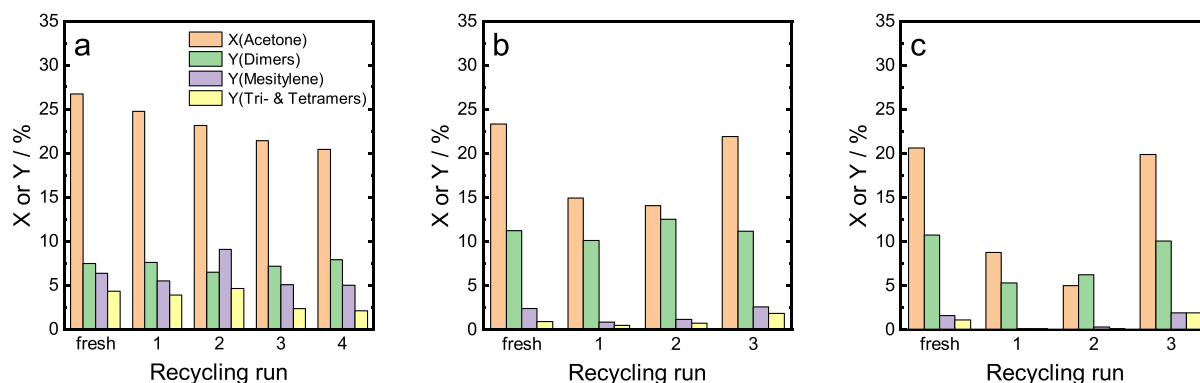


Fig. 2. Batch recycling experiments for Puro-lite CT275DR (a), H-BEA 35 (b), and HY-60 (c) at 150 °C (3 h), 5 wt% catalyst, 10 g acetone, 40 bar Ar. Recycled catalysts were calcined in air (550 °C, 6 h) from 2nd to 3rd cycle in figure (b) and (c).

shows a constant increase in dimer yield with a maximum of 15% at 240 min. Although the yield of total products for HY-60 is only 12%, the rates of formation for mesitylene and oligomers (tri- and tetramers) are comparable for both zeolites. Combined selectivity for mesitylene, tri- and tetramers (~20% for Puro-lite CT275DR and 8–9% for both zeolites at 240 min) slowly increases for all three catalysts over time (see Fig. S2). This results from the consecutive nature of the reaction where the conversion of intermediates such as mesityl oxide and trimeric phorones to secondary products, i.e., aromatics and oligomers, is fast compared to acetone conversion. Nevertheless, byproduct formation is observable for this reaction resulting in low quantities of less than 0.5% of the GC-area for acetic acid and isobutene from  $\beta$ -scission reaction (see Fig. S3) [18].

Acetone conversion and aromatics yield increase strongly for higher acid site densities which were determined via  $\text{NH}_3$ -TPD for zeolites and given by the manufacturer for the cation exchange resin (see Fig. S4). Here, Puro-lite CT275DR exhibits the highest amount of acid sites due to its sulfonic acid groups on the surface which strongly correlates with its highest activity. The general increase in activity with increasing amount of acid sites is independent of their strength and can also be found for weak acid centers. This could also be shown by comparing zeolite HY-30 and HY-60 where an approximately 30% increase in aromatics yield was found for HY-30 which features 70% more acid sites (see Fig. S5). While the aromatization of acetone benefits from higher acid site densities, the structure of the catalysts also affects their activity. For instance, the narrow pore size of ZSM-5 (0.47 nm [19]) does not lead to aromatization products of acetone in the liquid and gas phase [11,15]. In the case of H-

BEA 35, the pore size (0.67 nm) is also smaller than the kinetic diameter of mesitylene (0.87 nm) and thus mostly external acid sites contribute to the aromatization [11]. All catalysts fit the criterion of being active for the aromatization of acetone but their suitability for a potential scale-up needs to be evaluated by stability performance as catalyst deactivation hinders an economical use.

### 3.2. Assessing catalyst stability in batch and flow reactor

The stability of catalysts for the acetone aromatization is studied in batch autoclaves at 150 °C (Figure 2). After each reaction, the catalyst was filtered and washed thoroughly with acetone to remove organic depositions from the surface and then reused for subsequent reaction cycles after drying. Although a slight decrease in acetone conversion was observed using Puro-lite CT275DR, mesityl oxide and mesitylene yields showed no significant activity loss up to four experimental cycles (Figure 2a). After the first cycle, the catalyst mass had increased by almost 10% which remained for the consecutive runs and is likely linked to carbonaceous deposits [15]. Deposition of polymeric species generally deactivates active sites on catalysts, but interestingly it was not observed in the case of Puro-lite CT275DR. Therefore, we studied the reaction solutions and spent catalyst by monitoring pH and sulfur content, respectively. Highly acidic pH-values were found for the product solutions which increased from 1 to 3.5 in consecutive runs. Also, the sulfur content in the fresh and spent catalyst showed a significant reduction of 35% which directly translates to a loss in catalytically active sulfonic sites. This type of deactivation behavior of the highly

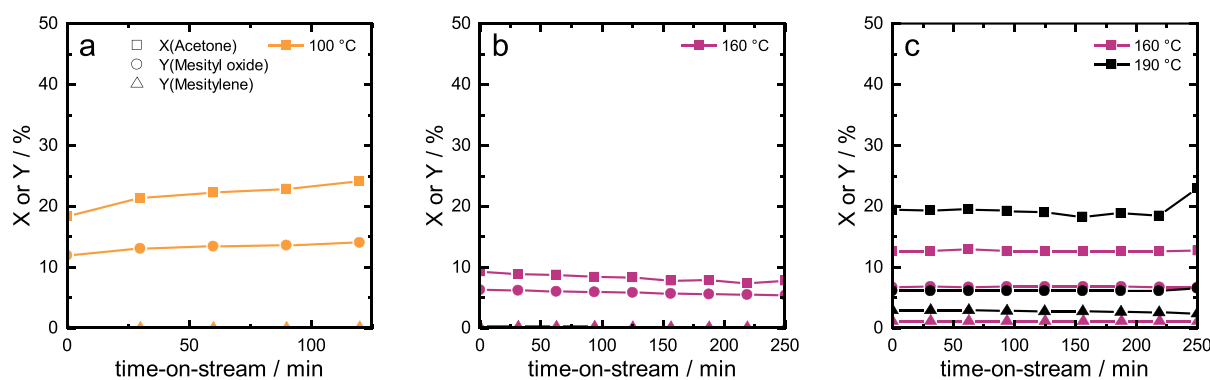


Fig. 3. Catalyst stability for acetone aromatization in liquid phase flow reactor for Puro-lite CT275DR (a), H-BEA 35 (b), and HY-zeolite (c). (square: acetone conversion, circle: mesityl oxide yield, and triangle: mesitylene yield).

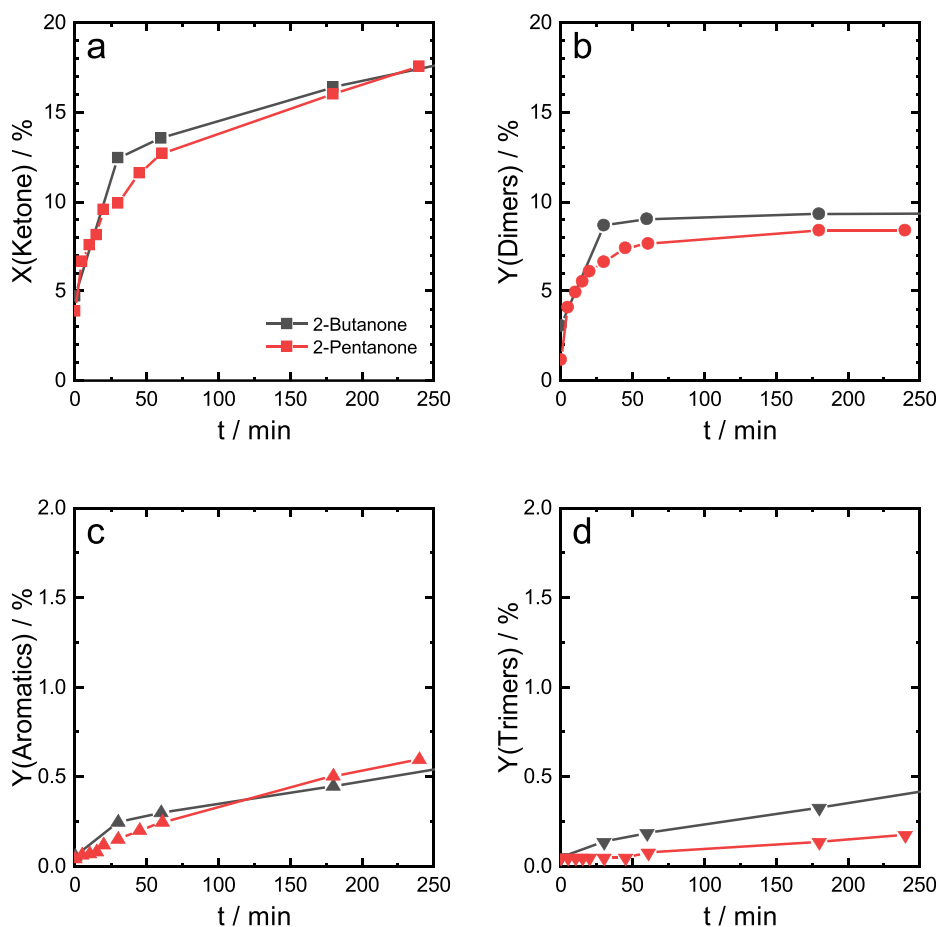


Fig. 4. Batch reaction progress for conversion (a) of 2-butanone and 2-pentanone with HY-60 at 160 °C and product yields of dimers (b), aromatics (c), and trimers (d).

active Purolite CT275DR catalyst was also observed in an esterification reaction by Saboya et al. [20] The finding can explain the concurrent decrease of active sites in the batch reactor responsible for constant acetone aromatization.

Figures 2b and 2c show a strong initial decrease in activity for both zeolites after the first cycle likely due to carbonaceous deposits (see Fig. S6). But an almost complete regeneration of active sites was achieved by simple calcination (550 °C, 6 h) which is widely practiced [21–23]. XRD analysis showed that the structural features remained unchanged after calcination (see Fig. S7). This means that all tested catalysts are generally recyclable according to their specific material properties. The observed leaching of active sites for Purolite CT275DR remains its biggest problem as it contradicts its use in a potential scale-up of continuous reaction conditions. For the latter, zeolite catalysts with regenerable activity have an advantage as automated regeneration processes such as implemented in fluid catalytic cracking exist in industry [24]. Furthermore, since neither precious metal catalysts nor hydrogen are involved in the deoxygenation reaction argon can be readily replaced with nitrogen for pressurizing the reactors to keep the reaction system in the liquid phase under batch reaction conditions and achieve similar yields (see Fig. S8).

In order to further understand the suitability of the selected catalysts for industrial importance, stability tests were performed in a flow reactor in the liquid phase at a weight hourly space velocity (WHSV) of

8 h<sup>-1</sup> (see Figure 3). Given the lower thermal stability of Purolite CT275DR it was tested at 100 °C to see its potential activity in a low-temperature continuous aromatization process. Although significant acetone conversion (up to 25%) and dimer formation (14%) were observed, no mesitylene was formed. An increase in reaction temperature to mimic previous batch experiment conditions at 150 °C led to agglomeration of the catalyst bed which ultimately blocked the flow reactor. The thermal degradation at elevated temperatures is intrinsic to the resin material, and thus renders it not suitable for flow conditions in the case of acetone aromatization.

The activity of the beta-zeolite in the flow reactor was very low with an acetone conversion below 10% and marginal formation of mesitylene observed at 160 °C (Figure 3b). The insignificant activity can likely be attributed to the dependence on external acid sites in the case of the beta-zeolite which are not active or too low in number for significant aromatization under the tested reaction conditions. This is in line with a previous study by Faba et al. [25] For HY-zeolite, on the other hand, a conversion of 12% and constant aromatics formation of 1.8% was found at 160 °C. An increase in temperature to 190 °C led to a significant increase in catalyst activity and mesitylene yield of 2.8%. Under the tested reaction conditions, the HY-catalyst was stable for more than 250 min-on-stream.

Given the stability in the flow reactor and the successfully applied regeneration under batch conditions, HY-zeolite can be considered as an



adequate catalyst for a potential industrial application of the aromatization of acetone in the liquid phase for both batch and flow reactors. An advantage of the liquid flow reactor is that no additional inert gas is required for pressurization or as carrier gas which can reduce costs.

### 3.3. Testing the HY-catalyst for higher alkyl methyl ketones in a batch reactor

While acetone is the simplest alkyl methyl ketone for the self-condensation reaction to biomass-derived 1,3,5-C<sub>6</sub>-aromatics, longer-chain alkyl methyl ketones such as 2-butanone and 2-pentanone can also be obtained in good yield from biomass [6,26,27]. Testing the suitability of the HY-zeolite with these higher ketones can extend its applicability for the formation of further alkyl aromatics. Batch experiments under reaction conditions similar to the one with acetone as starting material were therefore performed with 2-butanone and 2-pentanone (see Figure 4).

For both higher ketones, the time course experiments show a fast initial conversion of up to 10–15% in the first 50 min which is comparable with the acetone conversion activity of HY-60. Conversion then steadily increases over time to approximately 17–18% at 240 min. Dimer and aromatics formation is also observed and yields of both products increase with ketone conversion and time. For the intermediate dimer, a maximum yield is obtained within 50 min from when it remained constant. Yields of the aromatics and trimer products of the consecutive reaction of the dimers with another ketone molecule are constantly increasing over time. This shows that the catalyst remains active despite the larger molecular size of the compounds (kinetic diameter of 2-butanone: 0.52 nm [28]; 2-pentanone: 0.59 nm [29]). Considering the acetone conversion, dimer formation is comparable while yields of the consecutive products are roughly halved. This can likely be attributed to the lower overall reactivity of the higher alkyl methyl ketones compared with acetone due to steric hindrance.

## 4. Conclusions

Stable and efficient one-step conversion of ketones, a biomass-derived raw material, is realized using HY-zeolite as an acid catalyst at 150 °C. HY-zeolite is not only a suitable catalyst for the batch reactor but also showed high stability in the continuous liquid phase production of aromatics, e.g., mesitylene, in the flow reactor. Facile catalyst recovery and reusability of HY-zeolite in batch and flow conditions are essential for the establishment of a new environmentally benign process for alkyl methyl ketone aromatization.

Larger pores and a higher amount of acid sites are advantageous in the condensation reaction of ketones to aromatics in the liquid phase and determine catalyst activity and stability. While zeolite H-beta was more active in the batch reactor, a much higher activity of zeolite HY is observed in the flow reactor. The overall highest batch activity was found for the cation exchange resin Purolite CT275DR. However, it was not deemed suitable for a potential industrial application as it showed leaching of strong acid sites in recycling experiments and did not show substantial aromatization activity at 100 °C in the flow reactor. Further increasing the temperature (150 °C) eventually led to thermal degradation of the ion exchange resin in flow conditions.

### Credit author experiments

Phillip Reif performed the experiments. Phillip Reif, Navneet Kumar Gupta and Marcus Rose contributed to the design and implementation of the research. All authors analyzed the results and wrote the manuscript.

### Declaration of Competing Interest

The authors declare no conflict of interest.

### Acknowledgement

The authors gratefully acknowledge financial support from the German Federal Ministry of Education and Research (Grant No. 031B0680). NKG acknowledges the Alexander-von-Humboldt foundation for the financial support.

### Appendix A. Supplementary data

Supplementary data to this article can be found online at <https://doi.org/10.1016/j.catcom.2022.106402>.

### References

- [1] A.M. Niziolek, O. Onel, Y.A. Guzman, C.A. Floudas, Biomass-based production of benzene, toluene, and xylenes via methanol: process synthesis and deterministic global optimization, *Energy Fuel* 30 (2016) 4970–4998, <https://doi.org/10.1021/acs.energyfuels.6b00619>.
- [2] E. Barnard, J.J. Rubio Arias, W. Thielemans, Chemolytic depolymerisation of PET: a review, *Green Chem.* 23 (2021) 3765–3789, <https://doi.org/10.1039/D1GC00887K>.
- [3] A.K. Deepa, P.L. Dhepe, Solid acid catalyzed depolymerization of lignin into value added aromatic monomers, *RSC Adv.* 4 (2014) 12625, <https://doi.org/10.1039/c3ra47818a>.
- [4] E.A. Uslamin, N.A. Kosinov, E.A. Pidko, E.J.M. Hensen, Catalytic conversion of furanic compounds over Ga-modified ZSM-5 zeolites as a route to biomass-derived aromatics, *Green Chem.* 20 (2018) 3818–3827, <https://doi.org/10.1039/C8GC01528G>.
- [5] X. Tong, Y. Ma, Y. Li, Biomass into chemicals: conversion of sugars to furan derivatives by catalytic processes, *Appl. Catal. A* 385 (2010) 1–13, <https://doi.org/10.1016/j.apcata.2010.06.049>.
- [6] E.R. Sacia, M. Balakrishnan, M.H. Deaner, K.A. Goulas, F.D. Toste, A.T. Bell, Highly selective condensation of biomass-derived methyl ketones as a source of aviation fuel, *ChemSusChem* 8 (2015) 1726–1736, <https://doi.org/10.1002/cssc.201500002>.
- [7] G.S. Salvapati, K.V. Ramanamurthy, M. Janardanarao, Selective catalytic self-condensation of acetone, *J. Mol. Catal.* 54 (1989) 9–30, [https://doi.org/10.1016/0304-5102\(89\)80134-8](https://doi.org/10.1016/0304-5102(89)80134-8).
- [8] J.F. Adams, V.G. Papangelakis, Optimum reactor configuration for prevention of gypsum scaling during continuous sulphuric acid neutralization, *Hydrometallurgy* 89 (2007) 269–278.
- [9] E.V. Fufachev, B.M. Weckhuysen, P.C.A. Bruijninx, Tandem catalytic aromatization of volatile fatty acids, *Green Chem.* 22 (2020) 3229–3238, <https://doi.org/10.1039/D0GC00964D>.
- [10] A.G. Gayubo, A.T. Aguayo, A. Atutxa, R. Aguado, M. Olazar, J. Bilbao, Transformation of oxygenate components of biomass pyrolysis oil on a HZSM-5 zeolite. II. Aldehydes, ketones, and acids, *Ind. Eng. Chem. Res.* 43 (2004) 2619–2626, <https://doi.org/10.1021/ie030792g>.
- [11] J. Quesada, L. Faba, E. Díaz, S. Ordóñez, Effect of catalyst morphology and hydrogen co-feeding on the acid-catalysed transformation of acetone into mesitylene, *Catal. Sci. Technol.* 10 (2020) 1356–1367, <https://doi.org/10.1039/C9CY02288K>.
- [12] B. Yan, Z.-H. Liu, Y. Liang, B.-Q. Xu, Acrylic Acid Production by Gas-Phase Dehydration of Lactic Acid over K<sup>+</sup>-Exchanged ZSM-5: Reaction Variable Effects, Kinetics, and New Evidence for Cooperative Acid-Base Bifunctional Catalysis, *Ind. Eng. Chem. Res.* 59 (2020) 17417–17428, <https://doi.org/10.1021/acs.iecr.0c02148>.
- [13] R.M. Ravenelle, F. Schüßler, A. D'Amico, N. Danilina, J.A. van Bokhoven, J. A. Lercher, C.W. Jones, C. Sievers, Stability of zeolites in hot liquid water, *J. Phys. Chem. C* 114 (2010) 19582–19595, <https://doi.org/10.1021/jp104639e>.
- [14] P. Sun, D. Yu, Z. Tang, H. Li, H. Huang, NaY zeolites catalyze dehydration of lactic acid to acrylic acid: studies on the effects of anions in potassium salts, *Ind. Eng. Chem. Res.* 49 (2010) 9082–9087, <https://doi.org/10.1021/ie101093x>.
- [15] P. Reif, H. Rosenthal, M. Rose, Biomass-derived aromatics by solid acid-catalyzed aldol condensation of alkyl methyl ketones, *Adv. Sustainable Syst.* 4 (2020) 1900150, <https://doi.org/10.1002/adsu.201900150>.
- [16] Acetone, in: W.L. Howard, J.W.&.S. Inc, R.E. Kirk, D.F. Othmer (Eds.), *Kirk-Othmer Encyclopedia of Chemical Technology*, Wiley, New York, 2013, pp. 1–15.
- [17] Q. Jin, Y. Shen, S. Zhu, H. Li, Y. Li, Rare earth ions (La, Nd, Sm, Gd, and tm) regulate the catalytic performance of CeO<sub>2</sub>/Al<sub>2</sub>O<sub>3</sub> for NH<sub>3</sub>-SCR of NO, *J. Mater. Res.* 32 (2017) 2438–2445, <https://doi.org/10.1557/jmr.2017.125>.
- [18] S. Herrmann, E. Iglesia, Selective conversion of acetone to isobutene and acetic acid on aluminosilicates: kinetic coupling between acid-catalyzed and radical-mediated pathways, *J. Catal.* 360 (2018) 66–80, <https://doi.org/10.1016/j.jcat.2018.01.032>.
- [19] Ch. Baerlocher, L.B. McCusker, Database of Zeolite Structures. <http://www.iza-structure.org/databases/>. (Accessed 22 October 2021).
- [20] R.M.A. Saboya, J.A. Cecilia, C. García-Sancho, A.V. Sales, F.M.T. de Luna, E. Rodríguez-Castellón, C.L. Cavalcante, Assessment of commercial resins in the biolubricants production from free fatty acids of castor oil, *Catal. Today* 279 (2017) 274–285, <https://doi.org/10.1016/j.cattod.2016.02.020>.

- [21] Z. Ma, J.A. van Bokhoven, Deactivation and regeneration of H-USY zeolite during lignin catalytic fast pyrolysis, *ChemCatChem* 4 (2012) 2036–2044, <https://doi.org/10.1002/cctc.201200401>.
- [22] A.A. Costa, P.R. Braga, J.L. de Macedo, J.A. Dias, S.C. Dias, Structural effects of WO<sub>3</sub> incorporation on USY zeolite and application to free fatty acids esterification, *Microporous Mesoporous Mater.* 147 (2012) 142–148, <https://doi.org/10.1016/j.micromeso.2011.06.008>.
- [23] E. Xing, Z. Mi, C. Xin, L. Wang, X. Zhang, Endo- to exo-isomerization of tetrahydrocyclopentadiene catalyzed by commercially available zeolites, *J. Mol. Catal. A Chem.* 231 (2005) 161–167, <https://doi.org/10.1016/j.molcata.2005.01.015>.
- [24] E.T.C. Vogt, B.M. Weckhuysen, Fluid catalytic cracking: recent developments on the grand old lady of zeolite catalysis, *Chem. Soc. Rev.* 44 (2015) 7342–7370, <https://doi.org/10.1039/C5CS00376H>.
- [25] L. Faba, J. Gancedo, J. Quesada, E. Diaz, S. Ordóñez, One-pot conversion of acetone into Mesitylene over combinations of acid and basic catalysts, *ACS Catal.* 11 (2021) 11650–11662, <https://doi.org/10.1021/acscatal.1c03095>.
- [26] H. Yoneda, D.J. Tantillo, S. Atsumi, Biological production of 2-butanone in *Escherichia coli*, *ChemSusChem* 7 (2014) 92–95, <https://doi.org/10.1002/cssc.201300853>.
- [27] A. Corma, O. de La Torre, M. Renz, Production of high quality diesel from cellulose and hemicellulose by the sylvan process: catalysts and process variables, *Energy Environ. Sci.* 5 (2012) 6328, <https://doi.org/10.1039/c2ee02778j>.
- [28] P. Monneyron, M.-H. Manero, J.-N. Foussard, Measurement and modeling of single- and multi-component adsorption equilibria of VOC on high-silica zeolites, *Environ. Sci. Technol.* 37 (2003) 2410–2414, <https://doi.org/10.1021/es026206c>.
- [29] M.-H. Lai, R.Q. Chu, H.-C. Huang, S.-H. Shu, T.-W. Chung, Equilibrium isotherms of volatile alkanes, alkenes, and ketones on activated carbon, *J. Chem. Eng. Data* 54 (2009) 2208–2215, <https://doi.org/10.1021/jc800826d>.



---

## Supporting Information

### **Liquid phase aromatization of bio-based ketones over a stable solid acid catalyst under batch and continuous flow conditions**

*Phillip Reif<sup>1</sup>, Navneet Kumar Gupta<sup>1\*</sup>, Marcus Rose<sup>1\*</sup>*

<sup>1</sup>Technical University of Darmstadt, Department of Chemistry, Alarich-Weiss-Straße 8, 64287 Darmstadt, Germany.

**E-mail:** NKG: navneetguptatum@gmail.com; navneet.gupta@gast.tu-darmstadt.de

MR: marcus.rose@tu-darmstadt.de

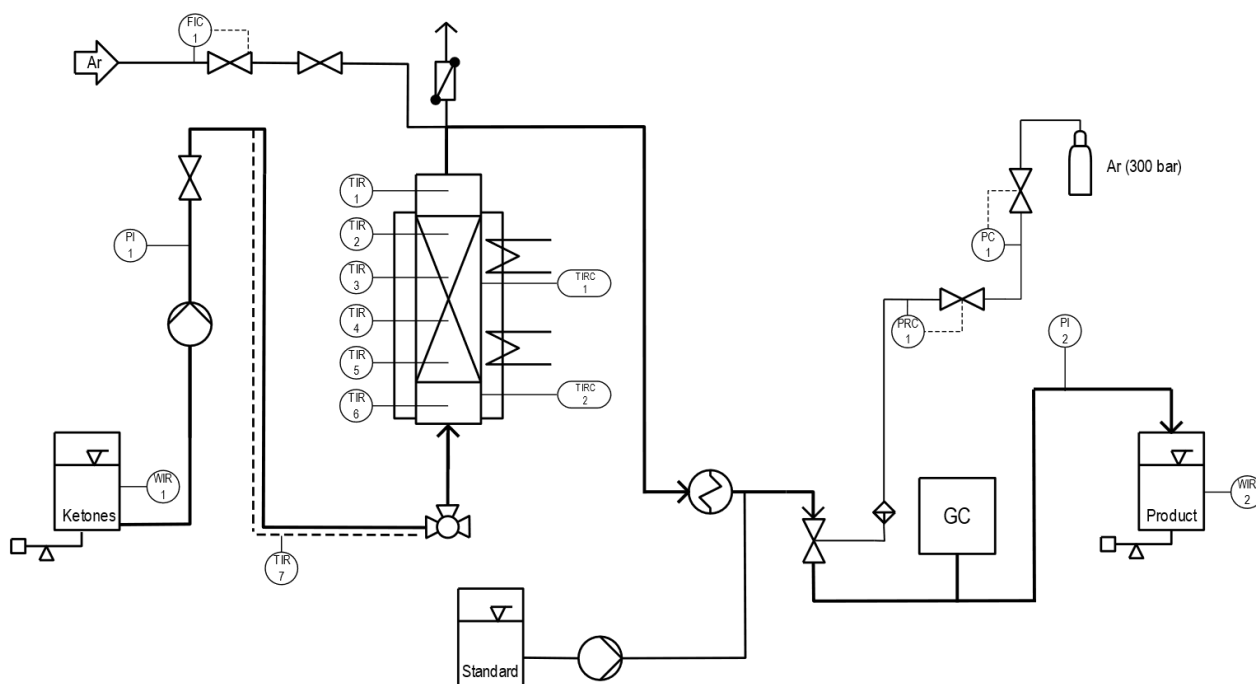


**Figure S1:** Process flow diagram of the liquid-phase fixed-bed reactor.

### Calculation of conversion X, product yield Y, and selectivity S:

Conversion of alkyl methyl ketone X:

$$X_{\text{Ketone}} = 1 - \frac{n_{\text{Ketone}}}{n_{\text{Ketone},0}}$$

with  $n$ : substance amount in mol

Product yields Y:

$$Y_i = \frac{|v_{\text{Ketone}}| n_i}{v_i n_{\text{Ketone},0}}$$

with  $v$ : stoichiometry of the reactant in the reaction

Product selectivity S:

$$S_i = \frac{Y_i}{X_{\text{Ketone}}}$$

The substance amounts are obtained via response factors  $RF$  based on the internal standard (IS) 1,4-dioxane obtained from GC-calibration, and the measured substance areas  $A$ . In case of acetone as starting ketone, calibration substances were used for mesityl oxide (dimer), mesitylene (aromatic), and isophorone (trimer).

$$\frac{A_i}{A_{IS}} = \frac{w_i}{w_{IS}} RF$$

with  $w$ : weight fraction

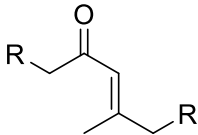
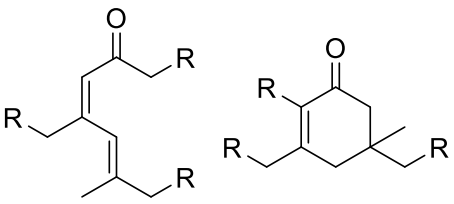
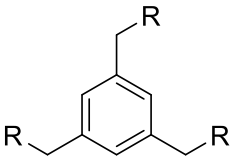
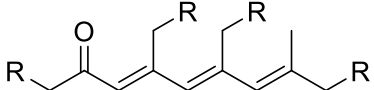
For the higher alkyl methyl ketones 2-butanone and 2-pentanone, only the ketones and the aromatic triethylbenzene were available for calibration. Therefore, the concept of the *effective carbon number* ( $ECN$ ) with the relative response factors  $RRF$  was used based on the molecular weight ( $MW$ ) and calculated  $ECN$  of the substance and a structurally similar reference substance  $R$ . [1]

$$RRF_i = \frac{MW_i}{MW_R} \cdot \frac{ECN_R}{ECN_i}$$

The reference substances are the corresponding dimers, trimers, and aromatics of the acetone condensation. The tetramers of the acetone condensation are based on the structurally similar dimer mesityl oxide. The many positional isomers existing for the products of higher ketones were grouped together and the corresponding area sums were used for calculation.

## Product characterization for 2-butanone and 2-pentanone aromatization

The product reaction solutions were vacuum distilled, and the fractions were analyzed via GC-MS as described in the experimental procedure. Product identification was based on the ratio of  $m/z$  and characteristic fragmentation patterns.

Structure + positional isomers	Product	Acetone	2-Butanone	2-Pentanone
		(R = H) / $m/z$	(R = CH <sub>3</sub> ) / $m/z$	(R = C <sub>2</sub> H <sub>5</sub> ) / $m/z$
	Dimer	98	126	154
	Trimer	138	180	222
	Aromatic	120	162	204
	Tetramer	178	234	290

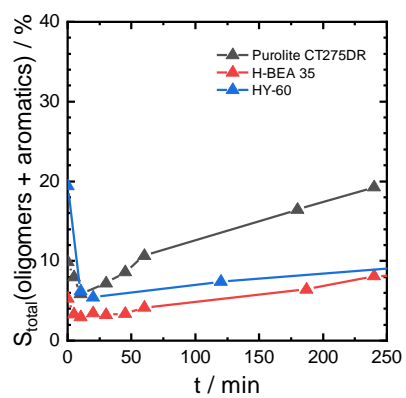


**Figure S2:** Progress of total selectivity for aromatics, tri- and tetramers for the selected catalysts at 150 °C. Reaction conditions: 150 mL acetone, 2.5 wt% catalyst, 30 bar Ar.

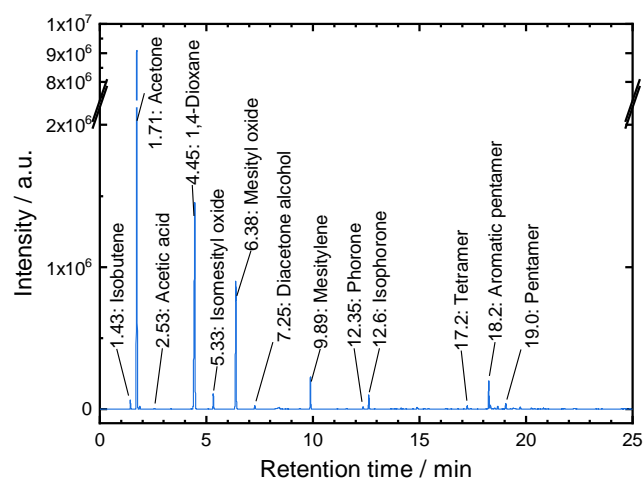


**Figure S3:** Representative GC-chromatogram of the product mixture using acetone as starting material for the reaction with HY-60 at 150 °C (3 h) with 1,4-dioxane as internal standard. The identified products amount to more than 95 % of the product GC-area.

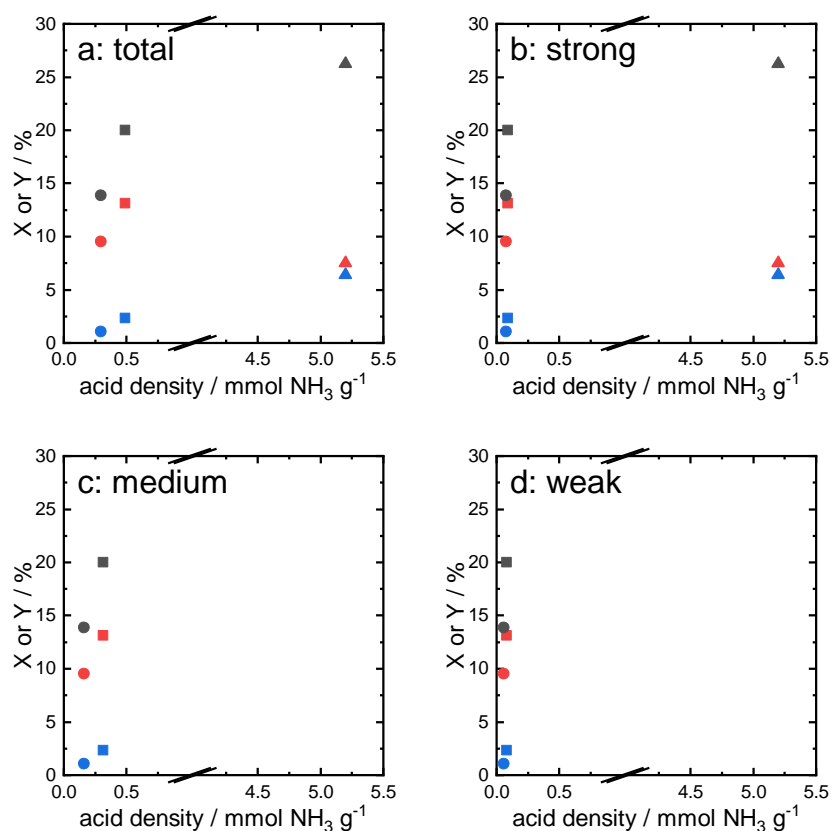


**Figure S4:** Catalyst activity vs. acid site density for total (a), strong (b), medium (c), and weak (d) acid strength. Catalysts are depicted by shapes (triangle: Purolite CT275DR, square: H-BEA 35, circle: HY-60). Conversion and product yields are marked by colors (black: X(acetone), red: Y(mesityl oxide), blue: Y(mesitylene)).

The acid density of solid acid catalyst was determined via NH<sub>3</sub>-TPD (see Experimental) and the strength of acid sites was estimated on their desorption temperatures based on the following classification: < 250 °C weak, 250-450 °C medium, and >450 °C strong.[2]

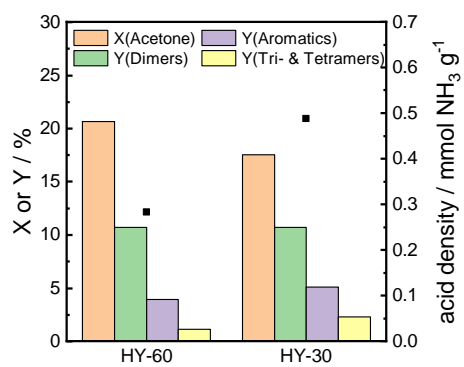


**Figure S5:** Comparison of HY-zeolites with different Si/Al ratios for the acetone conversion at 150 °C and 3 h. Also shown are the acid site densities determined via NH<sub>3</sub>-TPD (black dots).



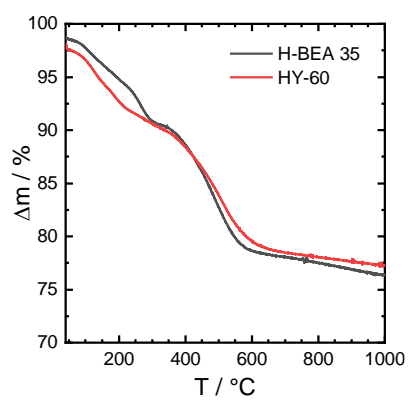


**Figure S6:** Thermogravimetric analysis of recycled zeolites H-BEA 35 and HY-60 used in the batch aromatization of acetone.

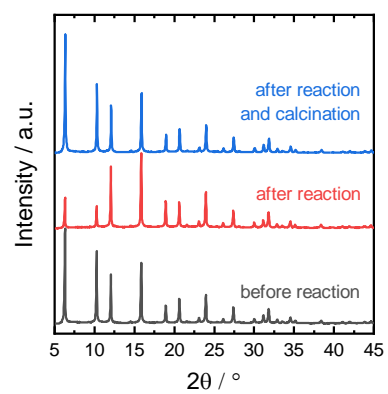


**Figure S7:** XRD patterns of HY-60 before and after the reaction of acetone and after calcination treatment of the spent catalyst.

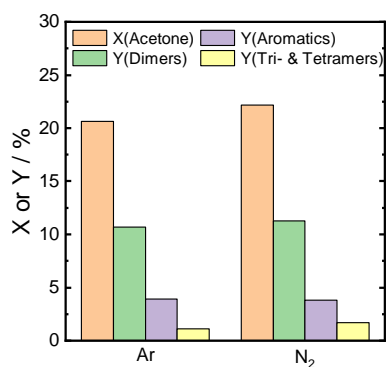


**Figure S8:** Results of batch reaction of acetone with HY-60 under argon or nitrogen atmosphere (40 bar) at 150 °C and 3 h.

## References

- [1] K. Dettmer-Wilde, *Practical Gas Chromatography: A Comprehensive Reference*, Springer Berlin / Heidelberg, Berlin, Heidelberg, 2014.
- [2] Q. Jin, Y. Shen, S. Zhu, H. Li, Y. Li, Rare earth ions (La, Nd, Sm, Gd, and Tm) regulate the catalytic performance of CeO<sub>2</sub>/Al<sub>2</sub>O<sub>3</sub> for NH<sub>3</sub>-SCR of NO, *J. Mater. Res.* 32 (2017) 2438–2445. <https://doi.org/10.1557/jmr.2017.125>.

### 4.3. Highly stable amorphous silica-alumina catalysts for continuous bio-derived mesitylene production under solvent-free conditions

Authors: P. Reif, N. K. Gupta, M. Rose

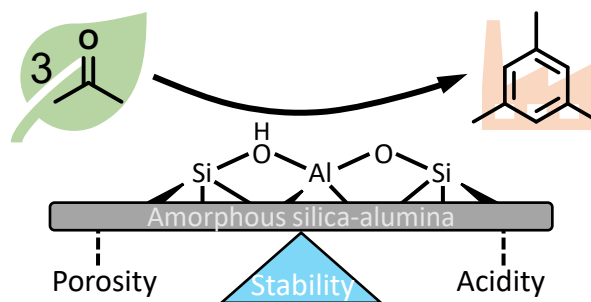
Journal: Green Chemistry

Date: 30 January 2023

DOI: <https://doi.org/10.1039/D2GC04116B>

© 2023 Published by The Royal Society of Chemistry.

This is an open access article under the CC BY 3.0 license. It is reproduced with permission from the Royal Society of Chemistry.



A technical process requires suitable catalytic activity, which zeolite H-Y lacked in the previous study despite its promising stability. Therefore, it was attempted to improve its aromatization activity by increasing the reaction temperature, but deactivation due to coking occurred above 200 °C. Simultaneously, amorphous silica-alumina was revisited as a catalyst, and the ASA Siralox 30 was evaluated under continuous flow conditions. Notably, Siralox 30 did not show signs of deactivation even at elevated reaction temperatures of 220 °C, where the steady-state mesitylene yield was higher compared to zeolite H-Y. This finding confirmed that catalyst stability in the liquid-phase aromatization of ketones benefits from the enhanced mass transport in larger catalyst pores. Based on this a detailed study of amorphous silica-alumina as aromatization catalysts was performed and published in *Green Chemistry*.<sup>[134]</sup> It was found that the large mesopores of ASA combined with their moderate density of acid sites results in the observed long-term catalytic stability in contrast to microporous zeolites with a high number of strong acid sites. Steady-state conditions of more than 50 h time-on-stream were achieved at 260 °C under supercritical conditions. By optimization of the process conditions, a maximum space-time-yield ( $W/F$  of 12.5  $\text{g}_{\text{cat}} \text{h mol}^{-1}$ ) of 10.1% for mesitylene with 66% total product selectivity was obtained. Characterization of the spent catalyst showed a low amount of coking and no structural changes. The large mesopores also allow a long-term stable conversion of the bulkier alkyl methyl ketone 2-butanone to its aromatic trimers under the established process conditions. To elucidate the efficiency of ASA in the aromatization of alkyl methyl ketones, the structure-activity relationship was analyzed. ASA are formed by doping alumina with silica, thus creating BAS on the catalyst surface, depending on the silica doping. The influence of silica content was studied and compared to pure silica and  $\gamma$ -alumina. For acetone aromatization, it was found that doping-increased acidity and enhanced BAS lead to an optimum in acid site strength and density at 30-40 wt% silica, which was supported by literature data. Higher silica loadings lead to a decrease in the number of BAS as the catalyst surface becomes

---

increasingly silica-dominated. The results of the study display that commercially available ASA combine remarkable catalytic stability with high product selectivity, making them suitable for a potential technical application in the conversion of biomass-derived ketones to aromatics. Based on this, a conceptual process for the continuous aromatization of acetone to mesitylene was proposed. One of its advantages is cost effectiveness, as the process requires no additional solvent and, by using ASA, does not rely on precious metals or hydrogen for deoxygenation. The demonstrated high stability in a fixed-bed reactor allows direct integration into existing continuous biorefinery streams, thus adding value and contributing to a bio-based chemical production. The products can be efficiently separated by distillation due to their large differences in boiling points. As a solvent-free process, it is also energy-efficient and saves operating costs. Through recycling of acetone and its dimer mesityl oxide, process efficiency can be further increased. A process based on ketones as feedstock and ASA as catalysts therefore represents an attractive pathway from biomass to aromatics and can be considered a significant contribution to a more sustainable production of aromatic-based compounds.



Cite this: *Green Chem.*, 2023, 25, 1588

## Highly stable amorphous silica-alumina catalysts for continuous bio-derived mesitylene production under solvent-free conditions†

Phillip Reif, <sup>a</sup> Navneet Kumar Gupta <sup>a,b</sup> and Marcus Rose <sup>a</sup>

Aromatization of alkyl methyl ketones obtained from biorefinery streams is a viable and attractive catalytic pathway to renewable aromatics, precursors for various important monomers and chemicals. To achieve high catalytic activity and stability under continuous conditions, mesoporous amorphous silica-alumina (ASA) catalysts are studied for the acid-catalyzed self-condensation of biomass-derived acetone to mesitylene in solvent-free conditions using a fixed-bed reactor. The catalytic efficiency of ASA catalysts depends on their structure and intrinsic acidity. In comparison to pure alumina, ASA Siralox 30 exhibits a 2.2 times higher catalytic activity for acetone conversion and 3.8 times higher mesitylene yield, demonstrating the importance of Brønsted acid sites (BAS) generated in ASA catalysts. The detailed kinetic studies and catalyst characterization indicate that mesitylene formation is favored over BAS and that the formation rate is enhanced with the relative strength of BAS. We demonstrate here that Siralox 30 (total product selectivity = 66%,  $W/F = 12.5 \text{ g}_{\text{cat}} \text{ h mol}^{-1}$ ) is an adequate and highly active catalyst for the continuous mesitylene synthesis with remarkable long-term operational stability (>50 hours-on-stream).

Received 2nd November 2022,  
Accepted 26th January 2023

DOI: 10.1039/d2gc04116b

rsc.li/greenchem

### 1. Introduction

The transition from fossil to renewable resources presents one of today's greatest challenges. Their steady depletion and contribution to global warming are driving factors for implementing a more sustainable circular economy which includes using biomass for chemicals and fuels production.<sup>1</sup> Especially for household products that frequently contain polymers, there is a strong consumer demand for green alternatives due to environmental concerns and awareness.<sup>2</sup> Many of these polymers possess aromatic monomers, *e.g.*, *p*-xylene for polyethylene terephthalate (PET), styrene for polystyrene (PS), toluene diisocyanate for polyurethanes (PUR), derived from benzene, toluene, and xylene (BTX) of which more than 122 Mt are produced annually, also for use in solvent and fuel applications.<sup>3</sup> As of today, aromatics are obtained by catalytic reforming of naphtha, a crude oil fraction.<sup>4</sup> Thus, using biomass as raw material feedstock for their production, ideally conceived as a drop-in solution, opens the door to a large variety of renewably

sourced products without requiring modification of the existing infrastructure downstream.

Several routes to biomass-derived aromatics have been reported. Among those, one important pathway is the selective Diels-Alder cycloaddition of furanic compounds, especially furan derivatives, with dienophiles such as bio-ethylene.<sup>5</sup> High costs associated with the production of furan and its derivatives from biomass are currently the biggest drawback.<sup>6</sup> Another fundamental route is the depolymerization of lignin by (catalytic) fast pyrolysis which yields a "bio-oil", a complex mixture of oxygenated aromatic compounds.<sup>7</sup> These require extensive purification, separation, and deoxygenation to obtain alkyl aromatics suitable for downstream processing. A more selective but less explored pathway is the self-condensation of alkyl ketones. The C-C coupling reaction of alkanones *via* robust acid/base-catalyzed condensation is an efficient way to achieve deoxygenated aromatics from existing biorefinery streams, *e.g.*, acetone from ABE-fermentation, in a single-step reaction without further need for metal-catalyzed dehydrogenation or upgrading *via* deoxygenation with hydrogen.<sup>8-11</sup> Furthermore, gas-phase fermentation by autotrophic acetogens offers a highly promising carbon-negative route to acetone.<sup>12</sup> Therefore, the efficient utilization of acetone *via* self-condensation for the formation of the aromatic product mesitylene (1,3,5-trimethylbenzene) is the focus of this study.

Previously, the self-condensation of acetone is mainly studied in the gas phase under atmospheric pressure, often at

<sup>a</sup>Technical University of Darmstadt, Department of Chemistry, Alarich-Weiss-Straße 8, 64287 Darmstadt, Germany. E-mail: marcus.rose@tu-darmstadt.de

<sup>b</sup>Centre for Sustainable Technologies, Indian Institute of Science, Gulmohar Marg, Mathikere, 560012 Bengaluru, India. E-mail: nkgupta@iisc.ac.in

† Electronic supplementary information (ESI) available. See DOI: <https://doi.org/10.1039/d2gc04116b>



high reaction temperatures above 400 °C using various solid acid catalysts such as zeolites, titania, zirconia, niobia, mesoporous aluminosilicates, and tantalum phosphate.<sup>13–17</sup> Despite the high catalytic activity, the formation of polycondensates on the strongly acidic catalysts leads to fast catalyst deactivation due to carbonaceous deposits which remains an inherent challenge.<sup>18</sup> Faba *et al.*, showed an increase in productivity for the gas-phase conversion of acetone over a mixed catalyst bed of TiO<sub>2</sub> and Al-MCM-41 at 250 °C but lacked the proof of long-term stability.<sup>17</sup>

Recently, we showed that zeolite HY is stable for the mesitylene formation in the liquid phase over several hours at 190 °C.<sup>19</sup> The larger pores of zeolite Y compared to other microporous zeolites proved to be beneficial for the catalyst stability.<sup>20</sup> Additionally, the liquid phase conditions allowed continuous removal of products from the catalyst bed, thus reducing carbonaceous deposits.<sup>21</sup> While zeolite HY was also applicable for the aromatization of larger alkyl methyl ketones, such as 2-butanone and 2-pentanone, its overall activity was still lacking regarding a potential process development for future integration into a biorefinery.<sup>19</sup> In the course of the catalyst development, combining high activity with long-term operational stability remains an ongoing problem that we sought to solve by using large pore amorphous aluminosilicates as acid catalysts.

Herein, we report that ASA afforded remarkable activity and selectivity for mesitylene from acetone under continuous conditions not only in liquid but also in supercritical phase. The ASA catalysts were beneficial due to their combination of larger mesopores and moderate overall acid site density of medium strength with a lower number of strong Brønsted acid sites.<sup>22–25</sup> The optimization of reaction conditions and long-term catalyst stability are examined for maximum mesitylene space–time–yield on ASA. Assessment of the acidity–activity–relationship for this material class is performed based on the degree of silica-doping.

## 2. Experimental

### 2.1 Materials

Commercial amorphous silica-alumina (denoted as ASA) were supplied by Sasol Germany GmbH and used after calcination in air at 550 °C for 6 h (2 K min<sup>-1</sup>, 100 NmL min<sup>-1</sup>). HY-5 catalyst was obtained by exchanging NaY three times with an aqueous solution of NH<sub>4</sub>NO<sub>3</sub> (1 M, 60 °C, 1 h) and subsequent calcination in air (2 K min<sup>-1</sup>, 550 °C, 6 h, 100 NmL min<sup>-1</sup>). γ-Al<sub>2</sub>O<sub>3</sub> (99.9%) was obtained from Alfa Aesar and Evonik Aeroperl 300/30 was used as pure SiO<sub>2</sub>.

Acetone (99%) was obtained from Sigma-Aldrich and used without further purification. For the GC standard solution, 1,4-dioxane (99.5%, Roth) was diluted with 1-butanol (99%, Grüssing).

For GC-calibration, acetone (99.9%, Sigma Aldrich), mesityl oxide (97%, Sigma Aldrich), mesitylene (99%, Acros Organics), isophorone (97%, Sigma Aldrich), 2-butanone (99%, Sigma Aldrich), and 1,3,5-triethylbenzene (97%, Sigma Aldrich) were used.

### 2.2 Catalytic studies in fixed-bed flow reactor

Catalytic studies were performed in a previously described fixed-bed reactor in upward flow configuration (Fig. S1†).<sup>19</sup> Briefly, 3 g of catalyst were placed in the isothermal zone in the center of the stainless-steel reactor (ID = 1.6 cm, length = 20 cm). The catalyst powders were pressed (8 ton, 5 min), crushed, and sieved to 100–200 micron particles to avoid mass transfer limitations (Fig. S2†). Neat acetone was fed into the reactor with an HPLC pump, and the reaction was performed at 200–300 °C and 75 bar to maintain liquid/supercritical conditions. The outlet of the reaction feed was continuously mixed with a standard solution of 1,4-dioxane (1.15 mol L<sup>-1</sup>) in 1-butanol downstream. The product solution was analyzed *via* online-gas chromatography (Shimadzu GC-2030, MEGA-5 column, 40–250 °C, 10 K min<sup>-1</sup>, H<sub>2</sub>) equipped with an FID (Fig. S3†). Acetone, mesityl oxide, mesitylene, isophorone, 2-butanone, and 1,3,5-triethylbenzene were calibrated with pure compounds while the other identified products were estimated *via* the concept of the effective carbon number combined with GC-MS.<sup>19,26</sup>

### 2.3 Catalyst characterization

Powder X-ray diffraction (XRD) measurements were performed on a Bruker D2-phaser using Cu-Kα-radiation ( $\lambda = 1.5406 \text{ \AA}$ ) with a radiation tube voltage of 30 kV and current of 40 mA. Diffraction patterns were measured in 10–80° 2 $\theta$  at 0.02° intervals and 1 s step time.

N<sub>2</sub>-physisorption was measured on a Quantachrome QuadraSorb at 77 K after evacuating the samples (approx. 30–100 mg) at 300 °C over night. The specific surface area ( $S_{\text{BET}}$ ) was obtained with the Brunauer–Emmett–Teller method. The micropore area was determined by the *t*-plot method.

Thermogravimetric analysis (TGA) of the spent catalysts was performed on a NETZSCH STA 449 FE Jupiter by heating (5 K min<sup>-1</sup>, 40–1000 °C) the samples (50 mg) in synthetic air (100 NmL min<sup>-1</sup>).

Temperature-programmed desorption of NH<sub>3</sub> (NH<sub>3</sub>-TPD) was used to measure the total amount of acid sites on the silica-alumina catalysts. For this, samples (100 mg) were dried in N<sub>2</sub> flow (100 NmL min<sup>-1</sup>) at 600 °C (10 K min<sup>-1</sup>, 3 h) and subsequently loaded with NH<sub>3</sub> (2 vol% NH<sub>3</sub> in N<sub>2</sub>, 20 mL min<sup>-1</sup>) at 140 °C. When the physisorbed NH<sub>3</sub> was desorbed, the samples were heated to 600 °C (10 K min<sup>-1</sup>) in N<sub>2</sub> flow (100 NmL min<sup>-1</sup>). The amount of chemisorbed NH<sub>3</sub> was detected by FT-IR.

## 3. Results and discussion

### 3.1 Catalyst stability of zeolite HY compared to amorphous silica-alumina

In our previous work, zeolite HY was identified as a suitable solid acid catalyst for the efficient and stable liquid phase conversion of biomass-derived ketones to aromatics due to its larger pore size and high amount of acid sites.<sup>19</sup> Catalytic activity of HY increased with temperature and at 190 °C steady-



state conditions were obtained for the continuous conversion of acetone to mesitylene. However, catalyst productivity was relatively low with 3% mesitylene yield at a weight hourly space velocity (WHSV) of  $7.8 \text{ h}^{-1}$ . When the reaction temperature was raised to  $200 \text{ }^\circ\text{C}$ , the initial productivity significantly increased to about twofold but the activity steadily decreased with time-on-stream due to catalyst deactivation (Fig. 1). In contrast, ASA Siralox 30 is found to be very stable when converting acetone to mesitylene under similar reaction conditions ( $200 \text{ }^\circ\text{C}$ ,  $\text{WHSV} = 7.8 \text{ h}^{-1}$ ). While its activity at  $200 \text{ }^\circ\text{C}$  is lower compared to zeolite HY, it shows a three-times increase in mesitylene yield to 4% for  $220 \text{ }^\circ\text{C}$ . Even at this elevated temperature, the catalyst activity remains very stable for more than 7 hours-on-stream and shows no deactivation. To understand the difference in stability of HY-5 and Siralox 30, relevant properties of the solid acid catalysts are compared in Table 1. The surface area of the mostly microporous zeolite HY-5 is  $778 \text{ m}^2 \text{ g}^{-1}$  and four-times higher than the one of Siralox 30 which is completely mesoporous (Fig. S4†). The number of surface acid sites is higher on HY-5 with  $0.53 \text{ mmol g}^{-1}$  compared to  $0.30 \text{ mmol g}^{-1}$  on Siralox 30. This results in a significantly higher activity of HY-5 at reaction temperatures below  $200 \text{ }^\circ\text{C}$  since mesitylene activity correlates with the number of acid sites.<sup>19</sup> Moreover, the strength of the acid sites on HY-5 is also greater than on Siralox 30 as evidenced by the higher temperature of the maximum  $\text{NH}_3$  desorption (Fig. S5†). Thermogravimetric

analysis of the spent catalysts in air determines a total mass loss of 20 wt% for HY-5 of which more than 17 wt% correspond to strongly bound, bulky carbonaceous deposits (Fig. S6†). Siralox 30, on the other hand, shows a minimal weight loss of 3.3 wt% from  $200\text{--}600 \text{ }^\circ\text{C}$  which could be due to weakly bound deposits. Thus, the stronger and greater number of acid sites on HY-5 are not only more active, but also lead to increased carbon deposition.<sup>27</sup> Those block the catalyst pores, and thus decrease the accessibility of active sites, as highlighted by the strongly diminished microporous surface area of spent HY-5 (Table 1). The observed slight increase in the mesoporous surface area of HY is due to carbon deposition as confirmed by TGA. In comparison, the surface area of spent Siralox 30 is almost completely retained due to its mesoporous structure and after calcination of the spent catalyst the number of surface acid sites is equivalent to the fresh sample.

Hence, at higher reaction temperatures (more than  $190 \text{ }^\circ\text{C}$ ), mass transport out of the zeolite HY pores is slow compared to the formation of bulkier molecules favored by its stronger acid sites, resulting in quick deactivation of the catalyst. However, Siralox 30 remains stable even at higher temperatures due to its better mass transport capabilities and lower number of stronger acid sites.<sup>25</sup> In this way, it is possible to greatly improve the activity of the catalyst with temperature without compromising stability. Therefore, the ASA Siralox 30 is a highly interesting solid acid catalyst for the liquid-phase aromatization of acetone and requires a deeper study of optimal reaction conditions for maximum activity and efficiency in the continuous flow process.

### 3.2 Process optimization for the efficient acetone aromatization using ASA

**Influence of reaction temperature.** Previous experiments have shown that the aromatization activity is strongly influenced by the reaction temperature, so the optimal temperature for mesitylene formation was initially assessed. Acetone conversion increases almost linearly with temperature from 17 to 63% between  $200$  and  $300 \text{ }^\circ\text{C}$  (Fig. 2). At harsh reaction temperatures of  $280 \text{ }^\circ\text{C}$  and above, there are notable fluctuations in the measured acetone conversions as represented by the increased error over five measurements at steady-state conditions. The selectivity to mesitylene shows a steady incline from 11% at  $200 \text{ }^\circ\text{C}$  to a maximum of 38% at  $260 \text{ }^\circ\text{C}$  but decreases for higher reaction temperatures as acetone is primarily converted to undetected products. The selectivity to the

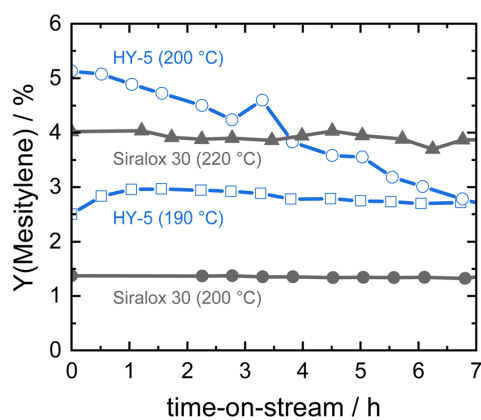


Fig. 1 Catalyst stability of silica-alumina HY-5 and Siralox 30 based on mesitylene yield at different reaction temperatures ( $7.8 \text{ h}^{-1}$ , 40 bar).

Table 1 Characterization data of fresh and spent HY-5 ( $200 \text{ }^\circ\text{C}$ ) and Siralox 30 ( $220 \text{ }^\circ\text{C}$ )

Catalyst	Textural properties					Crystallinity	Total amount of acid sites/ $\text{mmol NH}_3 \text{ g}^{-1}$	Mass loss/%
	BET surface area/ $\text{m}^2 \text{ g}^{-1}$	Microporous area/ $\text{m}^2 \text{ g}^{-1}$	Mesoporous area/ $\text{m}^2 \text{ g}^{-1}$	Total pore volume/ $\text{cm}^3 \text{ g}^{-1}$	Average pore diameter/nm			
HY-5	778	709	69	0.34	1.73	Crystalline	0.53	
Siralox 30	199	0	199	0.59	12.3	Amorphous	0.30	
HY-5 spent	230	121	109	0.16	2.74	Crystalline		20
Siralox 30 spent	190	0	190	0.58	11.6	Amorphous		3.3





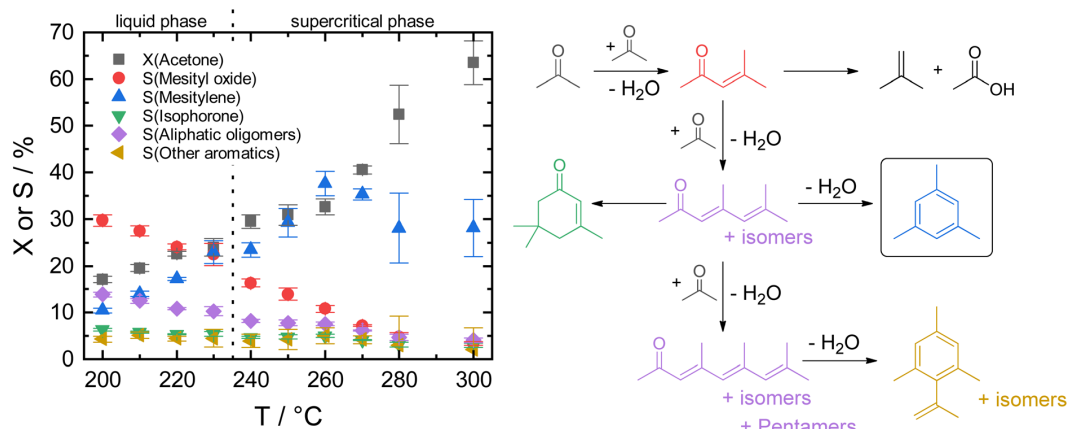


Fig. 2 Left: acetone conversion and product selectivity for Siralox 30 at different reaction temperatures (WHSV = 7.8 h<sup>-1</sup>, 75 bar) in liquid and supercritical acetone. Error bars give the standard deviation of the GC measurements at steady-state conditions. Right: a simplified network of the acid-catalyzed self-condensation of acetone.

dimer mesityl oxide decreases with reaction temperature as the consecutive aromatization to mesitylene is favored. While the selectivity to linear and branched aliphatic oligomers declines with temperature, the formation of the non-aromatic cyclic trimer isophorone is not significantly affected. At 240 °C and above, the formation of mesitylene is favored and identified as the main product. Total product selectivity at 260 °C is 66%, demonstrating that the reaction is effective even at elevated temperatures. The carbon balance for the conversion of acetone to mesitylene is 91% and no additional impact is observed when switching from liquid acetone to supercritical acetone above 235 °C.<sup>28</sup>

By varying the reaction temperature, a strong influence on the mesitylene activity is found with a maximum selectivity at 260 °C for Siralox 30. The following experiments were therefore carried out at 260 °C.

**Variation of the space-time-yield with Siralox 30.** Besides reaction temperature, space-time-yield is an important factor for process efficiency. In order to optimize the space-time-yield of the acetone aromatization with Siralox 30, the weight-to-flow ratio of catalyst mass  $W$  to acetone molar flow  $F$  is varied at 260 °C, the point of highest mesitylene selectivity. The acetone conversion and mesitylene yield increase for longer contact times which is represented by higher  $W/F$  ratios but mesitylene yield does not benefit from ratios higher than 12.5 g<sub>cat</sub> h mol<sup>-1</sup> where it is 10.1% (Fig. 3). The further increase in acetone conversion is a result of increased byproduct formation due to significantly longer catalyst contact times. The yield of mesityl oxide decreases for higher  $W/F$  ratios, indicating intermediate formation of the dimerization product and subsequent conversion to mesitylene. There was no significant effect of contact time on the formation of oligomers and isophorone. For a variation at 210 °C in liquid phase (Fig. S7†), a constant increase in mesitylene yield to only 8% was observed at a  $W/F$  ratio of 75. It can therefore be concluded

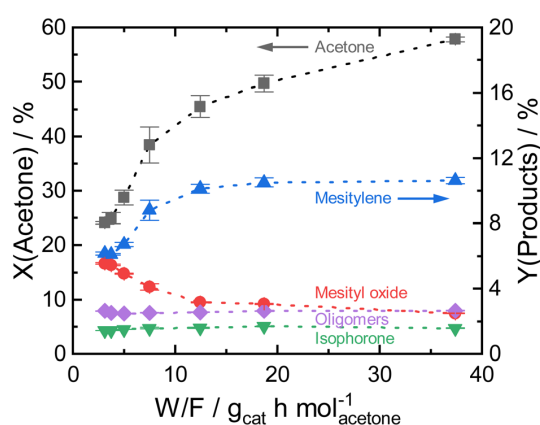


Fig. 3 Acetone conversion and product yields as a function of contact time for Siralox 30 at 260 °C. The dotted lines are only for visual guidance.

that the increased reaction temperature leads to more efficient catalysis of the acetone condensation and thus allows for faster contact times compared to lower reaction temperatures. A reaction temperature of 260 °C and a  $W/F$  ratio of 12.5 g<sub>cat</sub> h mol<sup>-1</sup> (corresponding to a WHSV of 4.66 h<sup>-1</sup>) are found as optimal conditions for the consistent formation of mesitylene with the ASA Siralox 30 in the continuous flow fixed-bed reactor.

**Stability test at optimized reaction conditions.** The stability of the Siralox 30 catalyst was evaluated under the optimum reaction conditions. In a long-term experiment, it could be shown that the catalyst remains stable for more than 50 hours-on-stream despite the comparatively harsher reaction conditions (Fig. 4a). This clearly demonstrates that the meso-



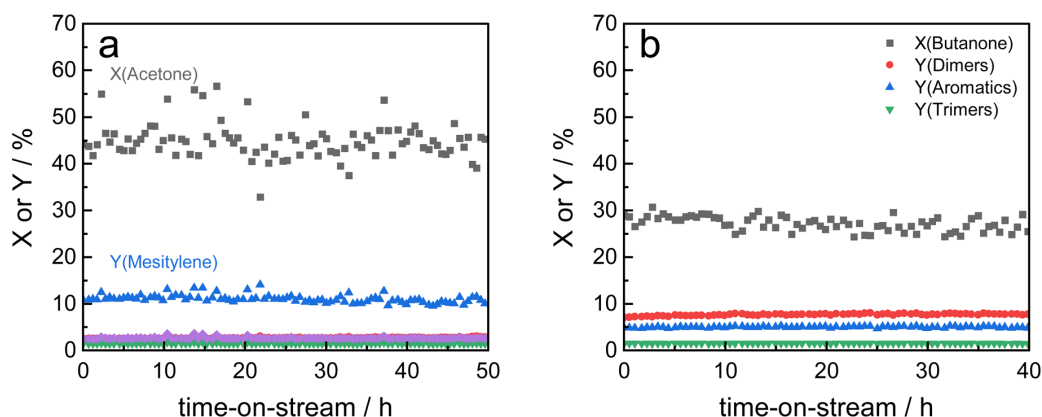


Fig. 4 Stability test of Siralox 30 under optimized reaction conditions (260 °C, 12.5  $\text{g}_{\text{cat}} \text{h mol}^{-1}$ , WHSV = 4.7  $\text{h}^{-1}$ ) in the conversion of acetone (a) and 2-butanone (b). Other products depicted in 4a: ● Y(Mesityl oxide), ▼ Y(Isophorone), ◆ Y(Oligomers).

porous ASA is a superior catalyst in the acetone aromatization to mesitylene.

Based on these findings, Siralox 30 was also tested for the conversion of 2-butanone under the optimized reaction conditions. The aromatic self-condensation product of 2-butanone is triethylbenzene that could be used as a potential precursor to styrene-type monomers. While Siralox 30 is stable for the conversion of this larger alkyl methyl ketone for more than 40 hours-on-stream, the catalytic activity is reduced compared to the conversion of acetone (Fig. 4b). For 2-butanone, the dimers present the main product with 8% yield whereas the yield of the aromatic triethylbenzenes is 5%. The lower catalyst activity is owed to the lower reactivity of 2-butanone and the steric hindrance due to its longer alkyl chain. The latter is also responsible that in comparison to acetone, a higher variety of isomers can be formed.<sup>19</sup> The total carbon balance for the conversion of 2-butanone is therefore 80%, whereas the total product selectivity for dimers, aromatics and trimers is 48%. As a side product propionic acid was detected in low amounts.

Nevertheless, the mesoporous structure of Siralox 30 with its larger pores is advantageous for the condensation as it is suitable for larger products without deactivation.

### 3.3 Influence of silica-content on catalytic activity of ASA

**Catalytic activity evaluation over different  $\text{SiO}_2$ -containing ASA.** For the production of the ASA of the Siralox family, silica is added to high-purity aluminas during synthesis.<sup>29</sup> Depending on the amount of silica, the silica-to-alumina ratio (SAR) is varied and thus material properties such as acidity (strength and density) and thermostability can be tuned.<sup>25</sup> To assess the influence of the SAR on the self-condensation of acetone, Siralox materials from 1–70 wt%  $\text{SiO}_2$  were studied under the optimum reaction conditions of 260 °C and 12.5  $\text{g}_{\text{cat}} \text{h mol}^{-1}$  and presented based on the steady-state conversion averaged over 10 hours-on-stream in Fig. 5. With silica-loading, the mesitylene yield (from 2.8 to 10.5%) and acetone conversion (from 19 to 42%) increase to a maximum at

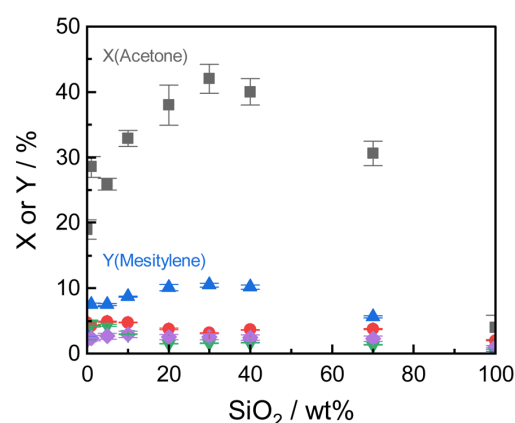


Fig. 5 Steady-state acetone conversion and product yields (▲ Y(Mesitylene), ● Y(Mesityl oxide), ▼ Y(Isophorone), ◆ Y(Oligomers)) for varying silica-content at optimized reaction conditions (260 °C, 12.5  $\text{g}_{\text{cat}} \text{h mol}^{-1}$ , 10 h-on-stream).

30 wt%  $\text{SiO}_2$ . For a further increase in silica-loadings, the conversion and yields decrease and are virtually zero for pure silica. Especially for the initial doping with 1 wt% silica, a strong increase in activity is observed for both mesitylene yield (7.5%) and acetone conversion (28%). The isophorone yield decreases with silica-content. Since bases promote the condensation to isophorone, the amphoteric nature of alumina exhibiting basic sites is relevant at low silica loadings.<sup>13,30,31</sup> The yields of mesityl oxide and oligomers increase up to 10 wt% silica, showing a maximum of 4.8 and 3%, respectively. With higher silica content, both yields decrease but remain constant up to 70 wt%  $\text{SiO}_2$ . Overall, an increase in mesitylene yield is accompanied by an increase in acetone conversion. This confirms that the mesitylene increase mainly stems from the consecutive reaction of mesityl oxide with acetone and subsequent aromatization. Based on the findings, a silica-content of



20–40 wt% gives the highest mesitylene yields with an optimum at 30 wt%. The trends observed in the flow reactor are supported by batch experiments at 230 °C for 3 h (see experimental details in SI and Fig. S8†). At these longer catalyst contact times, the maximum mesitylene yield at 30 wt% is more pronounced. The low activities of pure  $\gamma$ -Al<sub>2</sub>O<sub>3</sub> and pure SiO<sub>2</sub> found under flow and batch conditions highlight the effect of the silica-doping on the catalytic activity as additional active sites are created. Indeed, very large silica-loadings of 40 wt% and higher lead to a primarily silica surface with generally fewer surface acid sites.<sup>31</sup>

Under the optimized reaction conditions, all tested Siralox materials were stable at steady-state conditions for more than 10 hours-on-stream (Fig. S9†). The silica-content therefore does not play a significant role for the stability of the catalysts under reaction conditions. The TGA measurements of the spent ASA from the flow reactor show that the mass loss is about 7 wt% for silica-loadings of 10–40 wt% (Fig. S10†) after reaction at 260 °C. For very high and low silica-loadings, the mass loss is lower than 7 wt% due to decreased catalyst activity. For flow conditions, ~0.5 wt% less carbonaceous deposits are found compared to batch reactions which shows the efficiency of the continuous process with constant product removal from the catalyst bed.

The structural stability of the Siralox materials was assessed by XRD of the spent catalysts. The diffractograms (Fig. S11†) show that for the majority of materials, no significant change is visible. For Siralox 20 and 40, a small reflex at 49.2° can be observed, hinting to minor formation of the  $\gamma$ -AlO(OH) boehmite likely due to water formed in the aldol condensation. Surprisingly, Siralox 30 does not show the formation of boehmite which supports its suitability for scale-up in a continuous flow process.

**Influence of acidity of amorphous silica-alumina.** To understand why the Siralox materials show different activities in the aldol condensation of acetone, their nature and number of acid sites are assessed. The number of acid sites initially increases by doping  $\gamma$ -Al<sub>2</sub>O<sub>3</sub> with 1 wt% silica from 0.21 to 0.49 mmol g<sup>-1</sup>. However, the number of acid sites starts decreasing from 20 wt% SiO<sub>2</sub> and is strongly decreased for high silica-loadings as in Siralox 70 with 0.065 mmol g<sup>-1</sup> (Fig. S12†). No direct correlation with mesitylene yield can be found for the total number of acid sites obtained by NH<sub>3</sub>-TPD, indicating the importance of specific active acid sites. The desorption temperature of the chemisorbed NH<sub>3</sub> is an indicator for the strength of the probed acid sites, but in the case of the ASA, the large variety of acid sites leads to a broad desorption curve which renders it difficult to quantify or select individual sites for comparison based on their acid strength.<sup>22,32</sup> Instead, the temperature of the desorption maximum is used for estimation as it indicates the bond strength of a majority of acid sites.<sup>33</sup> Analogous to the number of acid sites, low silica-doping leads to an increase in the maximum desorption temperature from 260 °C to approximately 270 °C. For higher silica-contents, except for Siralox 40, the maximum temperature declines. Considering that the highest yields of mesitylene

were found for Siralox 20–40, a slightly decreased number of acid sites and strength appears beneficial for the stable formation of mesitylene found for ASA. This could be attributed to the fact that a high density of strong acid sites leads to faster deactivation due to the favored formation of larger byproducts, as seen for zeolite HY. By comparing the dimer yield with the NH<sub>3</sub>-desorption temperature, it becomes apparent that mesityl oxide benefits from the higher density of slightly stronger acid sites. As for the dimerization two acetone molecules need to react (and possibly be activated in close vicinity), the yield of mesityl oxide is mainly dictated by the amount and strength of acid sites.<sup>34</sup> Due to the structural complexity of ASA with multiple types of acid sites, results obtained by NH<sub>3</sub>-TPD are insufficient to explain the observed trends. Therefore, the nature and number of acid sites on which the reactions take place must be considered in more detail.

ASA exhibit a predominant amount of various Lewis acid sites (LAS) but also possess BAS in lower amounts (Fig. S13†).<sup>22,25</sup> The latter are created by doping the alumina with silica.<sup>31</sup> With increasing silica content, the number of LAS decreases while the formation of BAS increases up to a maximum at 40 wt% silica.<sup>23,31</sup> For silica-rich alumina of 90 wt% and above, no LAS are detected and the acidity is almost completely controlled by BAS. This is explained by the enrichment of the surface with silica which exceeds what would be expected from the bulk material composition. The majority of the material's surface at silica-loadings higher than 40 wt% is covered by silica and only contains small zones of the mixed aluminosilicate.<sup>31</sup> In fact, Daniell *et al.*, assessed the strength of the BAS and correlated it to the shift of the surface hydroxyl group  $\Delta\nu(\text{OH})$  at ~3748 cm<sup>-1</sup> on adsorption of CO on the Siralox materials by FTIR-spectroscopy.<sup>31</sup> The aluminosilicate surface shows a lower number of BAS which are strongly enhanced in strength by the addition of silica. Based on their

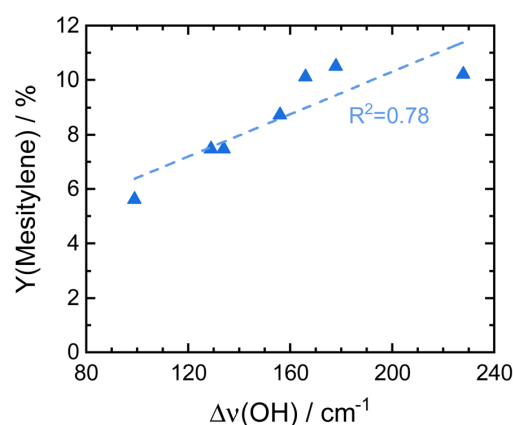
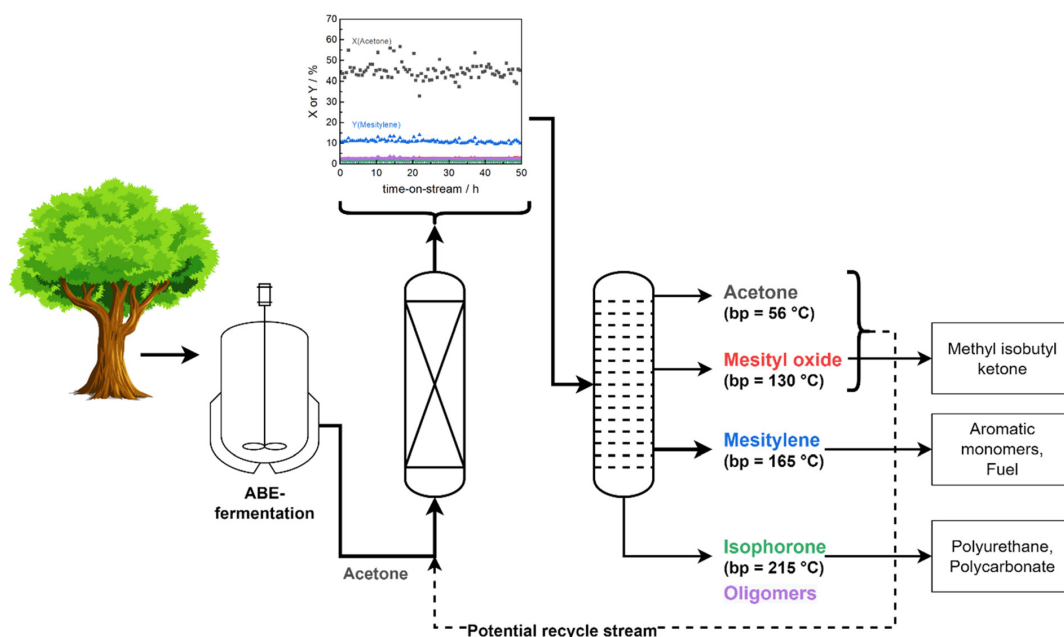


Fig. 6 Comparison of the here reported mesitylene yields for Siralox materials based on literature data for the strength of their BAS marked by the shift of vibrational frequencies for surface hydroxyl groups  $\Delta\nu(\text{OH})$  upon adsorption of CO on Siralox as determined by Daniell *et al.*<sup>31</sup>





**Fig. 7** Conceptual process for a continuous conversion of acetone obtained *via* ABE-fermentation of biomass-derived sugars to aromatics. Condensation products can be readily separated *via* distillation and recovered acetone and mesityl oxide can be recycled for increased process efficiency. Also depicted is the potential end-use of the separated condensation products. Depiction of biomass conversion and separation processes is simplified.

measurement, we found that the formation of mesitylene correlates well ( $R^2 = 0.78$ ) with the measured  $\Delta\nu(\text{OH})$  (Fig. 6). Accordingly, stronger BAS promote mesitylene formation under reaction conditions. For silica loadings higher than 60 wt%, the total number of acid sites and the strength of BAS decrease which results in the lower activities observed for these materials.<sup>23,31</sup> Therefore, materials with silica contents of 30–40 wt% are most beneficial for the formation of mesitylene.

The dimer mesityl oxide is preferably formed on ASA with low silica content which could stem from two effects: (1) mesityl oxide benefits from a higher number of LAS as observed by Panov and Fripiat<sup>34</sup> and (2) a lack of BAS at low silica loadings which are required to promote the consecutive aromatization with another acetone molecule. This concludes to both LAS and BAS being beneficial for the formation of mesityl oxide and dimers, while BAS promote the consecutive formation of mesitylene.

### 3.4 Conceptual process design for the aromatization of acetone

The remarkable stability of Siralox 30 combined with the high total product selectivity of 66% renders it suitable for a potential scale-up and further assessment of the industrial application in a continuous flow process. Separation of products can be readily achieved *via* distillation based on the differences in boiling points. A benefit of the solvent-free process is the more energy-efficient separation, as no additional solvent

needs to be vaporized and separated. Furthermore, recovered acetone and mesityl oxide can be recycled and added to the reactor feed to increase total efficiency (Fig. 7). Aromatics of the BTX-fraction can be obtained from mesitylene *via* industrially established transalkylation, thus offering a completely bio-based route for their production.<sup>35</sup> Generation of added value is also possible from the side products by their transformation to various important intermediates used in the polymer industry, *e.g.*, isophorone diisocyanate from isophorone for the polyurethane production.<sup>36</sup>

## 4. Conclusion

In conclusion, the continuous production of biomass-derived mesitylene from acetone can be achieved over ASA Siralox 30 under solvent-free continuous conditions in liquid as well as supercritical phase. At optimum conditions, Siralox 30 showed high stability without signs of deactivation for more than 50 hours-on-stream. Contributing to the stability is the mesoporous nature of Siralox 30 which facilitates mass transport and prevents deactivation by pore blocking from bulkier aromatic/aliphatic molecules as evidenced by the low amounts of carbonaceous deposits on the spent catalyst. Additionally, the larger pores allow the stable aromatization of 2-butanone to triethylbenzene with adequate yield, however activity is slightly decreased compared to the acetone-to-mesitylene conversion.



Variation in the degree of doping with silica influences the strength, amount, and nature of acid sites. Thus, it was found that the strength of BAS facilitates the mesitylene yield with an optimum silica-loading of 30–40 wt%.

Commercial availability of the low-cost catalyst, its remarkable stability, and a solvent-free continuous process present an excellent basis for a potential scale-up with the ASA Siralox 30. The fully integrated added value chains provide the opportunity for replacing fossil with biomass feedstock for a broad product spectrum with various applications.

## Author contributions

PR: conceptualization, investigation, formal analysis, visualization, writing – original draft; NKG: conceptualization, funding acquisition, writing – review & editing; MR: supervision, funding acquisition, project administration, writing – review & editing.

## Conflicts of interest

The authors declare no conflict of interest.

## Acknowledgements

PR and MR thank the German Federal Ministry of Education and Research (BMBF) for funding (Grant No. 031B0680). NKG gratefully acknowledges the Alexander-von-Humboldt foundation for financial support. We thank Martin Lucas for continuous technical support, Sasol Germany GmbH for providing the Siralox materials, and Kiyotaka Nakajima for his valuable input.

## References

- 1 J. Sherwood, The significance of biomass in a circular economy, *Bioresour. Technol.*, 2020, **300**, 122755, DOI: [10.1016/j.biortech.2020.122755](https://doi.org/10.1016/j.biortech.2020.122755).
- 2 Y. C. Yang, Consumer Behavior towards Green Products, *J. Econ. Bus. Manag.*, 2017, **5**(4), 160–167, DOI: [10.18178/joebm.2017.5.4.505](https://doi.org/10.18178/joebm.2017.5.4.505).
- 3 Mordor Intelligence., *Benzene-Toluene-Xylene (BTX) Market - Growth, Trends, COVID-19 Impact, and Forecasts (2022–2027)*. <https://www.mordorintelligence.com/industry-reports/benzene-toluene-xylene-btx-market> (accessed 2022-08-02).
- 4 M. R. Rahimpour, M. Jafari and D. Iranshahi, Progress in catalytic naphtha reforming process: A review, *Appl. Energy*, 2013, **109**, 79–93, DOI: [10.1016/j.apenergy.2013.03.080](https://doi.org/10.1016/j.apenergy.2013.03.080).
- 5 Y.-T. Cheng and G. W. Huber, Production of targeted aromatics by using Diels–Alder classes of reactions with furans and olefins over ZSM-5., *Green Chem.*, 2012, **14**(11), 3114, DOI: [10.1039/c2gc35767d](https://doi.org/10.1039/c2gc35767d).
- 6 A. Maneffa, P. Prieel and J. A. Lopez-Sanchez, Biomass-Derived Renewable Aromatics: Selective Routes and Outlook for *p*-Xylene Commercialisation, *ChemSusChem*, 2016, **9**(19), 2736–2748, DOI: [10.1002/cssc.201600605](https://doi.org/10.1002/cssc.201600605).
- 7 T. R. Carlson, G. A. Tompsett, W. C. Conner and G. W. Huber, Aromatic Production from Catalytic Fast Pyrolysis of Biomass-Derived Feedstocks, *Top. Catal.*, 2009, **52**(3), 241–252, DOI: [10.1007/s11244-008-9160-6](https://doi.org/10.1007/s11244-008-9160-6).
- 8 S. Herrmann and E. Iglesia, Selective conversion of acetone to isobutene and acetic acid on aluminosilicates: Kinetic coupling between acid-catalyzed and radical-mediated pathways, *J. Catal.*, 2018, **360**, 66–80, DOI: [10.1016/j.jcat.2018.01.032](https://doi.org/10.1016/j.jcat.2018.01.032).
- 9 E. R. Sacia, M. Balakrishnan, M. H. Deaner, K. A. Goulas, F. D. Toste and A. T. Bell, Highly Selective Condensation of Biomass-Derived Methyl Ketones as a Source of Aviation Fuel, *ChemSusChem*, 2015, **8**(10), 1726–1736, DOI: [10.1002/cssc.201500002](https://doi.org/10.1002/cssc.201500002).
- 10 P. Reif, H. Rosenthal and M. Rose, Biomass-Derived Aromatics by Solid Acid-Catalyzed Aldol Condensation of Alkyl Methyl Ketones, *Adv. Sustain. Syst.*, 2020, **4**(10), 1900150, DOI: [10.1002/adsu.201900150](https://doi.org/10.1002/adsu.201900150).
- 11 T. J. Benson, P. R. Daggolu, R. A. Hernandez, S. Liu and M. G. White, Catalytic Deoxygenation Chemistry, *Adv. Catal.*, 2013, **56**, 187–353, DOI: [10.1016/B978-0-12-420173-6.00003-6](https://doi.org/10.1016/B978-0-12-420173-6.00003-6).
- 12 F. E. Liew, R. Nogle, T. Abdalla, B. J. Rasor, C. Canter, R. O. Jensen, L. Wang, J. Strutz, P. Chirania, S. Tissera, A. P. de Mueller, Z. Ruan, A. Gao, L. Tran, N. L. Engle, J. C. Bromley, J. Daniell, R. Conrado, T. J. Tschaplinski, R. J. Giannone, R. L. Hettich, A. S. Karim, S. D. Simpson, S. D. Brown, C. Leang, M. C. Jewett and M. Köpke, Carbon-negative production of acetone and isopropanol by gas fermentation at industrial pilot scale, *Nat. Biotechnol.*, 2022, **40**(3), 335–344, DOI: [10.1038/s41587-021-01195-w](https://doi.org/10.1038/s41587-021-01195-w).
- 13 M. Paulis, M. Martín, D. B. Soria, A. Díaz, J. A. Odriozola and M. Montes, Preparation and characterization of niobium oxide for the catalytic aldol condensation of acetone, *Appl. Catal., A*, 1999, **180**(1), 411–420, DOI: [10.1016/S0926-860X\(98\)00379-2](https://doi.org/10.1016/S0926-860X(98)00379-2).
- 14 Z. Wu, J. Zhang, Z. Su, S. Lu, J. Huang, Y. Liang, T. Tan and F.-S. Xiao, Selective conversion of acetone to mesitylene over tantalum phosphate catalysts, *Chem. Commun.*, 2022, **58**(17), 2862–2865, DOI: [10.1039/d2cc00016d](https://doi.org/10.1039/d2cc00016d).
- 15 S. K. Bej and L. T. Thompson, Acetone condensation over molybdenum nitride and carbide catalysts, *Appl. Catal., A*, 2004, **264**(2), 141–150, DOI: [10.1016/j.apcata.2003.12.051](https://doi.org/10.1016/j.apcata.2003.12.051).
- 16 S. Herrmann and E. Iglesia, Elementary steps in acetone condensation reactions catalyzed by aluminosilicates with diverse void structures, *J. Catal.*, 2017, **346**, 134–153, DOI: [10.1016/j.jcat.2016.12.011](https://doi.org/10.1016/j.jcat.2016.12.011).
- 17 L. Faba, J. Gancedo, J. Quesada, E. Diaz and S. Ordóñez, One-Pot Conversion of Acetone into Mesitylene over Combinations of Acid and Basic Catalysts, *ACS Catal.*, 2021, **11**(18), 11650–11662, DOI: [10.1021/acscatal.1c03095](https://doi.org/10.1021/acscatal.1c03095).
- 18 L. Kubelková, J. Čjka, J. Nováková, V. Boszárček, I. Jirka and P. Jiáru, Acetone Conversion and Deactivation of Zeolites, in *Studies in Surface Science and Catalysis*, ed. P. A. Jacobs





- and R. A. van Santen, Elsevier, 1989, pp. 1203–1212. DOI: [10.1016/S0167-2991\(08\)62006-6](https://doi.org/10.1016/S0167-2991(08)62006-6).
- 19 P. Reif, N. K. Gupta and M. Rose, Liquid phase aromatization of bio-based ketones over a stable solid acid catalyst under batch and continuous flow conditions, *Catal. Commun.*, 2022, **163**, 106402, DOI: [10.1016/j.catcom.2022.106402](https://doi.org/10.1016/j.catcom.2022.106402).
- 20 J. Quesada, L. Faba, E. Díaz and S. Ordóñez, Effect of catalyst morphology and hydrogen co-feeding on the acid-catalysed transformation of acetone into mesitylene, *Catal. Sci. Technol.*, 2020, **10**(5), 1356–1367, DOI: [10.1039/C9CY02288K](https://doi.org/10.1039/C9CY02288K).
- 21 H. Takaya, N. Todo, T. Hosoya, T. Minegishi, M. Yoneoka and H. Oshio, Cleaning Effects of the Reactant in the Liquid-phase Isomerization of *m*-Xylene over a Silica-Alumina Catalyst under Pressure, *Bull. Chem. Soc. Jpn.*, 1971, **44**(9), 2296–2301, DOI: [10.1246/bcsj.44.2296](https://doi.org/10.1246/bcsj.44.2296).
- 22 G. Crépeau, V. Montouillout, A. Vimont, L. Marley, T. Cseri and F. Maugé, Nature, structure and strength of the acidic sites of amorphous silica alumina: an IR and NMR study, *J. Phys. Chem. B*, 2006, **110**(31), 15172–15185, DOI: [10.1021/jp062252d](https://doi.org/10.1021/jp062252d).
- 23 S. Nassreddine, S. Casu, J. L. Zotin, C. Geantet and L. Piccolo, Thiotolerant Ir/SiO<sub>2</sub>–Al<sub>2</sub>O<sub>3</sub> bifunctional catalysts: effect of support acidity on tetralin hydroconversion, *Catal. Sci. Technol.*, 2011, **1**(3), 408–412, DOI: [10.1039/c1cy00002k](https://doi.org/10.1039/c1cy00002k).
- 24 Z. Wang, Y. Jiang, O. Lafon, J. Trébosc, K. D. Kim, C. Stampfl, A. Baiker, J.-P. Amoureux and J. Huang, Brønsted acid sites based on penta-coordinated aluminum species, *Nat. Commun.*, 2016, **7**, 13820, DOI: [10.1038/ncomms13820](https://doi.org/10.1038/ncomms13820).
- 25 M. K. Mardkhe, K. Keyvanloo, C. H. Bartholomew, W. C. Hecker, T. M. Alam and B. F. Woodfield, Acid site properties of thermally stable, silica-doped alumina as a function of silica/alumina ratio and calcination temperature, *Appl. Catal., A*, 2014, **482**, 16–23, DOI: [10.1016/j.apcata.2014.05.011](https://doi.org/10.1016/j.apcata.2014.05.011).
- 26 J. T. Scanlon and D. E. Willis, Calculation of Flame Ionization Detector Relative Response Factors Using the Effective Carbon Number Concept, *J. Chromatogr. Sci.*, 1985, **23**(8), 333–340, DOI: [10.1093/chromsci/23.8.333](https://doi.org/10.1093/chromsci/23.8.333).
- 27 M. Guisnet, L. Costa and F. R. Ribeiro, Prevention of zeolite deactivation by coking, *J. Mol. Catal. A: Chem.*, 2009, **305**(2), 69–83, DOI: [10.1016/j.molcata.2008.11.012](https://doi.org/10.1016/j.molcata.2008.11.012).
- 28 D. Ambrose, C. Sprake and R. Townsend, Thermodynamic properties of organic oxygen compounds XXXIII. The vapour pressure of acetone, *J. Chem. Thermodyn.*, 1974, **6**(7), 693–700, DOI: [10.1016/0021-9614\(74\)90119-0](https://doi.org/10.1016/0021-9614(74)90119-0).
- 29 A. Meyer, K. Noweck, A. Reichenauer and J. Schimanski, Process for the preparation of a catalyst carrier based on aluminosilicates. US5045519A, 1991.
- 30 A. Gervasini, G. Bellussi, J. Fenyvesi and A. Auroux, Microcalorimetric and Catalytic Studies of the Acidic Character of Modified Metal Oxide Surfaces. 1. Doping Ions on Alumina, Magnesia, and Silica, *J. Phys. Chem.*, 1995, **99**(14), 5117–5125, DOI: [10.1021/j100014a036](https://doi.org/10.1021/j100014a036).
- 31 W. Daniell, U. Schubert, R. Glöckler, A. Meyer, K. Noweck and H. Knözinger, Enhanced surface acidity in mixed alumina–silicas: a low-temperature FTIR study, *Appl. Catal., A*, 2000, **196**(2), 247–260, DOI: [10.1016/S0926-860X\(99\)00474-3](https://doi.org/10.1016/S0926-860X(99)00474-3).
- 32 E. J. Hensen, D. G. Poduval, V. Degirmenci, D. J. M. Ligthart, W. Chen, F. Maugé, M. S. Rigutto and J. R. van Veen, Acidity Characterization of Amorphous Silica–Alumina, *J. Phys. Chem. C*, 2012, **116**(40), 21416–21429, DOI: [10.1021/jp309182f](https://doi.org/10.1021/jp309182f).
- 33 F. Lónyi and J. Valyon, On the interpretation of the NH<sub>3</sub>-TPD patterns of H-ZSM-5 and H-mordenite, *Microporous Mesoporous Mater.*, 2001, **47**(3), 293–301, DOI: [10.1016/S1387-1811\(01\)00389-4](https://doi.org/10.1016/S1387-1811(01)00389-4).
- 34 A. G. Panov and J. J. Fripiat, Acetone Condensation Reaction on Acid Catalysts, *J. Catal.*, 1998, **178**(1), 188–197, DOI: [10.1006/jcat.1998.2142](https://doi.org/10.1006/jcat.1998.2142).
- 35 Y. Li, H. Wang, M. Dong, J. Li, Z. Qin, J. Wang and W. Fan, Effect of zeolite pore structure on the diffusion and catalytic behaviors in the transalkylation of toluene with 1,2,4-trimethylbenzene, *RSC Adv.*, 2015, **5**(81), 66301–66310, DOI: [10.1039/C5RA09236A](https://doi.org/10.1039/C5RA09236A).
- 36 H. Sardon, L. Irusta and M. J. Fernández-Berridi, Synthesis of isophorone diisocyanate (IPDI) based waterborne polyurethanes: Comparison between zirconium and tin catalysts in the polymerization process, *Prog. Org. Coat.*, 2009, **66**(3), 291–295, DOI: [10.1016/j.porgcoat.2009.08.005](https://doi.org/10.1016/j.porgcoat.2009.08.005).



## Supporting Information

# Highly stable amorphous silica-alumina catalysts for continuous bio-derived mesitylene production under solvent-free conditions

*Phillip Reif,<sup>a</sup> Navneet Kumar Gupta,<sup>ab</sup> Marcus Rose<sup>\*a</sup>*

<sup>a</sup> Technical University of Darmstadt, Department of Chemistry, Alarich-Weiss-Straße 8, 64287  
Darmstadt, Germany

<sup>b</sup> Centre for Sustainable Technologies, Indian Institute of Science, Gulmohar Marg, Mathikere,  
560012 Bengaluru, India

**E-mail:** [marcus.rose@tu-darmstadt.de](mailto:marcus.rose@tu-darmstadt.de) (MR); [nkgupta@iisc.ac.in](mailto:nkgupta@iisc.ac.in) (NKG)

---

## Catalytic studies in batch experiments

For catalytic reactions under batch conditions, typically 10 g acetone and 5 wt% catalyst were added to the autoclave (45 mL, Parr) which was then pressurized with 40 bar Ar and heated to 230 °C while stirring at 500 rpm. After completion of the reaction, filtered samples of the reaction mixture were analyzed using gas chromatography (Shimadzu GC-2010 Plus with FID, Restek RTX-5 Amine, 40-250 °C, 10 K min<sup>-1</sup>, He) and 1,4-dioxane (99.5 %) as an internal standard. Furthermore, the identification of products was confirmed by GC coupled with mass spectrometry (Shimadzu GCMS-QP2010SE).



---

## Calculation of conversion $X$ , product yield $Y$ , and selectivity $S$ :

Conversion of alkyl methyl ketone  $X$ :

$$X_{\text{Ketone}} = 1 - \frac{n_{\text{Ketone}}}{n_{\text{Ketone},0}}$$

with  $n$ : substance amount in mol

Product yield  $Y$ :

$$Y_i = \frac{|v_{\text{Ketone}}| n_i}{v_i n_{\text{Ketone},0}}$$

with  $v$ : stoichiometry of the reactant in the reaction

Product selectivity  $S$ :

$$S_i = \frac{Y_i}{X_{\text{Ketone}}}$$

The substance amounts are obtained via response factors  $RF$  based on the internal standard (IS) 1,4-dioxane obtained from GC-calibration, and the measured substance areas  $A$ . In case of acetone as starting ketone, calibration substances were used for mesityl oxide (dimer), mesitylene (aromatic), and isophorone (trimer).

$$\frac{A_i}{A_{\text{IS}}} = \frac{w_i}{w_{\text{IS}}} RF$$

with  $w$ : weight fraction

---

For the higher alkyl methyl ketone 2-butanone, only the ketone and the aromatic triethylbenzene were available for calibration. Therefore, the concept of the effective carbon number (*ECN*) with the relative response factors *RRF* was used based on the molecular weight (*MW*) and calculated *ECN* of the substance and a structurally similar reference substance *R*.<sup>1-2</sup>

$$RRF_i = \frac{MW_i}{MW_R} \cdot \frac{ECN_R}{ECN_i}$$

The reference substances are the corresponding dimers and trimers of the acetone condensation. The many positional isomers existing for the products of 2-butanone were grouped together and the corresponding area sums were used for calculation.

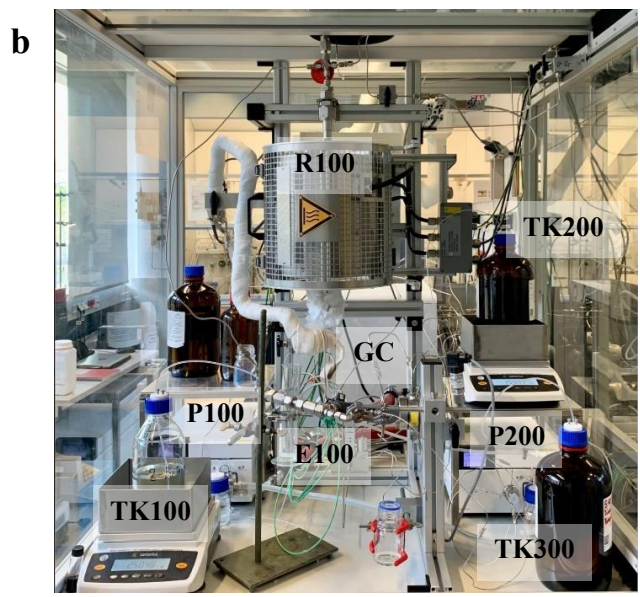
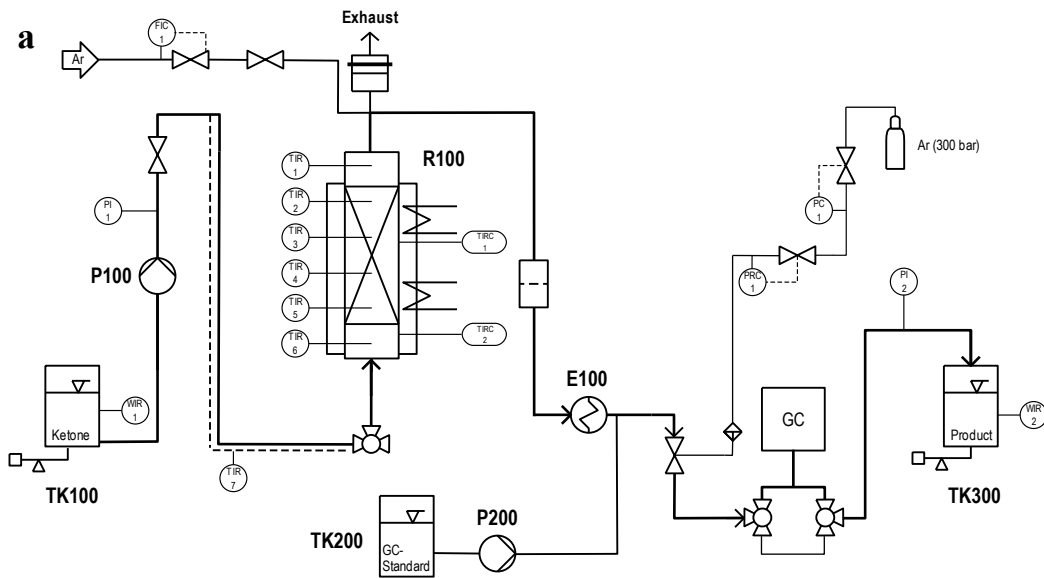


Figure S1: Process flow diagram of the catalytic fixed-bed reactor (a) and frontal view of the reactor (b).

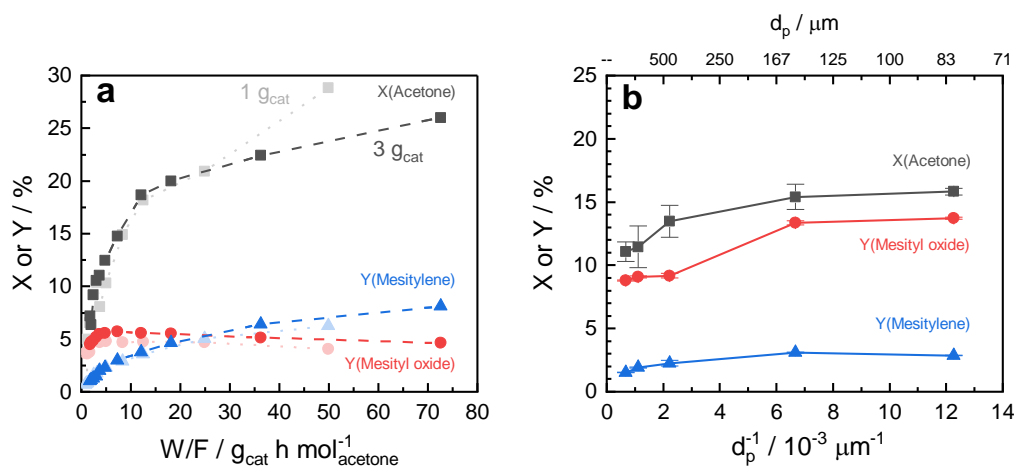


Figure S2: Assessment of external (a) and internal (b) mass transfer limitations at 210 °C.

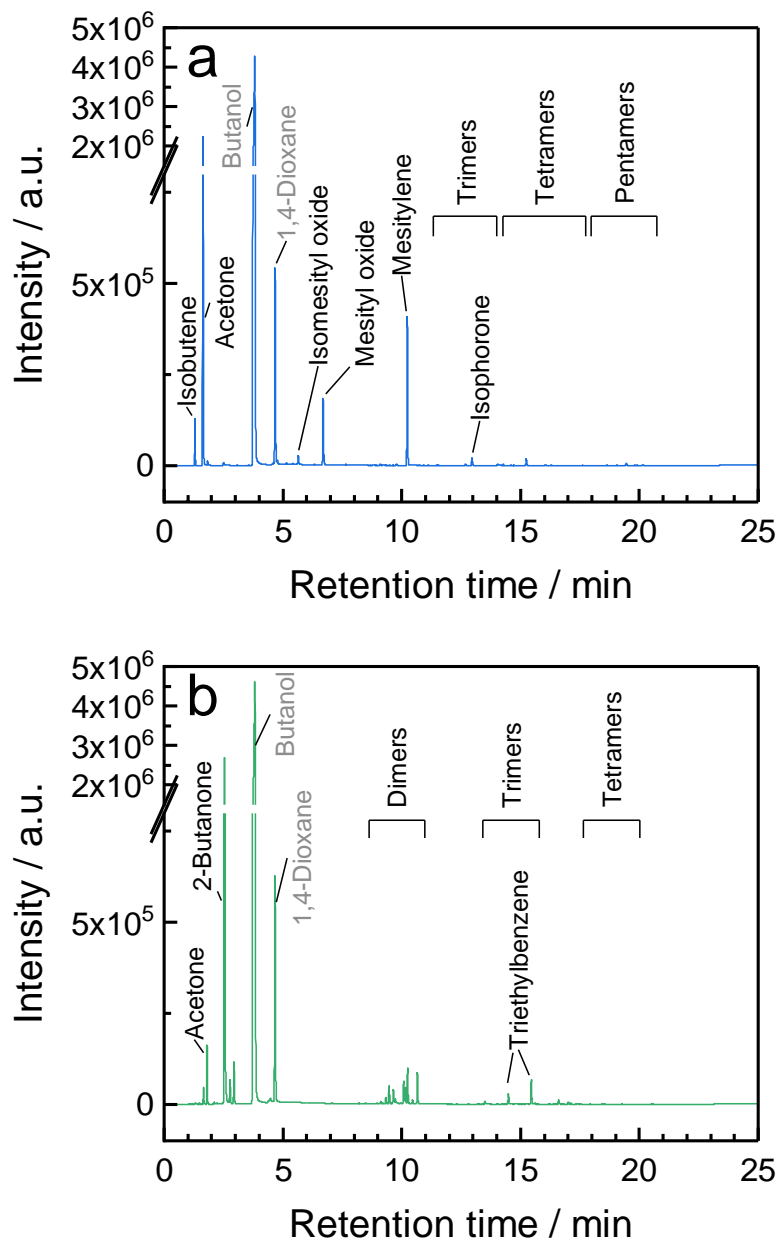


Figure S3: Representative GC-chromatograms of the product mixture for the conversion of acetone (a) and 2-butanone (b) at 260 °C in the fixed-bed reactor using Siralox 30. 1,4-Dioxane is used as internal standard and 1-butanol for dilution.

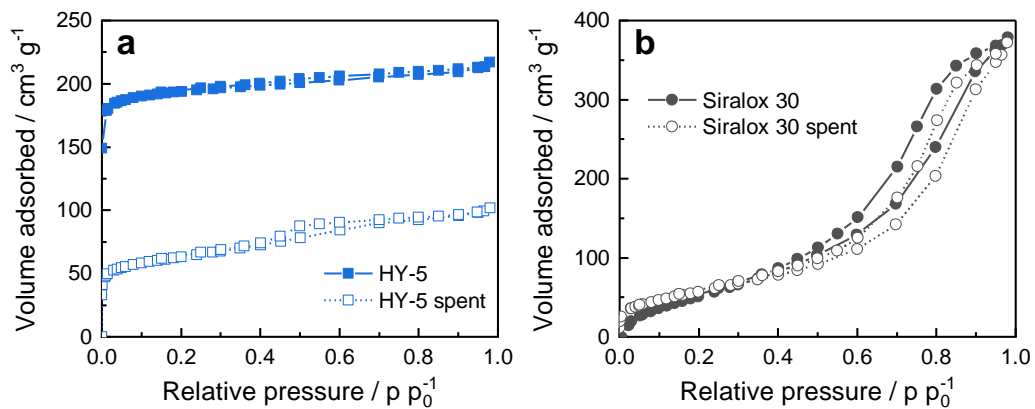


Figure S4: N<sub>2</sub>-Physisorption data for fresh and spent HY-5 (a) and Siralox 30 (b).

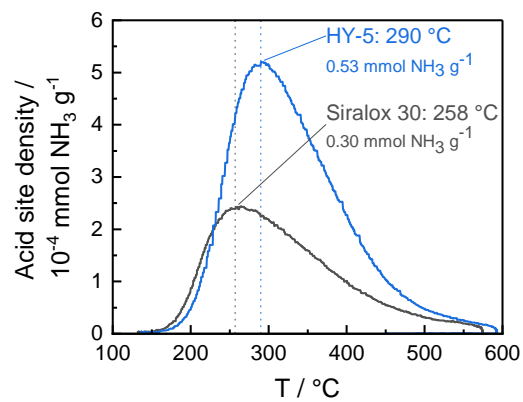


Figure S5: NH<sub>3</sub>-TPD curves for Siralox 30 and HY-5 catalyst and maxima of their desorption temperature.

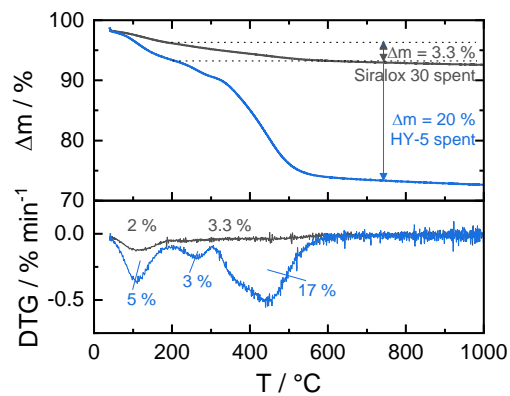


Figure S6: TGA and DTG curves for spent HY-5 and Siralox 30 catalyst in air. After the reaction HY-5 showed clear signs of black carbonaceous deposits while Siralox 30 remained grey-white. The chemical nature of the depositions was classified as following: < 180 °C: water and volatile species, 180-330 °C: “soft coke”, 330-750 °C: bulky carbonaceous deposits (“hard coke”) according to Sahoo et al.<sup>3</sup>



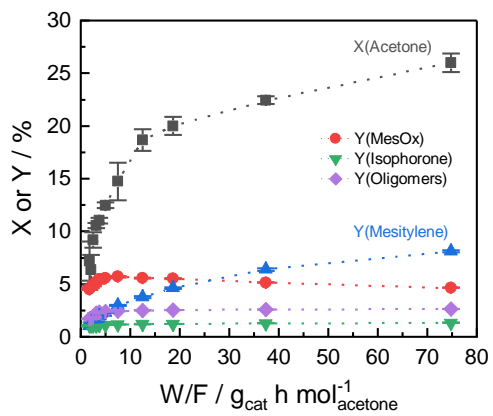


Figure S7: Acetone conversion and product yields for Siralox 30 at 210 °C for varying catalyst contact times.

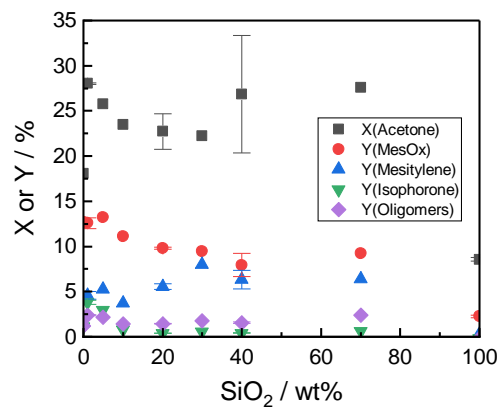


Figure S8: Acetone conversion and product yields of batch reactions at 230 °C (3 h) for varying silica content.

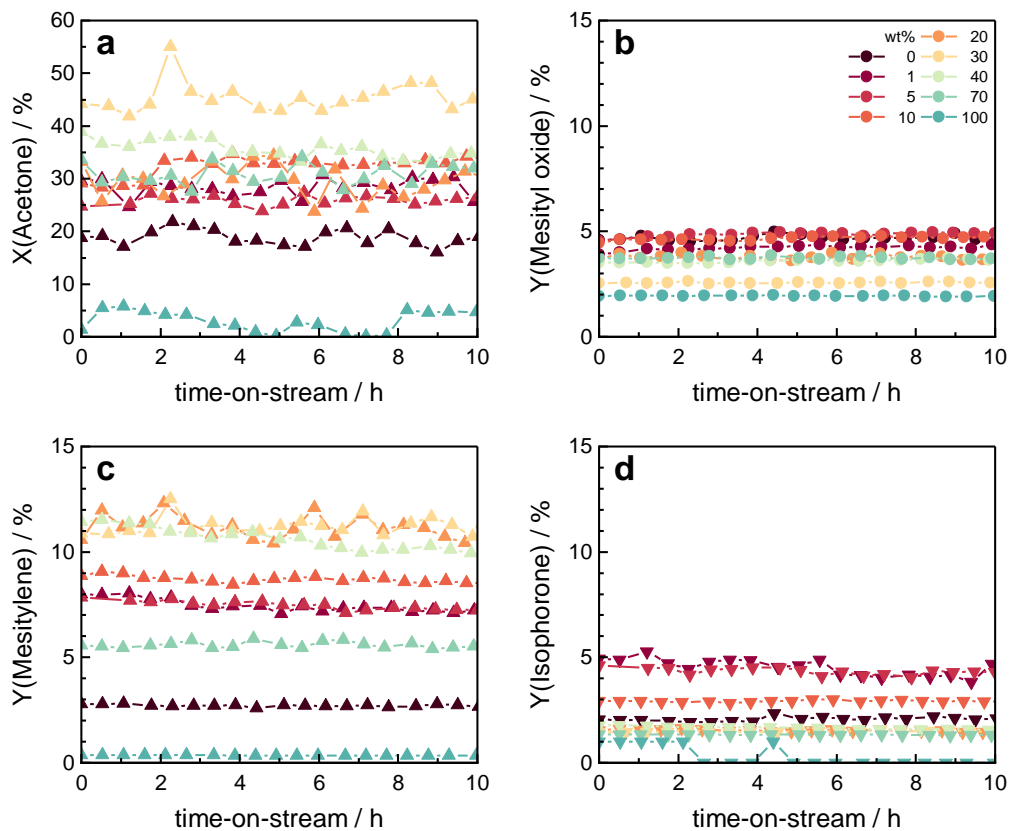


Figure S9: Silica-alumina catalyst stability based on acetone conversion (a) and product yields of mesityl oxide (b), mesitylene (c), and isophorone (d) for varying silica content (in wt%) in the flow reactor at 260 °C, 12.5 g<sub>cat</sub> h mol<sup>-1</sup>.

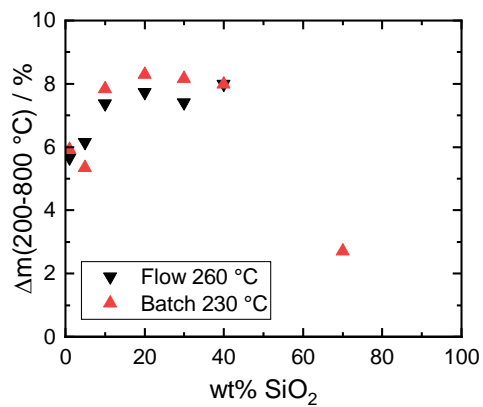


Figure S10: Mass loss of the spent catalysts determined by TGA ( $5 \text{ K min}^{-1}$ ,  $40\text{-}1000 \text{ }^\circ\text{C}$ ) in air.

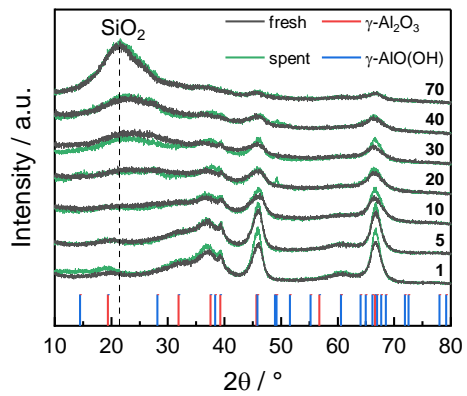


Figure S11: XRD spectra of fresh and spent (flow reactor, 260 °C, 12.5  $\text{g}_{\text{cat}} \text{ h mol}^{-1}$ ) Siralox catalysts of varying silica-content in wt%.

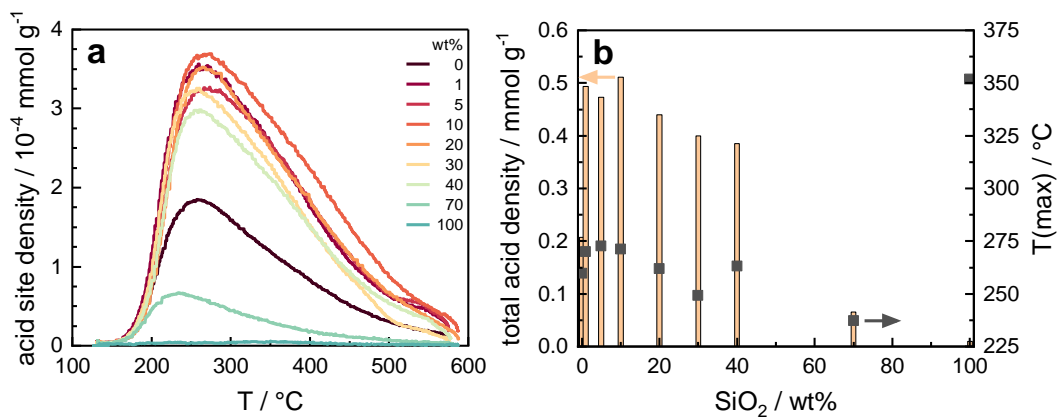


Figure S12:  $\text{NH}_3$ -TPD curves (a) and from there derived total number of acid sites and maximum desorption temperature (b) for silica-alumina with varying silica content (in wt%).

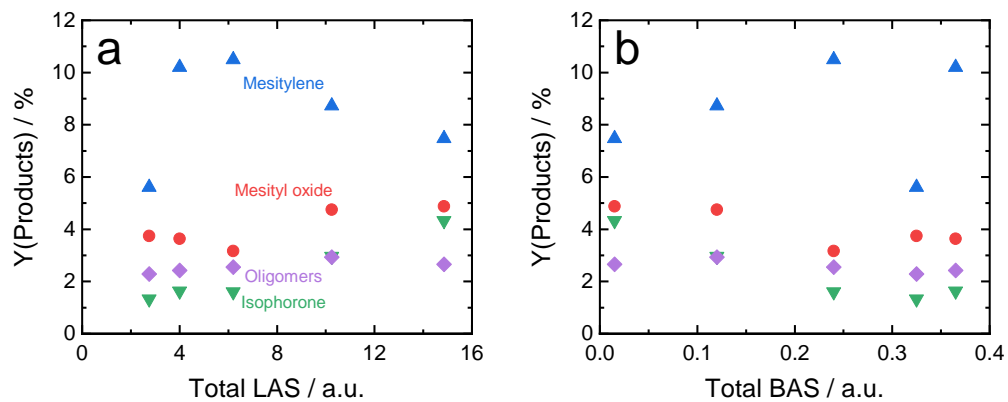


Figure S13: Product yields based on the total amount of Lewis acid sites (a) and Brønsted acid sites (b) measured by Nassreddine et al. via pyridine-desorption IR.<sup>4</sup>

---

## References:

- (1) Dettmer-Wilde, K.; Practical Gas Chromatography: A Comprehensive Reference, Springer Berlin / Heidelberg, Berlin, Heidelberg, **2014**.
- (2) Reif, P.; Gupta, N. K.; Rose, M. Liquid phase aromatization of bio-based ketones over a stable solid acid catalyst under batch and continuous flow conditions. *Catal. Commun.* **2022**, 163, 106402. DOI: 10.1016/j.catcom.2022.106402.
- (3) Sahoo, S. K.; Ray, S. S.; Singh, I. D. Structural characterization of coke on spent hydroprocessing catalysts used for processing of vacuum gas oils. *Appl. Catal., A* **2004**, 278 (1), 83–91. DOI: 10.1016/j.apcata.2004.09.028.
- (4) Nassreddine, S.; Casu, S.; Zotin, J. L.; Geantet, C.; Piccolo, L. Thiotolerant Ir/SiO<sub>2</sub>–Al<sub>2</sub>O<sub>3</sub> bifunctional catalysts: effect of support acidity on tetralin hydroconversion. *Catal. Sci. Technol.* **2011**, 1 (3), 408–412. DOI: 10.1039/c1cy00002k.



---

## 5. Conclusion and outlook

---

The transition to a net zero circular bioeconomy requires the production of chemicals from renewable biomass feedstocks. For many polymers, aromatics are a key building block for their respective monomers. The production of biomass-derived aromatics therefore provides important intermediates in the chemical value chain that are currently obtained from fossil resources. A less explored pathway from biomass to aromatics is the catalytic self-condensation of alkyl methyl ketones by cyclotrimerization. For example, acetone, the simplest alkyl methyl ketone and thus a model compound, is available from ABE fermentation of glucose, a mature technology that has even been used for industrial production in the past century. The main challenges of acetone aromatization to mesitylene catalyzed by (solid) acid catalysts are the rapid deactivation of the catalysts under the applied high-temperature gas-phase conditions and the complex network of consecutive and parallel reactions, which have hindered process scale-up so far. A better understanding of the structure-activity relationship will allow higher aromatics selectivity and identification of stable and active catalysts.

In a progressive series of publications, the acid-catalyzed aromatization of alkyl methyl ketones was studied step by step, leading to the development of a process concept based on a highly stable catalyst under continuous flow conditions. This was achieved by thorough catalyst characterization and reaction engineering in batch and fixed-bed reactors. By using solvent-free conditions and commercially available catalysts, an energy-efficient scale-up of the process would be feasible. In an initial screening of a wide variety of solid acid catalysts, the cation exchange resin Purolite CT275DR was found to be the most active under liquid-phase batch conditions due to its high number of BAS. Therefore, it was used to obtain an initial batch kinetic that showed a progressively slower becoming reaction. However, further characterization showed that the catalyst was not stable under reaction conditions due to leaching of active sites and thermal decomposition. In subsequent tests, zeolite H-Y was identified as a suitable alternative for batch and continuous flow reactions. Its activity could be completely restored by calcination, and steady-state mesitylene formation was achieved at 190 °C for 250 min time-on-stream. Furthermore, it was also suitable for the catalytic conversion of larger alkyl methyl ketones such as 2-butanone, a potential styrene precursor, and 2-pentanone to alkylated aromatics. The performance of zeolite H-Y shows the importance of larger catalyst pores for the stable aromatization of alkyl methyl ketones. Based on this finding, mesoporous amorphous silica-alumina were re-evaluated as acid catalysts. Siralox 30, consisting of 30 wt% SiO<sub>2</sub>, was found to be highly stable for more than 50 h time-on-stream even at an elevated reaction temperature of 260 °C. A maximum space-time-yield of 10.1 wt% mesitylene and 66% total product (dimers, trimers, aromatics) selectivity was obtained at a  $W/F$  of 12.5 g<sub>cat</sub> h mol<sup>-1</sup>. Varying the silica content showed that the catalyst activity depends on the density and strength of the acid sites. Optimal for aromatization was 30-40 wt% silica, which was supported by literature data. The catalyst Siralox 30 was also stable for the self-condensation of 2-butanone to

---

aromatics. Due to the superior stability and commercial availability of Siralox 30, a process concept was proposed in which unconverted acetone and dimers are recycled. The resulting solvent-free product mixture is efficiently separated by distillation due to the large differences in boiling points. Further value can be added to the separated product outlet streams by processing them into various useful products. To study the feasibility of the proposed process concept, the incorporation of a recycle stream for unconverted acetone into the reactor setup, and the isolation of mesitylene by distillation would be logical next steps in process development. By testing the catalyst stability over longer reaction times of weeks and months, accurate information on catalyst deactivation would be collected and potential fouling behavior could be observed. Studying the conversion of purified mesitylene in a downstream transalkylation reactor would allow estimation of overall process yield and selectivity for BTX-aromatics. Investigation of the activity on the catalyst surface under reaction conditions in a suitable setup and specific assessment of sites would provide further insight into the surface reaction mechanism. Based on such findings, a specialized catalyst system combining large or hierarchical catalyst pores with strong BAS in moderate amounts can be designed to further improve mass transport and activity. In summary, the study of the self-condensation of acetone successfully demonstrated the potential for the stable production of biomass-derived aromatics using solid acid catalysts. Through exploration and steadily increasing understanding of the catalytic requirements, a robust chemical pathway has been developed in the context of defossilizing the chemical industry and reducing carbon emissions.

---

## References

---

- [1] "Executive Order 14081. Advancing Biotechnology and Biomanufacturing Innovation for a Sustainable, Safe, and Secure American Bioeconomy", <https://public-inspection.federalregister.gov/2022-20167.pdf>, accessed: **11.04.2023**.
- [2] S. Asanova, D. Klitou, T. Lalanne, L. Azcona, K. Dervojeda, *Bio-based aromatics. Report on promising KETs-based product r. 2*, European Union, **2017**.
- [3] Y. C. Yang, *JOEBM*, **2017**, 5, 160, <https://doi.org/10.18178/joebm.2017.5.4.505>.
- [4] P. Skoczinski, M. Carus, G. Tweddle, P. Ruiz, D. de Guzman, J. Ravenstijn, H. Käb, N. Hark, L. Dammer, *Bio-based Building Blocks and Polymers. Global Capacities, Production and Trends 2022-2027*, nova-Institut GmbH, Hürth, Germany, **2023**.
- [5] P.R. Shukla, J. Skea, R. Slade, A. Al Khourdajie, R. van Diemen, D. McCollum, M. Pathak, S. Some, P. Vyas, R. Fradera, M. Belkacemi, A. Hasija, G. Lisboa, S. Luz, J. Malley, *Climate Change 2022: Mitigation of Climate Change. Contribution of Working Group III to the Sixth Assessment Report of the Intergovernmental Panel on Climate Change*, Ipcc, Cambridge, UK and New York, USA, **2022**.
- [6] R. Meys, A. Kätelhön, M. Bachmann, B. Winter, C. Zibunas, S. Suh, A. Bardow, *Science*, **2021**, 374, 71, <https://doi.org/10.1126/science.abg9853>.
- [7] E. Barnard, J. J. Rubio Arias, W. Thielemans, *Green Chem.*, **2021**, 23, 3765, <https://doi.org/10.1039/D1GC00887K>.
- [8] J. Stouten, A. A. Wróblewska, G. Grit, J. Noordijk, B. Gebben, M. H. M. Meeusen-Wierds, K. V. Bernaerts, *Polym. Chem.*, **2021**, 12, 2379, <https://doi.org/10.1039/D1PY00005E>.
- [9] Packaging World, "Coca-Cola, Suntory Cross the 100% Plant-Based Bottle Finish Line", <https://www.packworld.com/news/sustainability/article/22171823/cocacola-suntory-debut-100-plantbased-bottles>, accessed: **14.04.2023**.
- [10] F. Cavani, S. Albonetti, F. Basile in *Chemicals and fuels from bio-based building blocks* (Eds.: F. Cavani, S. Albonetti, F. Basile, A. Gandini), Wiley-VCH, Weinheim, Germany, **2016**, pp. 33–50.
- [11] A. E. Settle, L. Berstis, N. A. Rorrer, Y. Roman-Leshkóv, G. T. Beckham, R. M. Richards, D. R. Vardon, *Green Chem.*, **2017**, 19, 3468, <https://doi.org/10.1039/C7GC00992E>.
- [12] A. M. Niziolek, O. Onel, Y. A. Guzman, C. A. Floudas, *Energy Fuels*, **2016**, 30, 4970, <https://doi.org/10.1021/acs.energyfuels.6b00619>.
- [13] A. K. Deepa, P. L. Dhepe, *RSC Adv.*, **2014**, 4, 12625, <https://doi.org/10.1039/c3ra47818a>.
- [14] A. Jess, P. Wasserscheid, *Chemical Technology: An Integral Textbook*, Wiley-VCH, Weinheim, Germany, **2013**.

- 
- [15] M. R. Rahimpour, M. Jafari, D. Iranshahi, *Appl. Energy*, **2013**, *109*, 79, <https://doi.org/10.1016/j.apenergy.2013.03.080>.
- [16] Mordor Intelligence, "Benzene-Toluene-Xylene (BTX) Market - Growth, Trends, COVID-19 Impact, and Forecasts (2022 - 2027)", <https://www.mordorintelligence.com/industry-reports/benzene-toluene-xylene-btx-market>, accessed: **02.08.2022**.
- [17] J. A. Mendoza Mesa, F. Brandi, I. Shekova, M. Antonietti, M. Al-Naji, *Green Chem.*, **2020**, *22*, 7398, <https://doi.org/10.1039/D0GC01517B>.
- [18] A. Maneffa, P. Priece, J. A. Lopez-Sanchez, *ChemSusChem*, **2016**, *9*, 2736, <https://doi.org/10.1002/cssc.201600605>.
- [19] T. R. Carlson, G. A. Tompsett, W. C. Conner, G. W. Huber, *Top. Catal.*, **2009**, *52*, 241, <https://doi.org/10.1007/s11244-008-9160-6>.
- [20] S. Herrmann, E. Iglesia, *J. Catal.*, **2018**, *360*, 66, <https://doi.org/10.1016/j.jcat.2018.01.032>.
- [21] E. R. Sacia, M. Balakrishnan, M. H. Deaner, K. A. Goulas, F. D. Toste, A. T. Bell, *ChemSusChem*, **2015**, *8*, 1726, <https://doi.org/10.1002/cssc.201500002>.
- [22] D. T. Jones, D. R. Woods, *Microbiol. Rev.*, **1986**, *50*, 484, <https://doi.org/10.1128/mr.50.4.484-524.1986>.
- [23] H. Luo, L. Ge, J. Zhang, J. Ding, R. Chen, Z. Shi, *Bioresour. Technol.*, **2016**, *200*, 111, <https://doi.org/10.1016/j.biortech.2015.09.116>.
- [24] F. E. Liew, R. Nogle, T. Abdalla, B. J. Rasor, C. Canter, R. O. Jensen, L. Wang, J. Strutz, P. Chirania, S. de Tissera et al., *Nat. Biotechnol.*, **2022**, *40*, 335, <https://doi.org/10.1038/s41587-021-01195-w>.
- [25] S. A. Ali, K. E. Ogunronbi, S. S. Al-Khattaf, *Chem Eng Res Des*, **2013**, *91*, 2601, <https://doi.org/10.1016/j.cherd.2013.04.014>.
- [26] M. Balakrishnan, G. E. Arab, O. B. Kunbargi, A. A. Gokhale, A. M. Grippo, F. D. Toste, A. T. Bell, *Green Chem.*, **2016**, *18*, 3577, <https://doi.org/10.1039/C6GC00579A>.
- [27] L. Kubelková, J. Čjka, J. Nováková, V. Boszáček, I. Jirka, P. Jíaru, *Stud. Surf. Sci. Catal.*, **1989**, *49*, 1203, [https://doi.org/10.1016/S0167-2991\(08\)62006-6](https://doi.org/10.1016/S0167-2991(08)62006-6).
- [28] R. A. Sheldon, *Green Chem.*, **2014**, *16*, 950, <https://doi.org/10.1039/C3GC41935E>.
- [29] R. M. West, E. L. Kunkes, D. A. Simonetti, J. A. Dumesic, *Catal. Today*, **2009**, *147*, 115, <https://doi.org/10.1016/j.cattod.2009.02.004>.
- [30] B. Kamm, *Angew. Chem. Int. Ed.*, **2007**, *46*, 5056, <https://doi.org/10.1002/anie.200604514>.
- [31] A. J. Ragauskas, C. K. Williams, B. H. Davison, G. Britovsek, J. Cairney, C. A. Eckert, W. J. Frederick, J. P. Hallett, D. J. Leak, C. L. Liotta et al., *Science*, **2006**, *311*, 484, <https://doi.org/10.1126/science.1114736>.

- 
- [32] X. Wu, S. Xie, H. Zhang, Q. Zhang, B. F. Sels, Y. Wang, *Adv. Mater.*, **2021**, *33*, 2007129, <https://doi.org/10.1002/adma.202007129>.
- [33] Z. Zhang, J. Song, B. Han, *Chem. Rev.*, **2017**, *117*, 6834, <https://doi.org/10.1021/acs.chemrev.6b00457>.
- [34] M. W. Peters, J. D. Taylor, M. Jenni, L. E. Manzer, D. E. Henton (Gevo Inc.), US2011087000A1, **2010**.
- [35] L. Yu, S. Huang, S. Zhang, Z. Liu, W. Xin, S. Xie, L. Xu, *ACS Catal.*, **2012**, *2*, 1203, <https://doi.org/10.1021/cs300048u>.
- [36] J. Deischter, K. Schute, D. S. Neves, B. E. Ebert, L. M. Blank, R. Palkovits, *Green Chem.*, **2019**, *21*, 1710, <https://doi.org/10.1039/C9GC00483A>.
- [37] R. D. Cortright, P. G. Blommel (Virent Inc.), US2013185992 (A1), **2013**.
- [38] E. V. Fufachev, B. M. Weckhuysen, P. C. A. Bruijninx, *Green Chem.*, **2020**, *22*, 3229, <https://doi.org/10.1039/D0GC00964D>.
- [39] J. Sun, C. Liu, Y. Wang, C. Smith, K. Martin, P. Venkitasubramanian (Archer Daniels Midland Company; Washington State University), US2014121430 (A1), **2013**.
- [40] B. Boekaerts, B. F. Sels, *Appl. Catal., B*, **2020**, 119607, <https://doi.org/10.1016/j.apcatb.2020.119607>.
- [41] Clarence D. Chang, Anthony J. Silvestri, *J. Catal.*, **1977**, *47*, 249, [https://doi.org/10.1016/0021-9517\(77\)90172-5](https://doi.org/10.1016/0021-9517(77)90172-5).
- [42] P. Dejaifve, J. C. Védrine, V. Bolis, E. G. Derouane, *J. Catal.*, **1980**, *63*, 331, [https://doi.org/10.1016/0021-9517\(80\)90086-X](https://doi.org/10.1016/0021-9517(80)90086-X).
- [43] J. Zhang, W. Qian, C. Kong, F. Wei, *ACS Catal.*, **2015**, *5*, 2982, <https://doi.org/10.1021/acscatal.5b00192>.
- [44] P. Ryabchuk, K. Stier, K. Junge, M. P. Checinski, M. Beller, *J. Am. Chem. Soc.*, **2019**, *141*, 16923, <https://doi.org/10.1021/jacs.9b08990>.
- [45] Y. Ni, Z. Chen, Y. Fu, Y. Liu, W. Zhu, Z. Liu, *Nat. Commun.*, **2018**, *9*, 3457, <https://doi.org/10.1038/s41467-018-05880-4>.
- [46] Y. Wang, W. Gao, S. Kazumi, H. Li, G. Yang, N. Tsubaki, *Chem. Eur. J.*, **2019**, *25*, 5149, <https://doi.org/10.1002/chem.201806165>.
- [47] Z. Ma, J. A. van Bokhoven, *ChemCatChem*, **2012**, *4*, 2036, <https://doi.org/10.1002/cctc.201200401>.
- [48] B. Puértolas, A. Veses, M. S. Callén, S. Mitchell, T. García, J. Pérez-Ramírez, *ChemSusChem*, **2015**, *8*, 3283, <https://doi.org/10.1002/cssc.201500685>.
- [49] C. A. Mullen, A. A. Boateng, *Fuel Process. Technol.*, **2010**, *91*, 1446, <https://doi.org/10.1016/j.fuproc.2010.05.022>.

- 
- [50] J.-Y. Kim, J. H. Lee, J. Park, J. K. Kim, D. An, I. K. Song, J. W. Choi, *J. Anal. Appl. Pyrolysis*, **2015**, *114*, 273, <https://doi.org/10.1016/j.jaap.2015.06.007>.
- [51] R. Liu, M. Sarker, M. M. Rahman, C. Li, M. Chai, Nishu, R. Cotillon, N. R. Scott, *Prog. Energy Combust. Sci.*, **2020**, *80*, 100852, <https://doi.org/10.1016/j.pecs.2020.100852>.
- [52] Y.-T. Cheng, J. Jae, J. Shi, W. Fan, G. W. Huber, *Angew. Chem. Int. Ed.*, **2012**, *51*, 1387, <https://doi.org/10.1002/anie.201107390>.
- [53] E. A. Uslamin, N. A. Kosinov, E. A. Pidko, E. J. M. Hensen, *Green Chem.*, **2018**, *20*, 3818, <https://doi.org/10.1039/C8GC01528G>.
- [54] T. R. Carlson, J. Jae, Y.-C. Lin, G. A. Tompsett, G. W. Huber, *J. Catal.*, **2010**, *270*, 110, <https://doi.org/10.1016/j.jcat.2009.12.013>.
- [55] J.-Y. Kim, J. Moon, J. H. Lee, X. Jin, J. W. Choi, *Fuel*, **2020**, *279*, 118484, <https://doi.org/10.1016/j.fuel.2020.118484>.
- [56] Q. Bu, H. Lei, A. H. Zacher, L. Wang, S. Ren, J. Liang, Y. Wei, Y. Liu, J. Tang, Q. Zhang et al., *Bioresour. Technol.*, **2012**, *124*, 470, <https://doi.org/10.1016/j.biortech.2012.08.089>.
- [57] T. A. Palankoev, K. I. Dement'ev, D. V. Kuznetsova, G. N. Bondarenko, A. L. Maximov, *ACS Sustain. Chem. Eng.*, **2020**, <https://doi.org/10.1021/acssuschemeng.0c03215>.
- [58] D. Dodds, B. Humphreys in *Catalytic Process Development for Renewable Materials* (Eds.: P. Imhof, Jan Cornelis van der Waal), Wiley-VCH, Weinheim, Germany, **2013**, pp. 183–237.
- [59] G. W. Huber, A. M. Gaffney, J. Jae, Y. T. Cheng (Anellotech Inc.; University of Massachusetts), US2012203042 (A1), **2010**.
- [60] "LignoValue Pilot inaugurated. Europe's first and only pilot line of bioaromatics from lignin", <https://vito.be/en/news/lignovalue-pilot-inaugurated>, accessed: **18.05.2023**.
- [61] Y.-T. Cheng, G. W. Huber, *Green Chem.*, **2012**, *14*, 3114, <https://doi.org/10.1039/c2gc35767d>.
- [62] Z. Li, Y. Jiang, Y. Li, H. Zhang, H. Li, S. Yang, *Catal. Sci. Technol.*, **2022**, *12*, 1902, <https://doi.org/10.1039/D1CY02122B>.
- [63] A. A. Rosatella, S. P. Simeonov, R. F. M. Frade, C. A. M. Afonso, *Green Chem.*, **2011**, *13*, 754, <https://doi.org/10.1039/c0gc00401d>.
- [64] I. F. Teixeira, B. T. W. Lo, P. Kostetsky, M. Stamatakis, L. Ye, C. C. Tang, G. Mpourmpakis, S. C. E. Tsang, *Angew. Chem. Int. Ed.*, **2016**, *55*, 13061, <https://doi.org/10.1002/anie.201604108>.
- [65] Y. Román-Leshkov, C. J. Barrett, Z. Y. Liu, J. A. Dumesic, *Nature*, **2007**, *447*, 982, <https://doi.org/10.1038/nature05923>.
- [66] A. Morschbacker, *Polym. Rev.*, **2009**, *49*, 79, <https://doi.org/10.1080/15583720902834791>.
- [67] A. Morschbacker (Braskem S.A.), US2010069691 (A1), **2007**.
- [68] M. Shiramizu, F. D. Toste, *Chem. Eur. J.*, **2011**, *17*, 12452, <https://doi.org/10.1002/chem.201101580>.

- [69] H. J. Cho, L. Ren, V. Vattipalli, Y.-H. Yeh, N. Gould, B. Xu, R. J. Gorte, R. Lobo, P. J. Dauenhauer, M. Tsapatsis et al., *ChemCatChem*, **2017**, *9*, 398, <https://doi.org/10.1002/cctc.201601294>.
- [70] D. Wang, C. M. Osmundsen, E. Taarning, J. A. Dumesic, *ChemCatChem*, **2013**, *5*, 2044, <https://doi.org/10.1002/cctc.201200757>.
- [71] D.-H. Liu, H.-L. He, Y.-B. Zhang, Z. Li, *ACS Sustain. Chem. Eng.*, **2020**, *8*, 14322, <https://doi.org/10.1021/acssuschemeng.0c03544>.
- [72] C. L. Williams, C.-C. Chang, P. Do, N. Nikbin, S. Caratzoulas, D. G. Vlachos, R. F. Lobo, W. Fan, P. J. Dauenhauer, *ACS Catal.*, **2012**, *2*, 935, <https://doi.org/10.1021/cs300011a>.
- [73] Y. P. Wijaya, I. Kristianto, H. Lee, J. Jae, *Fuel*, **2016**, *182*, 588, <https://doi.org/10.1016/j.fuel.2016.06.010>.
- [74] C.-C. Chang, H. Je Cho, J. Yu, R. J. Gorte, J. Gulbinski, P. Dauenhauer, W. Fan, *Green Chem.*, **2016**, *18*, 1368, <https://doi.org/10.1039/C5GC02164B>.
- [75] R. Sheldon, R. Downing, *Appl. Catal., A*, **1999**, *189*, 163, [https://doi.org/10.1016/S0926-860X\(99\)00274-4](https://doi.org/10.1016/S0926-860X(99)00274-4).
- [76] J.-S. Chang, Q. Gao, A. K. Cheetham, S.-E. Park, G. Férey, *Chem. Commun.*, **2001**, 859, <https://doi.org/10.1039/b009160j>.
- [77] R. Lu, F. Lu, J. Chen, W. Yu, Q. Huang, J. Zhang, J. Xu, *Angew. Chem. Int. Ed.*, **2016**, *55*, 249, <https://doi.org/10.1002/anie.201509149>.
- [78] X. Tong, Y. Ma, Y. Li, *Appl. Catal., A*, **2010**, *385*, 1, <https://doi.org/10.1016/j.apcata.2010.06.049>.
- [79] L. Faba, J. Gancedo, J. Quesada, E. Diaz, S. Ordóñez, *ACS Catal.*, **2021**, *11*, 11650, <https://doi.org/10.1021/acscatal.1c03095>.
- [80] Z. Wu, J. Zhang, Z. Su, S. Lu, J. Huang, Y. Liang, T. Tan, F.-S. Xiao, *Chem. Commun.*, **2022**, *58*, 2862, <https://doi.org/10.1039/d2cc00016d>.
- [81] A. G. Gayubo, A. T. Aguayo, A. Atutxa, R. Aguado, M. Olazar, J. Bilbao, *Ind. Eng. Chem. Res*, **2004**, *43*, 2619, <https://doi.org/10.1021/ie030792g>.
- [82] E. L. Kunkes, E. I. Gürbüz, J. A. Dumesic, *J. Catal.*, **2009**, *266*, 236, <https://doi.org/10.1016/j.jcat.2009.06.014>.
- [83] M. Weber, W. Pompezki, R. Bonmann, M. Weber, *Acetone in Ullmann's Encyclopedia of Industrial Chemistry*, Wiley-VCH, Weinheim, Germany, **2013**.
- [84] G. S. Salvapati, K. V. Ramanamurty, M. Janardanarao, *J. Mol. Catal.*, **1989**, *54*, 9, [https://doi.org/10.1016/0304-5102\(89\)80134-8](https://doi.org/10.1016/0304-5102(89)80134-8).
- [85] M. Balakrishnan, E. R. Sacia, S. Sreekumar, G. Gunbas, A. A. Gokhale, C. D. Scown, F. D. Toste, A. T. Bell, *PNAS*, **2015**, *112*, 7645, <https://doi.org/10.1073/pnas.1508274112>.



- [86] S. Shylesh, D. Kim, A. A. Gokhale, C. G. Canlas, J. O. Struppe, C. R. Ho, D. Jadhav, A. Yeh, A. T. Bell, *Ind. Eng. Chem. Res.*, **2016**, *55*, 10635, <https://doi.org/10.1021/acs.iecr.6b03601>.
- [87] N. B. Lorette, *J. Org. Chem.*, **1957**, *22*, 346, <https://doi.org/10.1021/jo01354a619>.
- [88] E. I. Gürbüz, E. L. Kunkes, J. A. Dumesic, *Appl. Catal., B*, **2010**, *94*, 134, <https://doi.org/10.1016/j.apcatb.2009.11.001>.
- [89] S. Shylesh, S. Sreekumar, J. Gomes, A. Grippo, G. E. Arab, M. Head-Gordon, F. D. Toste, A. T. Bell, *Angew. Chem. Int. Ed.*, **2015**, *54*, 4673, <https://doi.org/10.1002/anie.201412470>.
- [90] S.-T. Tsai, C.-H. Chen, T.-C. Tsai, *Green Chem.*, **2009**, *11*, 1349, <https://doi.org/10.1039/b905744g>.
- [91] J. Fuhse, F. Bandermann, *Chem. Eng. Technol.*, **1987**, *10*, 323, <https://doi.org/10.1002/ceat.270100139>.
- [92] H. Siegel, M. Eggersdorfer, *Ketones in Ullmann's Encyclopedia of Industrial Chemistry*, Wiley-VCH, Weinheim, Germany, **2012**.
- [93] W. L. Howard, *Acetone in Kirk-Othmer Encyclopedia of Chemical Technology*, John Wiley & Sons, **2011**.
- [94] D. Hoell, T. Mensing, R. Roggenbuck, M. Sakuth, E. Sperlich, T. Urban, W. Neier, G. Strehlke, *2-Butanone in Ullmann's Encyclopedia of Industrial Chemistry*, Wiley-VCH, Weinheim, Germany, **2012**.
- [95] P. Anbarasan, Z. C. Baer, S. Sreekumar, E. Gross, J. B. Binder, H. W. Blanch, D. S. Clark, F. D. Toste, *Nature*, **2012**, *491*, 235, <https://doi.org/10.1038/nature11594>.
- [96] F. Mo, G. Dong, *Science*, **2014**, *345*, 68, <https://doi.org/10.1126/science.1254465>.
- [97] E.-B. Goh, E. E. K. Baidoo, J. D. Keasling, H. R. Beller, *Appl. Environ. Microbiol.*, **2012**, *78*, 70, <https://doi.org/10.1128/AEM.06785-11>.
- [98] H. Yoneda, D. J. Tantillo, S. Atsumi, *ChemSusChem*, **2014**, *7*, 92, <https://doi.org/10.1002/cssc.201300853>.
- [99] Y. Gong, L. Lin, J. Shi, S. Liu, *Molecules*, **2010**, *15*, 7946, <https://doi.org/10.3390/molecules15117946>.
- [100] K. Srirangan, X. Liu, L. Akawi, M. Bruder, M. Moo-Young, C. P. Chou, *Appl. Environ. Microbiol.*, **2016**, *82*, 2574, <https://doi.org/10.1128/AEM.03964-15>.
- [101] A. Corma, O. de La Torre, M. Renz, *Energy Environ. Sci.*, **2012**, *5*, 6328, <https://doi.org/10.1039/c2ee02778j>.
- [102] S. Shylesh, A. A. Gokhale, C. R. Ho, A. T. Bell, *Acc. Chem. Res.*, **2017**, *50*, 2589, <https://doi.org/10.1021/acs.accounts.7b00354>.
- [103] E. L. Kunkes, D. A. Simonetti, R. M. West, J. C. Serrano-Ruiz, C. A. Gärtner, J. A. Dumesic, *Science*, **2008**, *322*, 417, <https://doi.org/10.1126/science.1159210>.



- 
- [104] R. Kane, *Ann. Phys. Chem.*, **1838**, 120, 473, <https://doi.org/10.1002/andp.18381200711>.
- [105] F. W. Küster, A. Stallberg, *Justus Liebigs Ann. Chem.*, **1894**, 278, 207, <https://doi.org/10.1002/jlac.18942780205>.
- [106] W. Ipatiew, B. Dolgow, J. Wolnow, *Eur. J. Inorg. Chem.*, **1930**, 63, 3072, <https://doi.org/10.1002/cber.19300631123>.
- [107] F. Lin, Y.-H. Chin, *J. Catal.*, **2014**, 311, 244, <https://doi.org/10.1016/j.jcat.2013.11.018>.
- [108] W. T. Reichle, *J. Catal.*, **1980**, 63, 295, [https://doi.org/10.1016/0021-9517\(80\)90082-2](https://doi.org/10.1016/0021-9517(80)90082-2).
- [109] S. Herrmann, E. Iglesia, *J. Catal.*, **2017**, 346, 134, <https://doi.org/10.1016/j.jcat.2016.12.011>.
- [110] L. Faba, E. Díaz, S. Ordóñez, *Appl. Catal., B*, **2013**, 142-143, 387, <https://doi.org/10.1016/j.apcatb.2013.05.043>.
- [111] L. D. Dellon, C.-Y. Sung, D. J. Robichaud, L. J. Broadbelt, *Ind. Eng. Chem. Res*, **2019**, 58, 15173, <https://doi.org/10.1021/acs.iecr.9b03242>.
- [112] R. Adams, R. W. Hufferd, *Org. Synth.*, **1922**, 2, 41, <https://doi.org/10.15227/orgsyn.002.0041>.
- [113] J. F. Adams, V. G. Papangelakis, *Hydrometallurgy*, **2007**, 89, 269, <https://doi.org/10.1016/j.hydromet.2007.07.016>.
- [114] J. A. Mitchell, E. E. Reid, *J. Am. Chem. Soc.*, **1931**, 53, 330, <https://doi.org/10.1021/ja01352a049>.
- [115] S. Setiadi, M. Nasikin, *IJET-IJENS*, **2011**, 11, 72.
- [116] H. Kosslick, G. Lischke, G. Walther, W. Storek, A. Martin, R. Fricke, *Microporous Mater.*, **1997**, 9, 13, [https://doi.org/10.1016/S0927-6513\(96\)00087-9](https://doi.org/10.1016/S0927-6513(96)00087-9).
- [117] M. Zamora, T. López, M. Asomoza, R. Meléndrez, R. Gómez, *Catal. Today*, **2006**, 116, 234, <https://doi.org/10.1016/j.cattod.2006.02.087>.
- [118] D. Wang, Z. Liu, Q. Liu, *Ind. Eng. Chem. Res*, **2019**, 58, 6226, <https://doi.org/10.1021/acs.iecr.9b00175>.
- [119] B. Yan, Z.-H. Liu, Y. Liang, B.-Q. Xu, *Ind. Eng. Chem. Res*, **2020**, 59, 17417, <https://doi.org/10.1021/acs.iecr.0c02148>.
- [120] R. M. Ravenelle, F. Schüßler, A. D'Amico, N. Danilina, J. A. van Bokhoven, J. A. Lercher, C. W. Jones, C. Sievers, *J. Phys. Chem. C*, **2010**, 114, 19582, <https://doi.org/10.1021/jp104639e>.
- [121] P. Sun, D. Yu, Z. Tang, H. Li, H. Huang, *Ind. Eng. Chem. Res*, **2010**, 49, 9082, <https://doi.org/10.1021/ie101093x>.
- [122] M. Paulis, M. Martín, D. B. Soria, A. Díaz, J. A. Odriozola, M. Montes, *Appl. Catal., A*, **1999**, 180, 411, [https://doi.org/10.1016/S0926-860X\(98\)00379-2](https://doi.org/10.1016/S0926-860X(98)00379-2).
- [123] T. J. Benson, P. R. Daggolu, R. A. Hernandez, S. Liu, M. G. White, *Adv. Catal.*, **2013**, 56, 187, <https://doi.org/10.1016/B978-0-12-420173-6.00003-6>.

- 
- [124] A. D. Ivakhnov, T. E. Skrebets, M. V. Bogdanov, *Russ. J. Phys. Chem. B*, **2019**, *13*, 1125, <https://doi.org/10.1134/S199079311907008X>.
- [125] L. Kubelková, J. Čejka, J. Nováková, *Zeolites*, **1991**, *11*, 48, [https://doi.org/10.1016/0144-2449\(91\)80355-4](https://doi.org/10.1016/0144-2449(91)80355-4).
- [126] J. Quesada, L. Faba, E. Díaz, S. Ordóñez, *Catal. Sci. Technol.*, **2020**, *10*, 1356, <https://doi.org/10.1039/C9CY02288K>.
- [127] S. Wang, K. Goulas, E. Iglesia, *J. Catal.*, **2016**, *340*, 302, <https://doi.org/10.1016/j.jcat.2016.05.026>.
- [128] I. Yeboah, X. Feng, K. R. Rout, de Chen, *Ind. Eng. Chem. Res.*, **2021**, *60*, 15095, <https://doi.org/10.1021/acs.iecr.1c02994>.
- [129] F. Lin, H. Wang, Y. Zhao, J. Fu, D. Mei, N. R. Jaegers, F. Gao, Y. Wang, *JACS Au*, **2021**, *1*, 41, <https://doi.org/10.1021/jacsau.0c00028>.
- [130] H. Li, D. Guo, N. Ulumuddin, N. R. Jaegers, J. Sun, B. Peng, J.-S. McEwen, J. Hu, Y. Wang, *JACS Au*, **2021**, *1*, 1471, <https://doi.org/10.1021/jacsau.1c00218>.
- [131] G. Li, D. T. Ngo, Y. Yan, Q. Tan, B. Wang, D. E. Resasco, *ACS Catal.*, **2020**, *10*, 12790, <https://doi.org/10.1021/acscatal.0c02987>.
- [132] P. Reif, H. Rosenthal, M. Rose, *Adv. Sustain. Syst.*, **2020**, *4*, 1900150, <https://doi.org/10.1002/adsu.201900150>.
- [133] P. Reif, N. K. Gupta, M. Rose, *Catal. Commun.*, **2022**, *163*, 106402, <https://doi.org/10.1016/j.catcom.2022.106402>.
- [134] P. Reif, N. K. Gupta, M. Rose, *Green Chem.*, **2023**, *25*, 1588, <https://doi.org/10.1039/D2GC04116B>.

---

---

## Erklärungen

---

### Erklärungen laut Promotionsordnung

#### §8 Abs. 1 lit. c der Promotionsordnung der TU Darmstadt

Ich versichere hiermit, dass die elektronische Version meiner Dissertation mit der schriftlichen Version übereinstimmt und für die Durchführung des Promotionsverfahrens vorliegt.

#### §8 Abs. 1 lit. d der Promotionsordnung der TU Darmstadt

Ich versichere hiermit, dass zu einem vorherigen Zeitpunkt noch keine Promotion versucht wurde und zu keinem früheren Zeitpunkt an einer in- oder ausländischen Hochschule eingereicht wurde. In diesem Fall sind nähere Angaben über Zeitpunkt, Hochschule, Dissertationsthema und Ergebnis dieses Versuchs mitzuteilen.

#### §9 Abs. 1 der Promotionsordnung der TU Darmstadt

Ich versichere hiermit, dass die vorliegende Dissertation selbstständig und nur unter Verwendung der angegebenen Quellen verfasst wurde.

#### §9 Abs. 2 der Promotionsordnung der TU Darmstadt

Die Arbeit hat bisher noch nicht zu Prüfungszwecken gedient.

Darmstadt, den

---

Phillip Reif

---

## Erklärung zum Eigenanteil an den Veröffentlichungen der kumulativen Dissertation

Im Folgenden ist aufgelistet, mit welchem Anteil ich an den Veröffentlichungen beteiligt war.

Mein Anteil an der folgenden Veröffentlichung beträgt 60%:

1. P. Reif, H. Rosenthal, M. Rose, Biomass-Derived Aromatics by Solid Acid-Catalyzed Aldol Condensation of Alkyl Methyl Ketones, *Adv. Sustain. Syst.* **2020**, *4*, 1900150.

Mein Anteil an der folgenden Veröffentlichung beträgt 85%:

2. P. Reif, N. K. Gupta, M. Rose, Liquid phase aromatization of bio-based ketones over a stable solid acid catalyst under batch and continuous flow conditions, *Catal. Commun.* **2022**, *163*, 106402.

Mein Anteil an der folgenden Veröffentlichung beträgt 85%:

3. P. Reif, N. K. Gupta, M. Rose, Highly stable amorphous silica-alumina catalysts for continuous bio-derived mesitylene production under solvent-free conditions, *Green Chem.* **2023**, *25*, 1588.

---

Datum

---

Phillip Reif

---

## Erklärung zur Begutachtung der Veröffentlichungen

Erstgutachter: Prof. Dr. Marcus Rose

Zweitgutachter: Prof. Dr. Markus Busch

Weder der Erstgutachter (Prof. Dr. Marcus Rose) noch der Zweitgutachter (Prof. Dr. Markus Busch) der vorliegenden kumulativen Doktorarbeit waren an der Begutachtung nachstehender Veröffentlichungen beteiligt:

1. P. Reif, H. Rosenthal, M. Rose, Biomass-Derived Aromatics by Solid Acid-Catalyzed Aldol Condensation of Alkyl Methyl Ketones, *Adv. Sustain. Syst.* **2020**, *4*, 1900150.
2. P. Reif, N. K. Gupta, M. Rose, Liquid phase aromatization of bio-based ketones over a stable solid acid catalyst under batch and continuous flow conditions, *Catal. Commun.* **2022**, *163*, 106402.
3. P. Reif, N. K. Gupta, M. Rose, Highly stable amorphous silica-alumina catalysts for continuous bio-derived mesitylene production under solvent-free conditions, *Green Chem.* **2023**, *25*, 1588.

---

Datum

---

Erstgutachter  
(Prof. Dr. Marcus Rose)

---

Zweitgutachter  
(Prof. Dr. Markus Busch)